63-3-3

LOW NOISE MILLIMETER DETECTOR

FINAL REPORT

7 JANUARY 1963

Prepared By

C. H. Brunquell

Contract #AF30(602)-2651

Prepared For

Rome Air Development Center

Research and Technology Division

Air Force Systems Command

United States Air Force

Griffis Air Force Base

New York

MICROWAVE ASSOCIATES, INC.

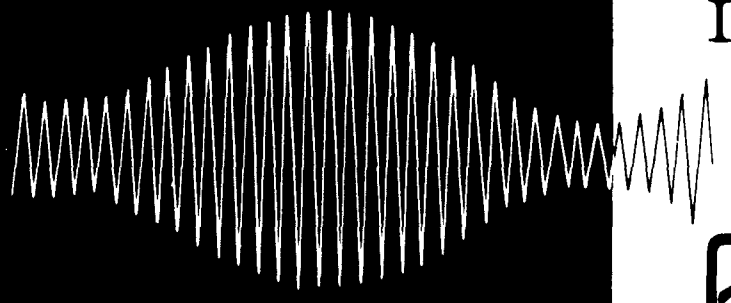

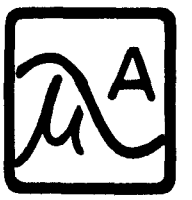

RADC-TDR-63-44

7 January 1963

LOW NOISE MILLIMETER DETECTOR

Prepared By

Clyde H. Brunquell

MICROWAVE ASSOCIATES, INC.
BURLINGTON, MASSACHUSETTS

FINAL REPORT

Contract #AF30(602)-2651

Project #5578

Task #557801

Prepared For

Rome Air Development Center

Research and Technology Division

Air Force Systems Command

United States Air Force

Griffis Air Force Base

New York

PATENT NOTICE: When Government drawings, specifications, or other data are used for any purpose other than in connection with a definitely related Government procurement operation, the United States Government thereby incurs no responsibility nor any obligation whatsoever and the fact that the Government may have formulated, furnished, or in any way supplied the said drawings, specifications or other data is not to be regarded by implication or otherwise as in any manner licensing the holder or any other person or corporation, or conveying any rights or permission to manufacture, use, or sell any patented invention that may in any way be related thereto.

ASTIA NOTICE: Qualified requestors may obtain copies of this report from the ASTIA Document Service Center, Dayton 2, Ohio. ASTIA Services for the Department of Defense contractors are available through the "Field of Interest Register" on a "need-to-know" certified by the cognizant military agency of their project or contract.

FOREWORD

This investigation of new and improved crystal detectors for use in the 2 mm region was conducted at Microwave Associates, Inc., Burlington, Massachusetts by Clyde H. Brunquell and Dudley Brewster in the Point-Contact Diode Development Group supervised by John V. Jenkinson, in the Semiconductor Research and Development Department directed by Dr. Arthur Uhlir, Jr.

Epitaxial silicon material was prepared by John Brownson and Simon Stopek. Noise temperature ratio measurements were conducted by William E. Doherty, Jr.

The Author would like to acknowledge the cooperation of G. S. Heller and J. B. Thaxter of Lincoln Laboratories in the establishment of a power level at 140 Gc.

ABSTRACT

Work conducted on the design and development of 2-millimeter wavelength circular guide point contact detectors is summarized in this report.

Circular waveguide formed the basis of the 2-millimeter detector design after preliminary comparison with existing rectangular waveguide detectors at 4-millimeter wavelengths. A waveguide diameter of 0.090", with a dumb bell type of adjustable shorting plunger was found to give the best performance.

Test results of Tangential Signal, figure of merit and conversion loss is reported. Results indicate that a 2-mm video detector can be fabricated with a -35 dbm Tangential Signal Sensitivity at 10 μA bias and 1 Mc video band width. Calculations of the "minimum detectable signal" MDS from figure of merit measurements indicate the goal of a minimum detectable signal of 10^{-10} watts was met. A harmonic generator and a calibrated 2-mm attenuator were constructed. The report contains design data for these components, and the results obtained from their use.

TABLE OF CONTENTS

TABLE OF CONTENTS (continued)

LIST OF ILLUSTRATIONS

LIST OF ILLUSTRATIONS (continued)

LIST OF TABLES

LIST OF APPENDICES

SECTION I - INTRODUCTION

This final report contains an account of the investigations on 2-millimeter wavelength detectors. The objective of the program has been the development of point contact crystal diodes for operation at 140 Gc.

In Section 2, experimental work with 4 and 2 millimeter circular guide detectors is described. For the most part, this portion of the research has dealt with diodes operating in the 2-millimeter wavelength band. The solutions of the electromagnetic equations for the case of TE_{1n} waves in a circular waveguide are presented. Some testing procedures are outlined, and a number of experimental results are presented herein.

Appendices I and II present the development of crystal harmonic generators and a calibrated 2-millimeter attenuator. These components were used in the instrumentation for testing the 2-millimeter circular guide detectors.

SECTION II - DISCUSSION

CHAPTER 1. RF DESIGN STUDY BASED ON 4 MM MODELS

A. INTRODUCTION

When the present program was first started it was thought that Coin silver rectangular waveguide 0.040 by 0.080 inch I.D. cross section (RG-138/U) might be used as a holder for a 2 mm detector. This guide has a $T.E._{10}$-mode cutoff frequency of 73.8 kMc and propagates only the dominant mode at frequencies below approximately 148 kMc. Because of the high attenuation and close tolerances inherent at these frequencies, careful fabrication techniques, including precision milling and electroforming are generally used. It was decided that a different type of waveguide transmission be used that would lend itself more readily to common shop practices. The TE_{11}-mode circular waveguide has the desirable characteristic that it can be fabricated easily and accurately on any standard lathe.

Circular waveguide geometry lends itself to the fabrication of a diode holder with the diode integrally mounted in the waveguide along with a variable-position short circuit. The problem of designing a short-circuiting plunger for circular waveguide is much more straight forward, in theory, than the problem of designing one for rectangular waveguide. An additional and very simple means of matching the diode to the input waveguide would be the rotation of the diode and the holder about the axis of the circular waveguide. This type of tuning corresponds to the lateral offsetting of the diode in rectangular guide to effect an impedance transformation.

In the fabrication and testing of a circular-guide 2 mm diode the comparison with existing detectors cannot readily be made. In light of this problem it would be rather difficult to evaluate the technique of circular

guide detection versus rectangular guide. Therefore, preliminary tests on a circular guide detector were performed at 4 millimeter wavelengths where comparisons with existing detectors could be readily made. Favorable results were obtained; therefore, the 2 millimeter detector was based on the circular type.

B. DESIGN

(1) When the electromagnetic equations are applied to circular guides, they fit best when placed in cylindrical-coordinate form. The solutions to the electromagnetic equations in this form usually appear as Bessel's functions. The cutoff wavelength and also the conditions for higher-order waves are related to the radius (a) of the guide by way of the zeroes of the particular Bessel function appropriate to the case in question.

For proper operation of our circular guide detector the counterpart in circular guide of the TE_{10}-mode in a rectangular guide must be propagated. This mode is the TE_{11}-mode (Figure 1) and is the first to appear in a circular guide. For that reason it is often referred to as the dominant wave in a circular guide.

The design of our detector is based upon the solution of the electromagnetic equations for the case of TE_{1n} waves in a circular guide.

In the case of the propagation constant,

$$\Gamma = \sqrt{\chi^2 - \beta^2} = \sqrt{\frac{k^2}{a^2} - \frac{4\pi^2}{\lambda^2}}$$

where k represents the roots for which $J_1'(2\pi a/\lambda) = 0$. k = 1.841, 5.331, 8.536, etc. For circular waveguides, cutoff occurs when $\Gamma = 0$ or when

$$(1.1) \qquad \lambda_c = \frac{2\pi a}{k}, \quad \lambda_c = \text{cutoff wavelength}$$

for the TE_{11} or dominant wave

$$(1.2) \qquad \lambda_c = \frac{2\pi a}{1.841} = 3.42\ a$$

and it may be shown that

$$(1.3) \qquad \lambda_g = \frac{\lambda}{\sqrt{1-\nu^2}}$$

where $\nu = \frac{fc}{f} = \frac{\lambda}{\lambda_c}$ λ = free space wavelength
λ_g = guide wavelength

Circular guide for dominant mode operation at 4 millimeter wavelengths is 0.189" I.D. in cross section. From equation 1.2 λ_c is found to be 0.323" (8.2 mm), or a cutoff frequency of 36.6 kMc. Substitution into equation (1.3) gives a guide wavelength of 0.199" (5.05 mm) at 69.720 kMc.

To avoid the excitation of higher order modes a smaller diameter guide detector was also fabricated. An I.D. cross section of 0.125" was used. Equation (1.2) reveals a λ_c of 0.214" (5.43 mm) and substitution of this figure into equation (1.3) gives a λ_g of 0.277" (7.04 mm) at 69.720 kMc. A λ_c of 5.43 mm corresponds to an fc of 55.2 kMc.

C. FABRICATION OF 4 MM TEST CRYSTALS

Figure #2 shows the 4.3 millimeter detector. This design incorporates an integral mounting of the diode and waveguide. The body was machined to the specifications in Figure #3 and fitted with the flange illustrated in Figure #8 which mates with the Phillips claw flange after removal of the claws. The flange is soft soldered to the body and the unit is then cleaned, degreased and gold plated. This form of coupling allows for matching the diode to the waveguide by rotating the diode about the waveguide axis.

Two whisker designs were prepared for evaluation. The first whisker was a "C"-bend of 0.0025" diameter tungsten. The tungsten wire was welded to the whisker screw and formed on a 0.0025" diameter "C"-bend die. After forming, the wire was cut and pointed by electrolytic means.[3] The electrolyte used for the pointing operation is an aqueous solution containing 10 percent by weight of potassium hydroxide. The cathode is a Nickel mesh. The pointing operation is accomplished by placing the whiskers in a vertical position with their lower ends in the electrolyte and applying 2 volts a.c. until the current drops to zero. The drop in current at constant voltage arises from the decrease in wetted area as the tungsten is dissolved. The shaping of the point depends on the formation of a meniscus of a suitable shape about the wire. The "C"-bend screw and whisker are illustrated in Figure #4. The second whisker was an "S"-spring of 0.0035" diameter tungsten. The wire was soldered in the whisker screw and formed on a 0.0035" diameter "S"-bend die. After forming, the wire was cut to length and then pointed mechanically. The "S"-bend screw and whisker are illustrated in Figure #5.

Boron-doped P-type single-crystal silicon was sliced and polished. The silicon had resistivities of .00064 - .00042 ohm-cm. The slices were then heated in an oven to a temperature of 1250°C. The oven was purged for five minutes with N_2. After the purge the slices were prefired with H_2 for thirty minutes. An epitaxial layer was deposited on the silicon by passing a mixture of H_2 + $SiCl_4$ over the slices for a period of 5.5 minutes. An H_2 purge of five minutes followed by a 5 minute N_2 purge ended the surface preparation of the silicon. The untreated face of the slices were lapped and plated with nickel and silver. Dice were cut from the slices and soldered to crystal screws as illustrated in Figure #6. Before final assembly the

silicon was etched for ten minutes in a 24 percent solution of hydroflouric acid, rinsed in hot water, and washed with Solox. The silicon was etched in 48 percent Hydroflouric to remove oxide from the epitaxial layer.

Four shorting plungers were fabricated to evaluate the best possible type that should be used. The first type of shorting is illustrated in Figure #7A. It was a flat face cylindrical plunger relying solely on low contact resistance. The second type of plunger is illustrated in Figure #7B. This type had a flat face that is indented one-half a guide wavelength ($\lambda g/2$ from equation 1.3) back from the end of the short. This also relys on a low contact resistance plus the reflection of a voltage minimum from the face to the discontinuity at the plunger end. The third type of short is illustrated in Figure #7C. It was a cylindrical plunger with a conical indent at its face. It was hoped that this type of short would work similar to the flat face short but not be too critical in tuning. The fourth type of short illustrated in Figure #7D was the dumb bell type.(2) This shorting plunger consists of low and high impedance sections one-quarter of a guide-wavelength in length. The alternation of low and high impedances makes the attainment of low contact resistance less important than it would be in a plain cylindrical plunger relying soley on low contact resistance. It may be shown that the current in the contact is reduced below that in the main waveguide by the factor Z_{01}/Z_{02} by the alternation of the low characteristic impedance Z_{01} and the high characteristic impedance Z_{02}. Plunger losses are reduced by the square of this ratio compared with those in a plain cylindrical plunger having the same contact resistance.

The diodes were assembled as illustrated in Figures #9 and #10. Figures #11 through #16 illustrate the additional parts of the diode needed for assembly. Upon assembly the whisker and screw subassembly were positioned

in the diode to place the point contact at the approximate center of the guide. All adjusting of the unit was done by means of the silicon screw subassembly. The units were adjusted on the waveguide for a maximum Tangential Signal Sensitivity with a 0.5 μsec. pulse. Figures #17, 18 and 19 illustrate the adjust and test equipment setup. The units were attached to the waveguide by means of a transition illustrated in Figure #20.

D. RESULTS

The "C"-bend whisker smashed easily and the resulting diodes were unstable. While adjusting the diodes, it was found that an extremely light contact pressure was necessary. The "S"-bend whisker adjusted smoothly and resulted in what appeared to be a stable unit.

Tangential Signal Sensitivity tests were made to compare the circular guide detector and existing 4.3 millimeter detectors. The results were very satisfactory in that the circular guide with the flat face short, the indented flat face short and the conically indented short had sensitivities 2 to 10 db better than existing rectangular guide detectors. The dumb bell short exhibited a 1 to 2 db increase in sensitivity over the other 3 shorts. The 0.189" diameter design exhibited up to 6 db more sensitivity than the 0.125" diameter waveguide design.

E. CONCLUSIONS

The results showed that a video detector comparable to existing rectangular guide detectors may be fabricated in circular waveguide propagating the TE_{11}-mode.

These results justify proceeding with the design and fabrication of a 2 millimeter detector in circular guide. This design will be centered about the dumb bell short which exhibited a superiority over the other shorts as a low loss shorting plunger.

CHAPTER 2. 2-MILLIMETER DETECTOR DIODE

A. INTRODUCTION

Chapter 1 of this report described the design and fabrication of a 4.3 millimeter wavelength circular guide detector. Tests indicated senitivities comparable to existing rectangular guide detectors. The present chapter reports the design and fabrication of a 2-millimeter wavelength circular guide detector.

B. DESIGN

As in the design of the 4.3 millimeter wavelength detector equations 1.2 and 1.3 are true for dominant mode operation at 2-millimeter wavelengths. These equations were

$$\lambda_c = \frac{2\pi a}{1.841} = 3.42\, a \qquad (1.2)$$

$$\lambda_g = \frac{\lambda}{\sqrt{1 - \gamma^2}} \qquad (1.3)$$

Three different guide diameter detectors were fabricated. A circular guide of 0.090" diameter is capable of propagating higher order modes at 140 kMc. The cutoff wavelength of a guide of this size is found from equation (1.2) to be .154" (3.91 mm) which corresponds to cutoff frequency of 76.8 kMc. The guide wavelength at 139.44 kMc from equation (1.3) is 0.105" (2.575 mm).

A circular guide of 0.070" diameter will suppress the excitation of higher order modes other than the dominant mode at 140 kMc. The cutoff wavelength of this guide is 0.1205" (3.06 mm) corresponding to a cutoff of 98.1 kMc. The guide wavelength at 139.44 kMc is 0.119" (3.03 mm).

A third size guide of 0.0625" diameter will also suppress the excitation of higher order modes other than the dominant mode at 140 kMc. The cutoff wavelength of this guide is 0.107" (2.72 mm) corresponding to a cutoff frequency of 110.5 kMc. The guide wavelength at 139.44 kMc is 0.138" (3.51 mm).

C. FABRICATION

Four styles of 2 millimeter wavelength circular guide detector designs were fabricated. Each new detector mount came about to improve the mechanical design of the preceding diode. The first design was exactly the same as the 4.3 millimeter detector with the exception of the change in the circular guide cross sectional area. The second design followed the first very closely. A mechanical change that was incorporated in this unit was to machine the micrometer adaptor coupling (Figure #14) integrally with the body. This body is illustrated in Figure #21. The change eliminated any discontinuity in the waveguide that may have previously been caused by improper seating of the coupler in the body. The third design incorporated a significant improvement in the ruggedness and simplicity of the shorting plunger mechanism. A new micrometer was specified as in Figure #22 and the plunger, Figure #23, was reworked to thread into the micrometer shaft. The body was changed to the specifications in Figure #24 so that the micrometer adaptor was integral with the body. This made for a much more compact and easily fabricated unit. The body designs to this point all require that the flange illustrated in Figure #8 be soft-soldered on the input waveguide. A fourth body design, illustrated in Figure #25,A and B, specified that the flange be machined as an integral part of the body. The flange was set back from the waveguide edge to produce a lip that is concentric with the waveguide. This lip mates with a concentric depression in the mating flange and insures proper

alignment of the diode assembly with the input waveguide. All four designs were cleaned, degreased and gold plated before assembly.

Three whisker designs were prepared for evaluation. The first whisker was the "S"-spring of 0.0035" diameter tungsten, illustrated Figure #5, used in the fabrication of the 4.3 millimeter diode. The second whisker was an "S"-spring of 0.0030" diameter tungsten. This whisker had a shorter amplitude than the 0.0035" diameter "S"-spring. Both "S"-bend whiskers were fabricated as described in the fabrication of the 4.3 millimeter detector. In the case of the 0.003" diameter "S"-spring the whisker was formed on a 0.003" short amplitude "S"-spring die. This configuration is illustrated in Figure #26. The third design was a "C"-bend of 0.0015" diameter tungsten. The tungsten wire was welded to a 0.025" diameter Nickel pin soldered in the whisker screw. The "C"-bend was formed on a 0.0015" diameter "C"-bend die designed to produce a large amplitude "C"-bend. The wire was cut and pointed by electrolytic means described in a previous section. The "C"-bend screw and whisker are illustrated in Figure #27.

Three types of silicon were prepared for study at 2-millimeter wavelengths. The first was the P-type epitaxial silicon used in the comparison tests at 4.3 millimeter wavelengths. The second silicon prepared was aluminum doped, P-type, polycrystalline material with resistivities of .0175 - .0185 ohm-cm. The third type was boron doped, P-type, single crystal silicon with resistivities of .020 - .022 ohm-cm. Both the aluminum and Boron doped silicon crystals were prepared as follows. The crystals were slice and polished. The slices were baked for one hour at $1050^{o}C \pm 25^{o}C$ in an oxygen atmosphere. The unpolished surface was sand blasted and plated with nickel and silver. Dice were cut from the slices and soldered to crystal screws as

illustrated in Figure #6. Before final assembly the silicon was etched for ten minutes in a 24 percent solution of hydroflouric acid, rinsed in hot water, and washed with solox. The silicon was etched to remove oxide from the epitaxial layer.

The diodes were assembled as illustrated in Figures #9, #10, #28 and #29. Upon assembly the whisker and screw subassembly were positioned in the diode to place the point contact at the approximate center of the guide. Adjusting was done by means of the silicon-screw subassembly. The units were adjusted on the waveguide with R.F. power at 140 kMc obtained from the second harmonic from a 70 kMc klystron. The design of the harmonic generator for this purpose is described in the appendix. The klystron was modulated with a 1,000 cycles square wave and the output from the detector was observed on a Hewlett Packard 415B Standing Wave Indicator.

D. RESULTS

In the early part of the project, power measurement techniques had not been developed to determine the power output of the harmonic generators which have been developed here. It follows that the sensitivity of the detectors could not be determined.[4] A measure of the useable dynamic range of the detected signal provides a knowledge of the sensitivity of the detector. For example, a dynamic range of 35 db means that the maximum detected signal is 35 db above the noise level observed on the indicator when the power at the fundamental frequency to the harmonic generator is removed. The difference in the dynamic range between two units is a relative measurement of the units. As diode sensitivities are improved with design and harmonic generator efficiencies increase, the dynamic range will also increase. In order for data of this kind to have meaning the value of the power at the fundamental frequency

to the harmonic generator must be known. Table I presents an indication of the dynamic range of various early diodes used in both the harmonic generator and the detector. The data indicates a slightly larger dynamic range (5 to 19 db for a 1.0 mW input) for a guide diameter of 0.090". This makes the 0.090" diameter desirable for a 140 kMc detector mount. The ease in which the 0.090" diameter guide can be fabricated compared to the 0.0625" and 0.070" diameter guides also enhances its use. As the guide diameter is reduced, it becomes more difficult to accurately bore the cylindrical guide to any length through the brass body. It was decided to continue the 140 kMc detector operations in the 0.090" diameter guide.

This measure of sensitivity leaves much to be desired in that it characterizes the harmonic generator and detector as a pair and not singularly. To characterize the diodes separately the level of the R.F. power must be known. To determine this power level diodes #0 through #7 were constructed to be used as standards. These diodes were calibrated at Lincoln Laboratories to establish a power level. A 140 kMc power source was calibrated at Lincoln Laboratories by means of a calorimeter constructed by J. B. Thaxter of that Laboratory. The power as indicated by the calorimeter is consistently 20% $\pm$ 5% below the best estimates of the true power level present. Measurements were made at three different power levels, 1 μwatt, 10 μwatts and 100 μwatts. Table II represents the calibration data at zero bias taken on the seven diodes tested. Dynamic range measurements were taken on these diodes to be used to determine the conversion efficiency of the 4 to 2 millimeter harmonic generation. This efficiency is discussed in the appendix along with the design of the generator. The open circuit voltage (δV) as read on a Hewlett Pakcard Model 412A D.C. vacuum tube voltmeter were taken to rate the detectors in terms of a "figure of merit". Upon return to our laboratory

with the diodes anyone of the three power levels listed above could be established by varying the level of the fundamental power to the harmonic generator until the data of Table II is reproduced.

The figure of merit $M^{(5)}$ is defined by

$$M = \frac{\gamma}{\sqrt{R_V + R_A}}$$

where R_A is an arbitrary resistance used to represent the amplifier noise and has almost always been taken as 1200 ohms, γ, which may be termed the "Voltage sensitivity" of the diode, is the constant of proportionality between the open-circuit output voltage δv resulting from an input microwave power (P):

$$\delta V = \gamma P$$

The symbol R_V designates the video resistance or effective output impedance of a crystal rectifier which is essentially resistive at the highest common video frequencies. At low output frequencies, the shunting capacitance contributed by the diode holder is of no consequence, so that the video resistance can be determined by a measurement of small-signal resistance at audio frequency. For example, one can attach a bridge to the output terminals. The result should be indifferent to the presence or absence of small microwave signal. Of course, the d-c bias for the intended use must be applied during this measurement. For the zero bias measurements we used a high-impedance audio frequency current generator and an a-c vacuum tube voltmeter; the resistance is then directly proportional to the meter reading. For biased R_V measurements, the open-circuit output voltage with a small audio-modulated microwave signal applied to the input was measured. Then, the video resistance is found by trial as the setting of a resistance box in shunt with the output terminals that result in a reduction of the output voltage to one-half of the open-circuit voltage. Figure #30 illustrates the test equipment built

for this purpose. Table III presents the Rv values and the calculated figure of merit at zero bias and a 1 μwatt C.W. input. The figure of merit varied between 5.2 to 18.8. As may be noted in the table, the video resistance is quite large at zero bias. This accounts for the relatively small figure of merits displayed in the chart. To reduce the video resistance the diodes were tested under forward biased conditions. Before conducting further tests diodes #0 and #7 were placed aside as standards to be checked periodically against diodes #1, 2, 4, 5 and 6. Diode #1 was lost due to a faulty cable and it was decided to replace the cable with 58/u coaxial cable and a Microdot adaptor Model #33-103. Diodes #2, 4, 5 and 6 were tested under biased conditions as described above and the results presented in Table IV. As may be noted, if the zero biased figure of merit readings in Table III are compared with those in Table IV that a correlation does not exist. Previous work at X and M band frequencies has shown that a correlation does exist between figure of merit measurements with both CW and audio-modulated microwave power inputs. This would indicate that the diodes have changed their characteristics. A check on a d.c. characteristic curve tracer showed the diodes to be highly conductive in the reverse direction. A check of diodes #0 and #7 also showed a vast change in their characteristics. Further study pointed to the light contact pressure required by the 0.0035" "S"-bend whisker to obtain maximum sensitivity. It was decided to try two new whisker designs, the 0.0030" "S"-bend and the 0.0015" C-bend, and observe their stability characteristics. Table V presents the diodes made as an attempt to make a stable diode. Four different silicons were used for comparison of sensitivities as well as stability. Two of these silicon types were epitaxial to see if the characteristic change that had occurred was not due to the epitaxial layer diffusion process. Twice daily the potential across the diode at 50 μamps in the forward

and reverse direction was recorded. The variance in this potential versus time is plotted in Figure #31. Inspection of these shows the 0.0015" C-bend tungsten whisker to be of adequate stability for use in this type of diode.

With the change in the standard diodes a new power level detector had to be found. An F.X.R. Model Z325S Thermistor Power Detector Cartridge and Model F208A Detector Mount was purchased. To be used as an absolute power measuring detector the thermistor required calibration against a known absolute power detecting device such as a calorimeter. This calibration was performed at Lincoln Laboratories by means of the calorimeter mentioned previously in this report. The Thermistor sensitivity is comparable to that of the calorimeter. Power as indicated by the calorimeter is consistently 20% $\pm$ 5% below the best estimates of the true power level present.

To facilitate our testing of the detectors, a calibrated 2-millimeter wavelength attenuator was constructed as described in the appendix. With the use of the attenuator the power input to the harmonic generator could be kept constant at a level of most efficient doubler operation. The 140 kMc power output could instantly be varied without regard to the non-linear performance of the harmonic generator.

With the aid of the thermistor and the calibrated attenuator a 1 μwatt audio-modulated 2-millimeter power level was established. The new diodes were measured for open-circuit voltage and video resistance at both zero bias and forward biased conditions. As may be seen from Table IV the figure of merit was a maximum at approximately 20 μa of forward current. Three bias values of 0, +10 and +20 μa were selected as test conditions for the diodes. Table VI presents the video resistance and open circuit voltages of the diodes in Table V under the test conditions stated above. Diodes 6A

and 3B were lost due to a static discharge through the point contact. Diode #12 was forwarded to RADC as a Laboratory sample. Table VII presents the calculated figure of merit from the data in Table VI. 10 μa of bias resulted in a maximum figure of merit of 75.4.

A measure of diode sensitivity is "minimum detectable signal" (MDS). This can be defined as the microwave power which is required to produce an output power equal to the noise power. In other words, when a true r.m.s. power meter is placed at the output of the video amplifier, the MDS is the r-f power that must be applied to the crystal detectors so that the output power meter reading increases by 3 db.

The output signal-to-noise ratio is

$$\frac{E}{N} = \frac{P}{\sqrt{4KTB}} M \quad \text{(Eq 23 Chapter 11, Ref. \#5)}$$

where $$1 = \frac{(MDS)}{\sqrt{4KTB}} M \quad \text{by definition of (MDS)}$$

so that $$MDS = \frac{\sqrt{4KTB}}{M}$$

where K = Boltzmann's constant = 1.38×10^{-23} joules/^{o}K

T = 300 ^{o}K

B = Video bandwidth = 10 cps and is characteristic of typical tuned detectors

M = Zero bias figure of merit

$$MDS = \frac{\sqrt{4\ (1.38 \times 10^{-23})\ 300\ (10)}}{M}$$

$$MDS = \frac{4.07 \times 10^{-10}}{M} \text{ watts} = \frac{4.07 \times 10^{-7}}{M} \text{ mW}$$

$$MDS = (63.9 + 10 \log_{10} M) \text{ dbm at } 300^{o}K$$

For diode #11 Table VII, M = 46.5 Thus,

$$MDS = - (63.9 + \log_{10} 46.5) = -80.6 \text{ dbm} = 8.72 \times 10^{-12} \text{ watts}$$

This is a minimum detectable signal better than the contract goal of a 10^{-10} watts.

To further evaluate and characterize the diodes of Table V tests were conducted at below ambient temperatures. Both the video resistance and open circuit voltage were measured as the operating temperature of the diodes was lowered to -150°C. This temperature was obtained in the laboratory by cooling forming gas (80% nitrogen, 20% hydrogen) with liquid nitrogen and then passing the cooled gas over the diode. Before cooling, the gas was passed through a tube of desicant to remove water vapor to prevent icing. The diode was enclosed to prevent icing due to the freezing of the water vapor in the atmosphere when the forming gas was removed. A Chromel-Alumel thermocouple was attached to the body of the diode to monitor its temperature. By controlling the rate of flow of the gas the temperature of the diode could be maintained at any value between ambient and -150°C long enough for the desired electrical measurements to be taken. Figure #32 illustrates setup. Because this test could have destructive effects on the diodes, not all of the diodes of Table V were tested under these conditions. Tables VIII and IX present the figure of merit data at below-ambient temperatures. Because of the vast drop in the open circuit voltage output with decreasing temperature the power level was increased as indicated in the data. Figure #33 is a plot of the figure of merit of the diodes of Tables VIII and IX with temperature. Inspection of Figure #33 reveals a rather large deteriation in the figure of merit with decreasing tempterature. As may be seen in the data of Table VIII this decrease is proportional to the deteriation of open-circuit voltage output.

To determine independently the sensitivity of the diodes, Tangential Signal Sensitivity measurements were taken. The CW microwave power level @ 140 kMc was first determined by the thermistor. The klystron was then modulated with a 0.5 μsecond pulse generated by a General Radio Unit Pulser Type #1217-A. The reflector of the klystron power supply is repeaked so that all of the microwave power is contained in the output pulse. The pulse is then detected by the diode. The output from the diode is fed through a Tektronix wide band pre-amplifier type 121 into a Tektronix Type 541A oscillascope. The pulse-modulated microwave input power to the detector is then reduced by means of the 2 millimeter calibrated attenuator until the bottom of the detected pulse is tangential to the noise level of the diode. The level of the microwave input power under this condition, as determined by the attenuator setting and its original level, when related to a 1 milliwatt level is the Tangential Signal Sensitivity of the diode. Table X presents the Tangential Signal Sensitivity of these diodes under zero and forward biased conditions of 10 and 20 μamps. At zero bias a T.S.S. of 33.5 was measured and at 10 and 20 μa forward bias a T.S.S. greater than 35 dbm was measured. Diodes 6A, 3B and 12 were lost during this test due to a faulty connection in the biasing circuit of the test setup. These values of Sensitivity as measured on these 2-millimeter detectors compare favorably with existing 4-millimeter detectors.

Up till now the diodes were tested only as detectors. Their capabilities as mixers are also of interest. A fundamental limitation on the sensitivity of a microwave receiver employing a crystal mixer arises from the fact that in the frequency-conversion process not all of the available power in the r-f signal is converted into power at the intermediate frequency. This conversion loss is, therefore, a crystal property affecting its mixer performance.

In the measurement of the conversion loss of the crystals at 140 kMc, there are no standard crystals available to establish the basis of measurement.(6) The d-c incremental method of loss measurement is the method used to establish an absolute calibration of standard crystals. The equation for conversion loss may be written

$$Lo = \frac{g_b}{2Po\left(\frac{d\,I}{d\,P}\right)^2} \cdot \frac{4g_b \frac{\partial I}{\partial V}}{\left(gb + \frac{\partial I}{\partial V}\right)^2} \quad (I)$$

we may take Po to be the average power, P + 1/2 dP. $\partial I/\partial V$ is the i-f conductance of the converter under the conditions of measurement. If gb is equal to $\partial I/\partial V$, the factor

$$\frac{4gb \frac{\partial I}{\partial V}}{\left(gb + \frac{\partial I}{\partial V}\right)^2} \quad (II)$$

isunity and the loss is given by

$$Lo = \frac{gb}{2Po\left(\frac{dI}{dP}\right)^2} \quad (III)$$

This method is ordinarily used in fixed-tuned measurements and gb is chosen to be equal to the mean i-f conductance of the type of crystal to be measured. For any one crystal the factor (II) is generally less than unity but the error involved in using equation (III) instead of equation (I) is less than 1/2 db if

$$1/2\ gb < \frac{\partial I}{\partial V} < 2\ gb$$

For routine measurements the factor (II) is usually dropped, but it must be included in accurate work.

A schematic diagram of the circuit used in the measurement of loss is shown in Figure #34. The crystal is loaded by the 1K ohm resistance shunting the meter resistance of 1K ohms. The total load is 500 ohms and is approximately equal to gb. The current supplied by the battery balances out the crystal current

at some standard r-f power level P and makes the crystal current in the microammeter zero. The r-f power is then increased by dP, producing a change in rectified current which is indicated by the meter.

The loss is obtained from equation III by measurement of Po, dP and dI. gb is approximately 500 ohms. The change in current dI is directly indicated on the microammeter. The r-f power Po is measured with the thermistor and is a property of the apparatus only. The change in power dP is produced by a change in attenuation between the crystal and the r-f oscillator. This change is produced by the 2-millimeter calibrated attenuator. During the operation of this contract over 600 hours of use were placed on the DX151 klystron. This resulted in a 5 db drop in its output power which limited Po to 24 microwatts. At such a low level good mixer performance is not expected.

Diode #1B was tested and readjusted for maximum dI in an attempt to decrease the poor indicated conversion loss. A conversion loss of -46.6 db was obtained under these conditions. Table XI presents the results of these measurements. These conversion loss values are somewhat to be expected since existing 4-millimeter detectors were found to have a 20-25 db conversion loss.

An investigation was conducted to determine how the output noise temperature ratio of a 2 mm detector varied with forward bias and frequency. The unit was tested at various d-c forward bias levels. The test equipment consisted of a d-c bias circuit, a Millivac Model VS-64A preamplifier, and a Quan-Tech Model 303 Spectrum Analyzer. Figure #35 is a plot of noise temperature ratio (in db) vs forward bias measured at 40 Kc/S. Figure #36 shows the noise temperature spectra obtained at the indicated bias levels.

These results show that a low-frequency cutoff of 100 Kc/S or more is desirable if these diodes are used as biased video detectors; otherwise, sensi-

tivity calculations that have been given above for the unbiased detector are not affected, since there can be no I_F noise without bias.

E. CONCLUSIONS

The results show that a video detector at 2-millimeters may be fabricated in circular waveguide propagating the TE_{11}-mode. The results indicate that this form of construction results in diode sensitivities comparable to rectangular waveguide structures.

The whisker comparison tests and low temperature figure of merit tests indicate that further experiments should be carried out using the 0.0015" diameter "C"-bend tungsten whisker. The shape of the "C" bend may be modified to decrease the contact pressure and improve the mechanical stability.

SECTION III - CONCLUSIONS

The investigation conducted under this contract has been concerned primarily with the analysis, development and testing of a point contact video detector for use at millimeter wavelengths. Primary emphasis has been placed on the 140 Gc region of the spectrum, though the applicability of many of the techniques extends over a broader frequency range.

The solution of the electromagnetic equations for the case of the TE_{1n} waves in a circular guide was successfully applied to the design of millimeter wavelength detectors. Diodes were constructed in circular guide with sensitivities at 4.3 millimeters exceeding that of existing rectangular waveguide detectors. 2-millimeter wavelength detectors were constructed in circular guide which exhibited satisfactory sensitivities. A variety of crystal and whisker configurations were used, but the best results were ordinarily obtained with the Aluminum doped Silicon, "C" bend tungsten whisker combination. Various

changes in structure were also made to obtain better performance. The dumb bell type of shorting plunger proved to be the best design for lower losses and performance.

A Tangential Signal Sensitivity of -35 dbm at 10 μa bias was obtained. A figure of merit of 46.5 was obtained at zero bias and at +10 μa bias a maximum figure of merit of 75.4 was obtained. Calculations from the zero bias figure of merit resulted in a minimum detectable signal (MDS) of 8.72×10^{-12} watts. This exceeds the goal of a minimum detectable signal of 10^{-10} watts.

The low temperature measurements of figure of merit were much lower than those at ambient temperature. This may be explained by the ionization of the impurities in the Silicon. At room temperature, the thermal excitation energy of the elections is sufficient to ionize some of the impurity centers. As the temperature is decreased, thermal excitation energy is decreased and less and less carriers are ionized. This decrease in the fraction of ionized carriers decreases the conductivity of the semiconductor. Thus the decrease in the figure of merit measurements at below ambient temperatures is a result of the carriers being frozen out on the impurity centers and the conductivity being low.

REFERENCES

(1) Principles and Applications of Waveguide Transmission, George C. Southworth, D. VanNostrand Company, Chapter 5.

(2) Microwave Transmission Circuits, Volume 9, Radiation Laboratory Series, Edited by George L. Ragan, First Edition, McGraw-Hill, Section 8.8.

(3) Crystal Rectifiers, Volume 15, Radiation Laboratory Series, Torrey and Whitmer, McGraw-Hill, Section 10.6.

(4) Millimeter Wave Component Research, Final Report Contract AF19(604)-5475, Electronic Communications, Inc.

(5) Crystal Rectifiers, Volume 15, Radiation Laboratory Series, Torrey and Whitmer, McGraw-Hill, Page 346.

(6) Crystal Rectifiers, Volume 15, Radiation Laboratory Series, Torrey and Whitmer, McGraw-Hill, Section 7.4.

(7) Very High-Frequency Techniques, McGraw-Hill.

(8) Principles and Applications of Waveguide Transmission, George C. Southworth, D. VanNostrand Company, Page 275.

FIGURE 1

FIELD CONFIGURATIONS IN RECTANGULAR AND CIRCULAR GUIDE

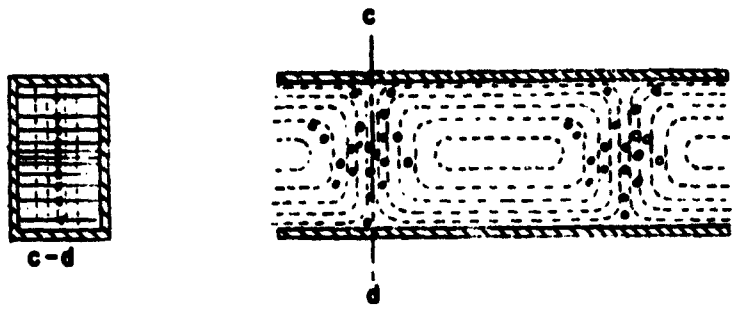

ORIENTATION OF LINES OF ELECTRIC AND MAGNETIC FORCE IN A DOMINANT (TE_{10}) WAVE IN A RECTANGULAR GUIDE.

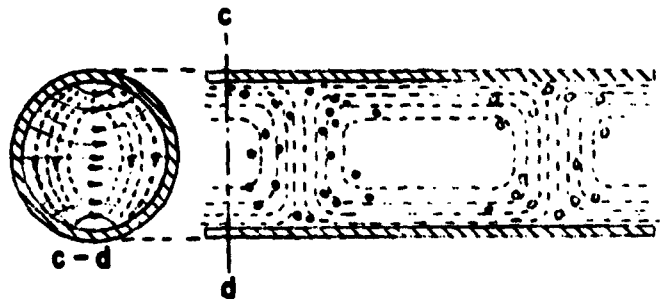

ORIENTATION OF LINES OF ELECTRIC AND MAGNETIC FORCE IN A DOMINANT (TE_{11}) WAVE IN A CIRCULAR GUIDE.

—— LINES OF ELECTRIC FORCE ---LINES OF MAGNETIC FORCE

•— TOWARD OBSERVER •— AWAY FROM OBSERVER

FIGURE 2

4.3 MILLIMETER CIRCULAR GUIDE DETECTOR

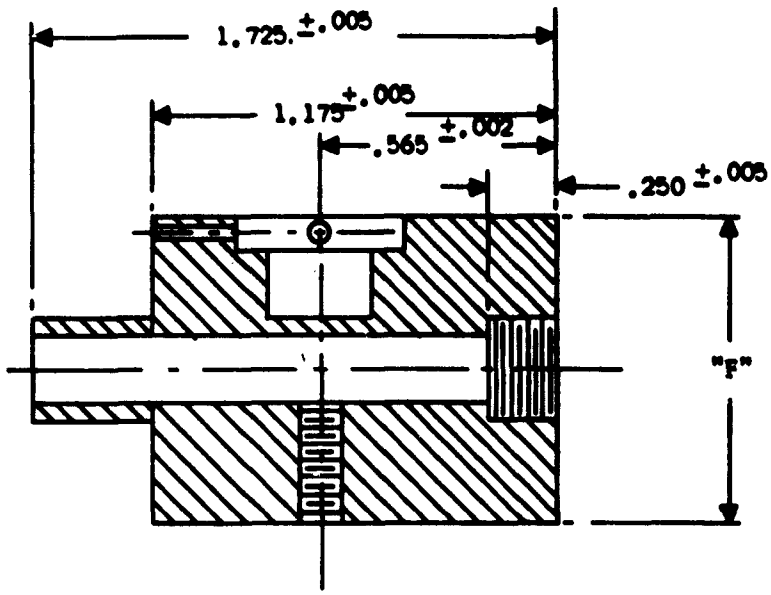

SECTION AA

MATERIAL:
BRASS

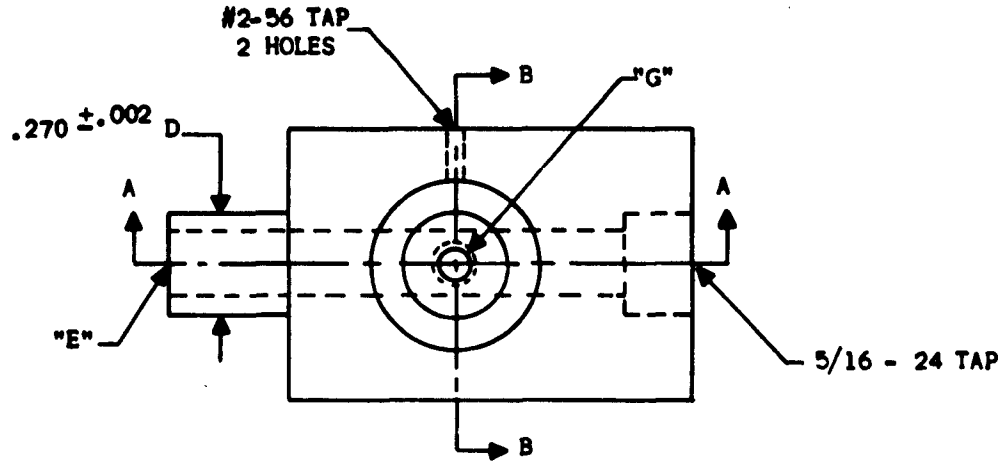

NOTE:
DIMENSION "E" IS TO BE CONCENTRIC WITH BOTH THE .270 ±.002 D. AND THE 5/16-24 TAPPED HOLE WITHIN ±.001.

FIGURE 3

4.3 MILLIMETER CIRCULAR GUIDE DETECTOR MOUNT

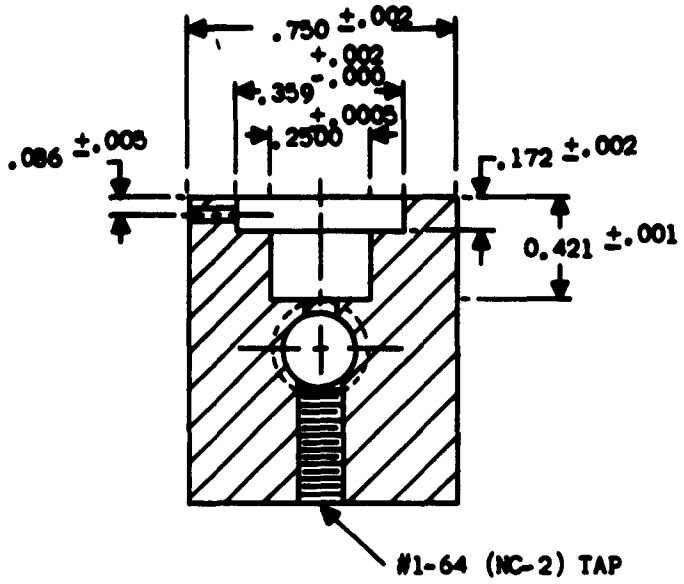

SECTION BB

DIM. / TYPE	E	F	G
1.	0.189 REAM	$1.082^{+.002}_{-.000}$	$0.050 \pm .001$ DIA.
2.	0.125 REAM	$1.018^{+.002}_{-.000}$	$0.050 \pm .001$ DIA.
3.	0.070 REAM	$0.963^{+.002}_{-.000}$	$0.020 \pm .001$ DIA.
4.	0.090 REAM	$0.983^{+.002}_{-.000}$	$0.020 \pm .001$ DIA.
5.	0.0625 REAM	$0.956^{+.002}_{-.000}$	$0.020 \pm .001$ DIA.

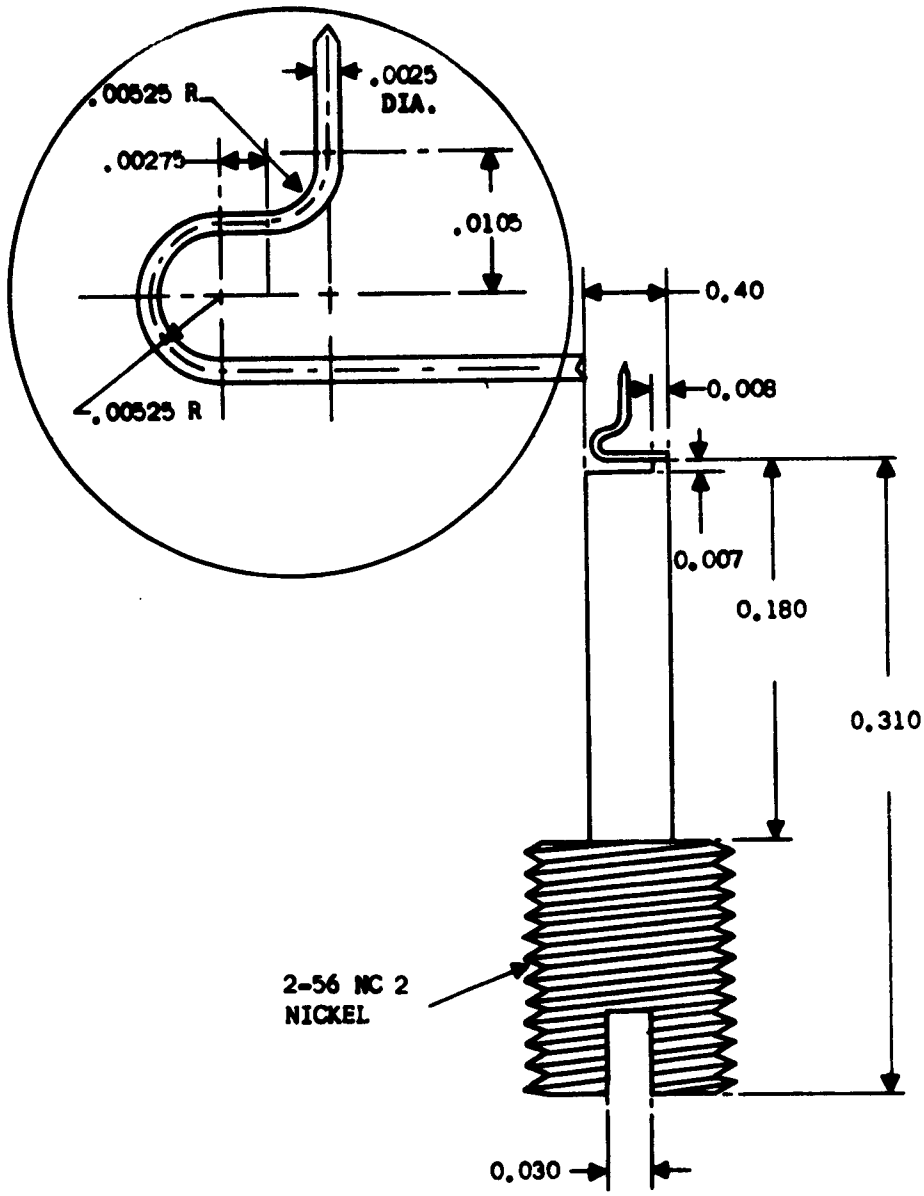

FIGURE 4

"C"-BEND WHISKER AND SCREW SUB-ASSEMBLY

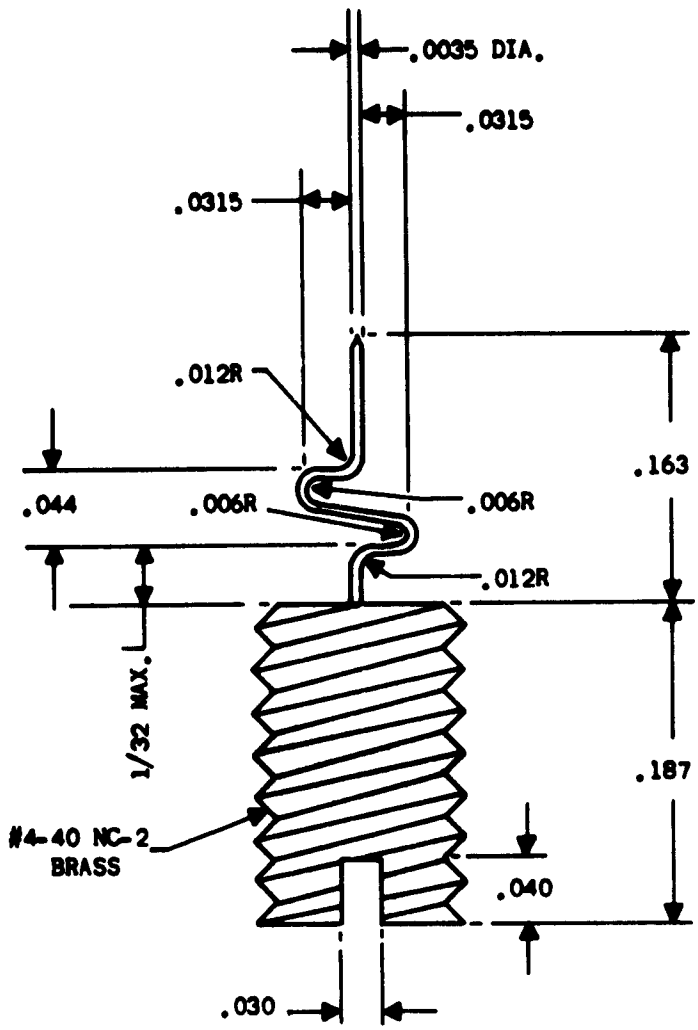

NOTES:

1. CONCENTRICITY - .012 T.I.R. (WHISKER TO SCREW)
2. ALIGNMENT OF TOP & BOTTOM LEGS - .010 T.I.R.

FIGURE 5

"S"-BEND WHISKER AND SCREW SUB-ASSEMBLY

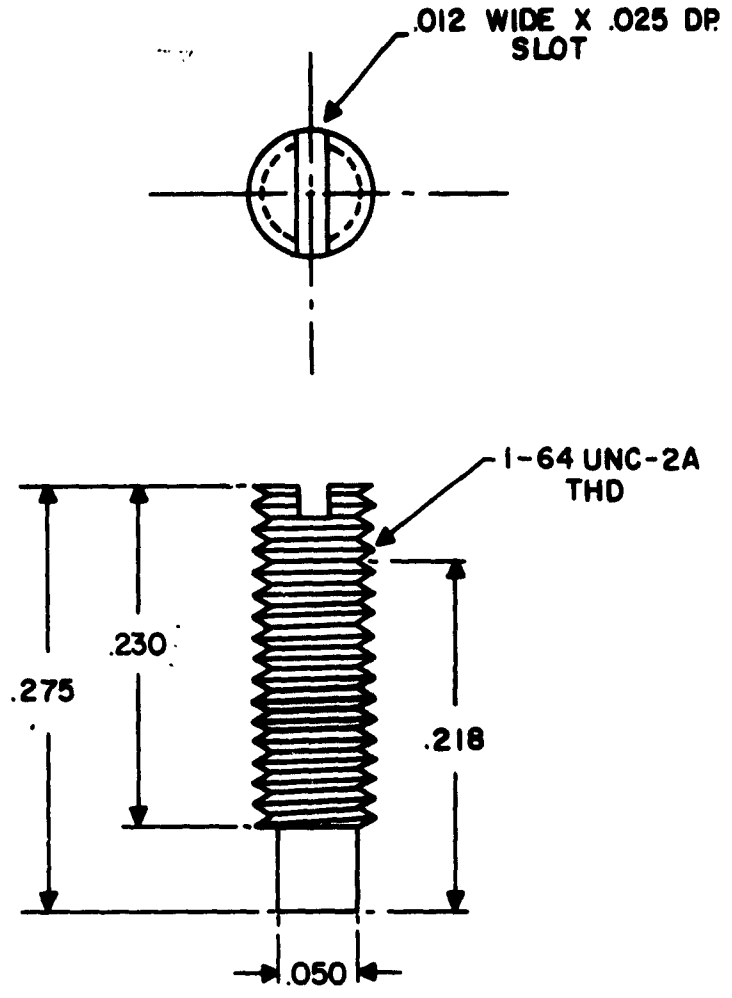

MATERIAL:
BRASS

FIGURE 6

SILICON SCREW

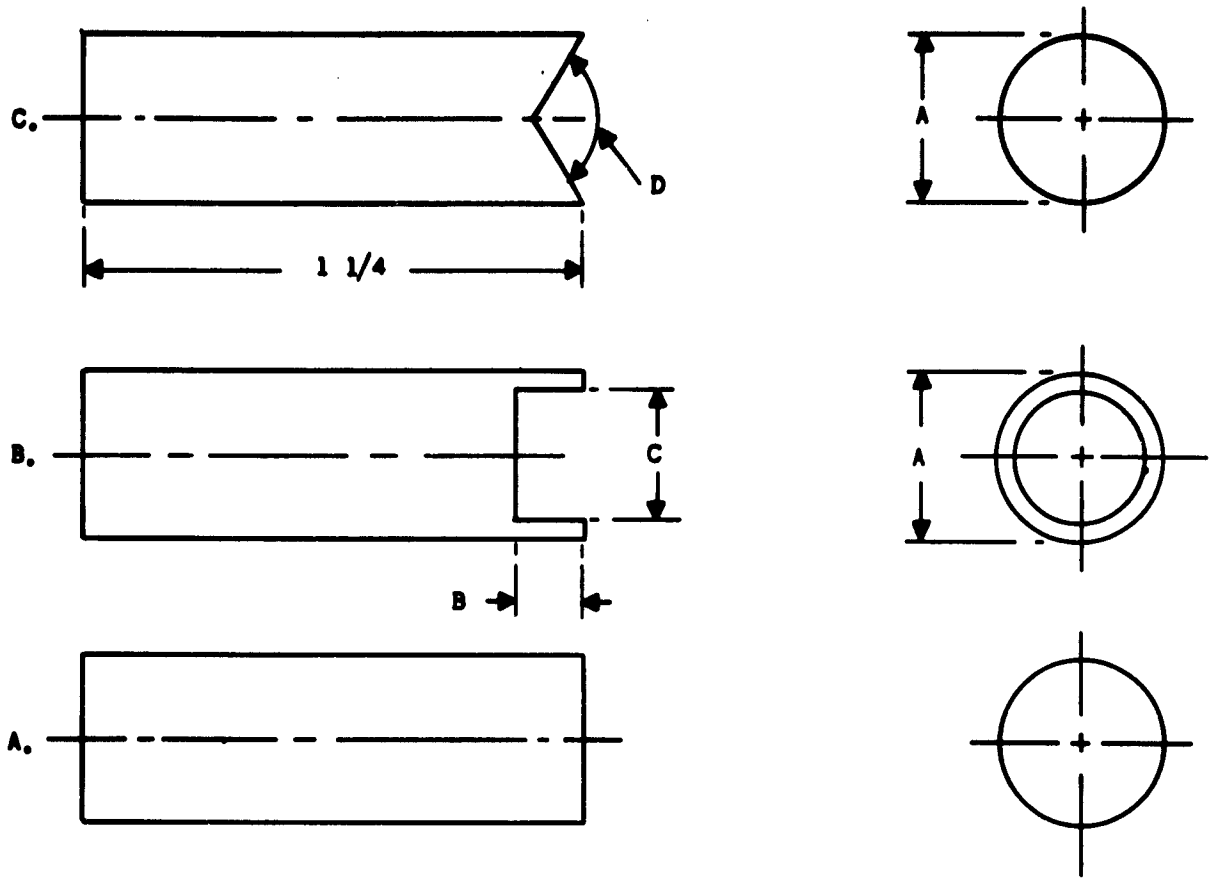

DIM. / TYPE	A	B	C	D
1	.189	.100	.150	DRILL TAPER #12
2	.125	.138	.090	DRILL TAPER 1/8

MATERIAL:
BRASS

FIGURE 7, A, B, C, D

CIRCULAR GUIDE SHORTS

D.

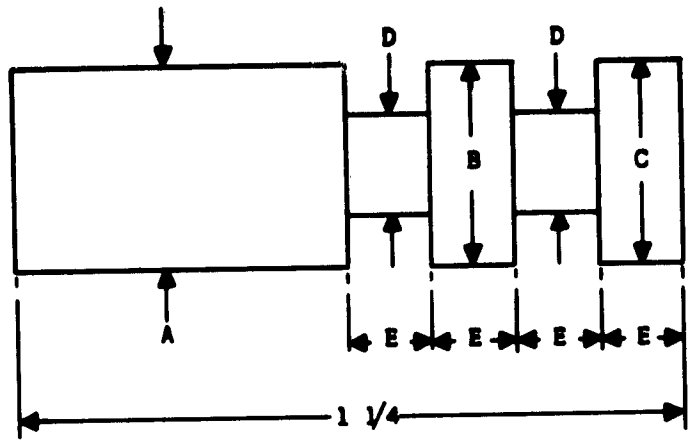

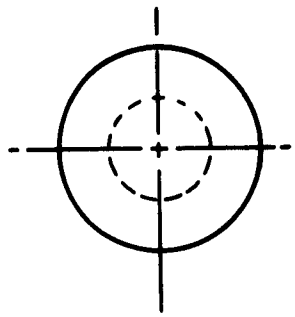

TYPE	A	B	C	D	E
1	.1875	.175	.170	.090	.050
2	.1225	.110	.105	.050	.069

MATERIAL:
BRASS

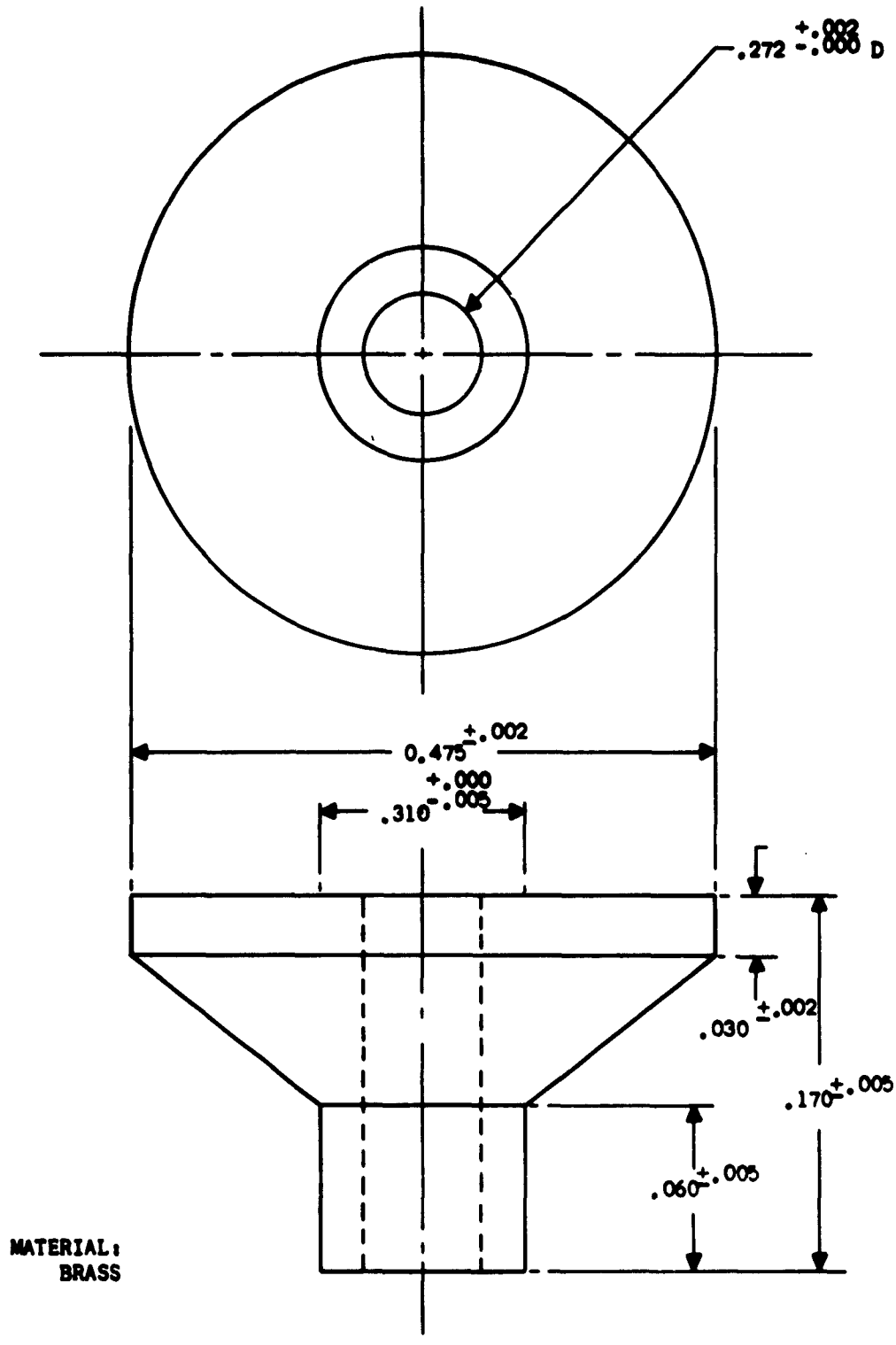

FIGURE 8

FLANGE

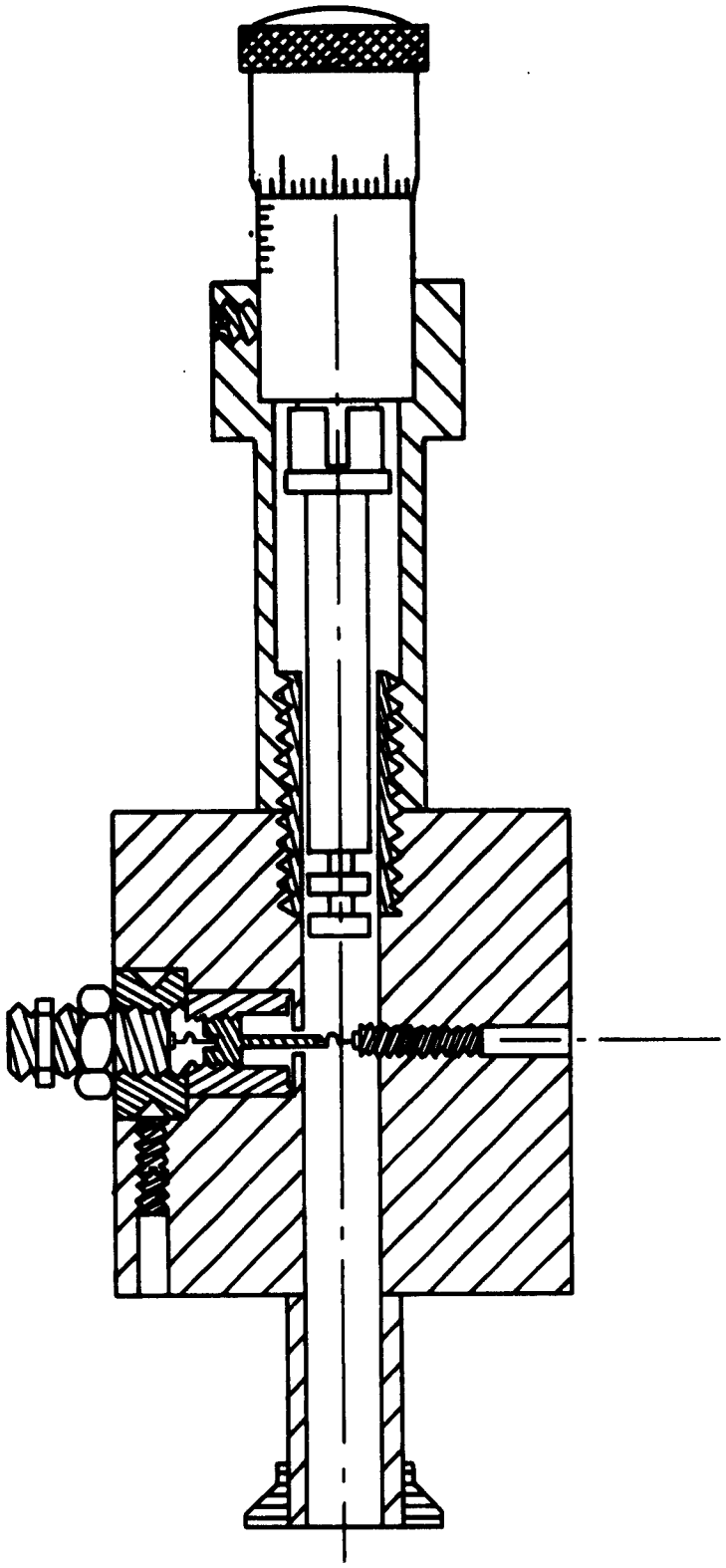

FIGURE 9

4 MILLIMETER DIODE ASSEMBLY

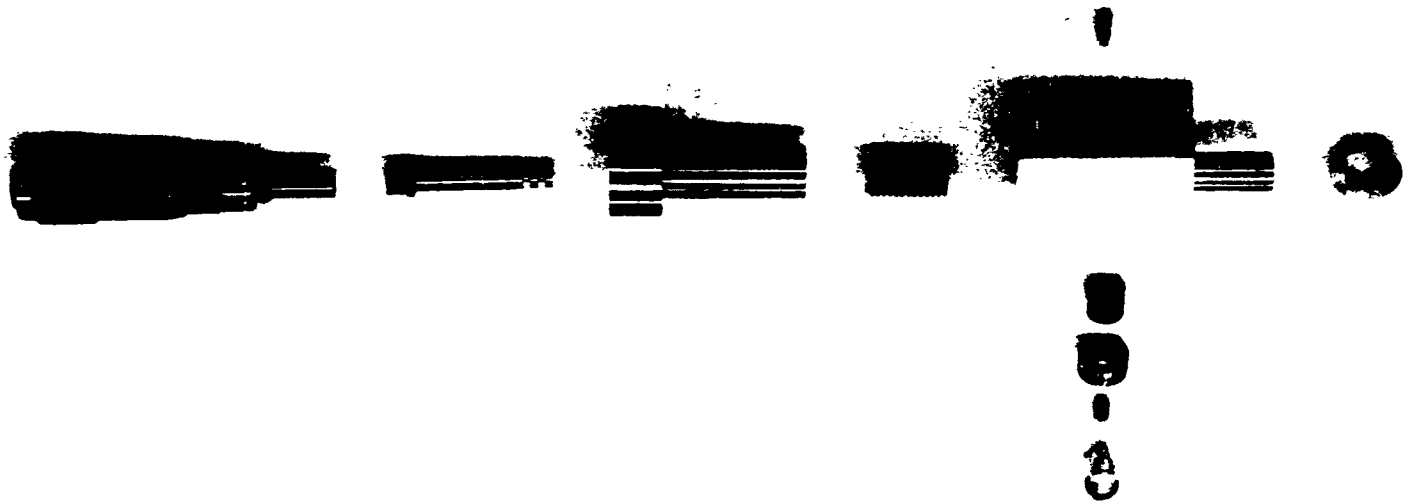

FIGURE 10

EXPLODED VIEW 4 MILLIMETER VIDEO DETECTOR

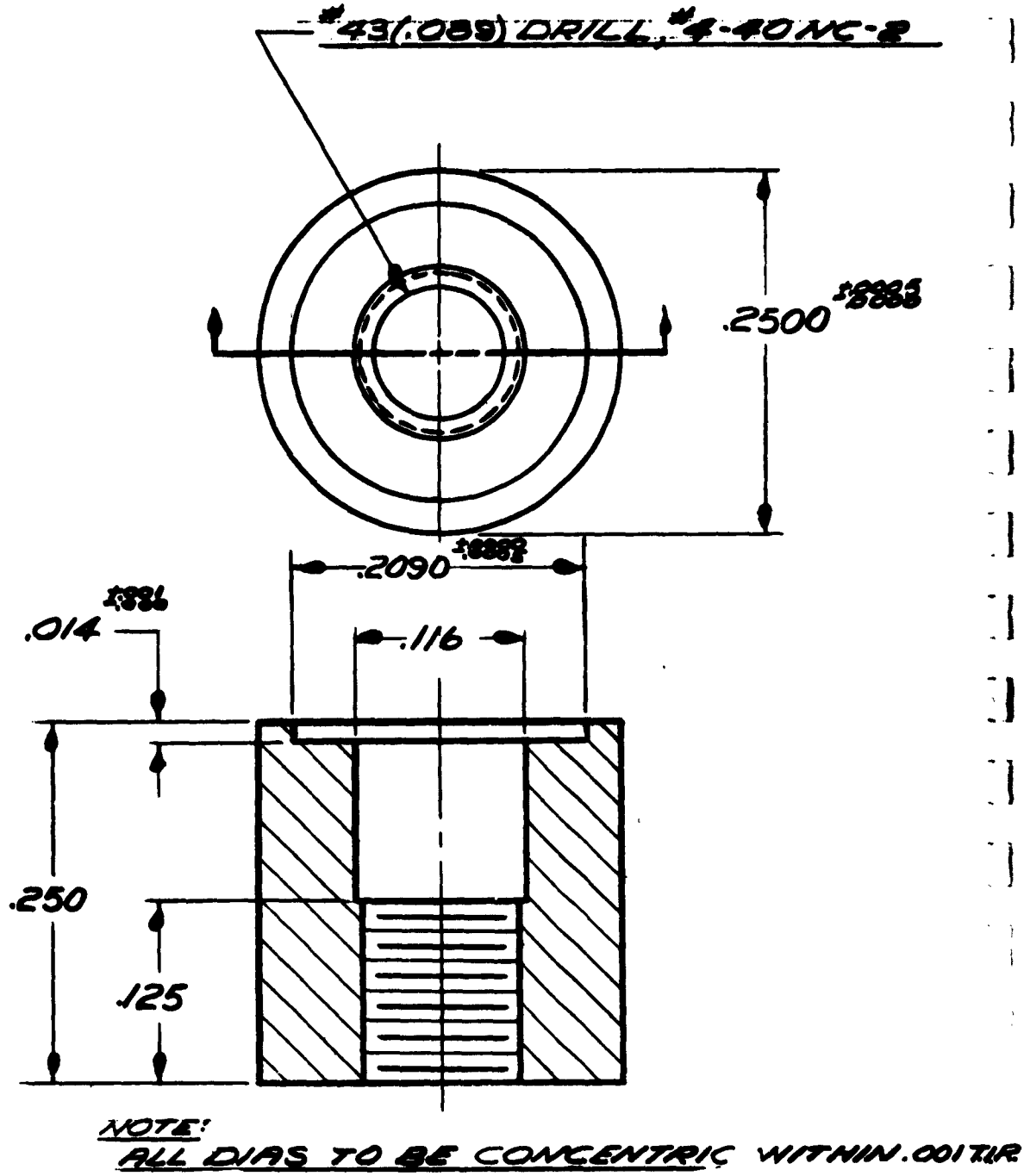

FIGURE 11

BUSHING

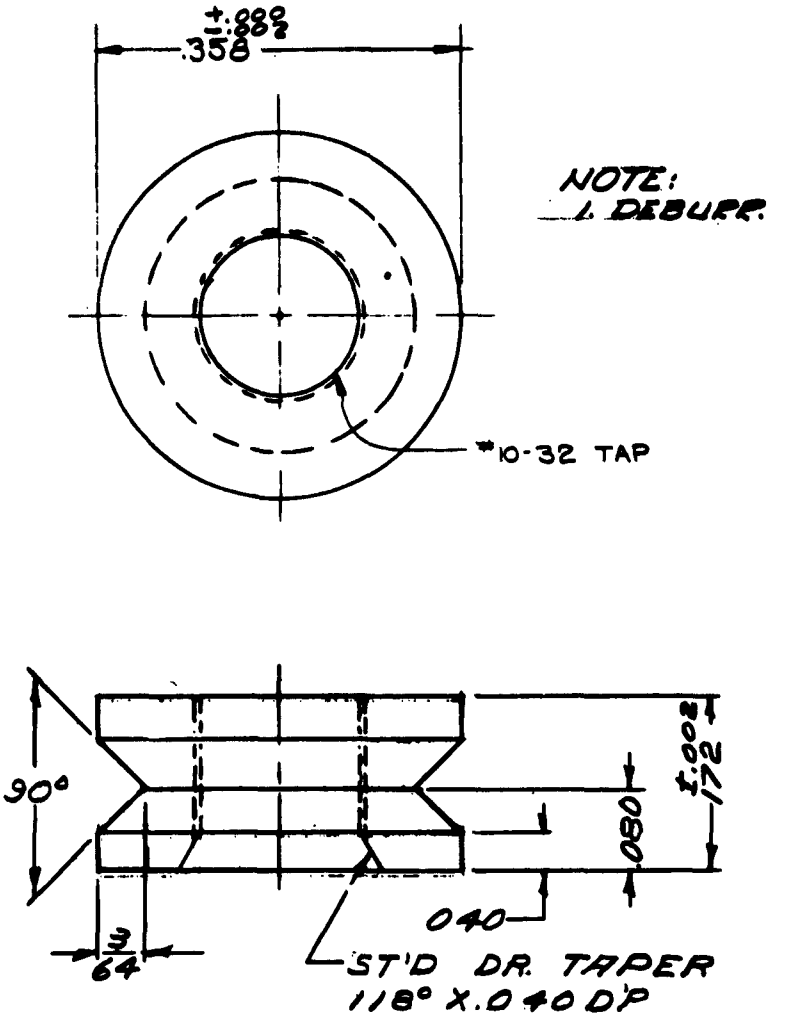

FIGURE 12

PLUG

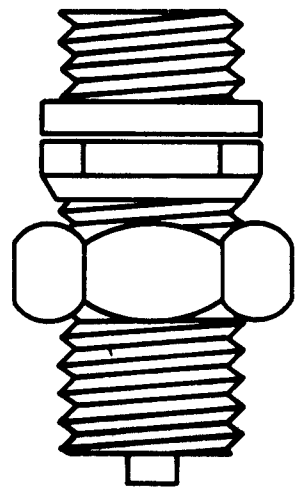

FIGURE 13

MICRODOT BULKHEAD RECEPTACLE

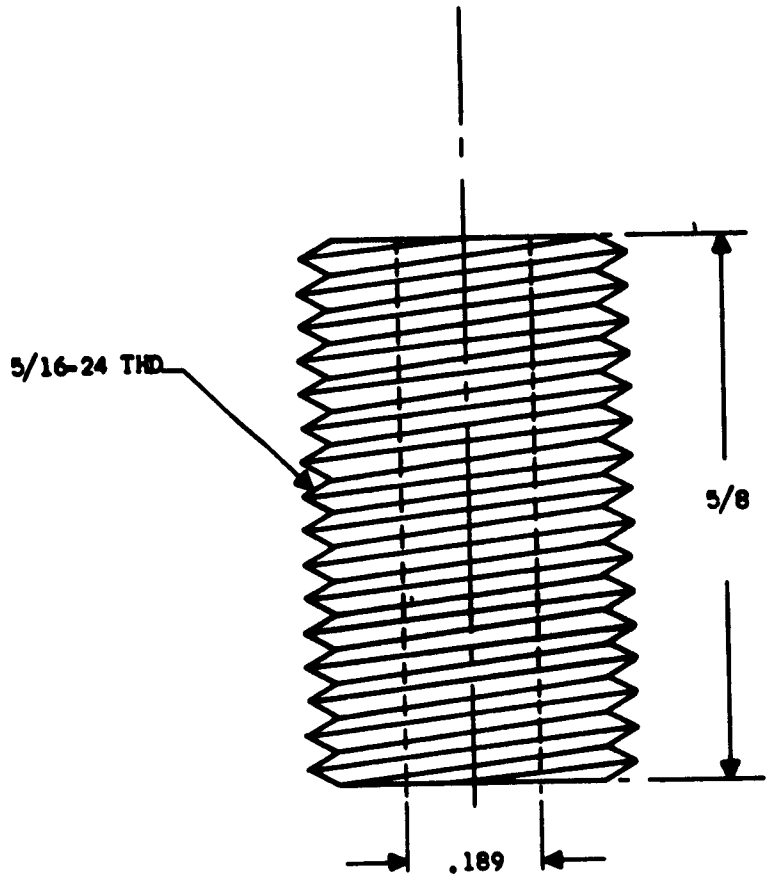

MATERIAL:
BRASS

FIGURE 14

ADAPTOR COUPLING

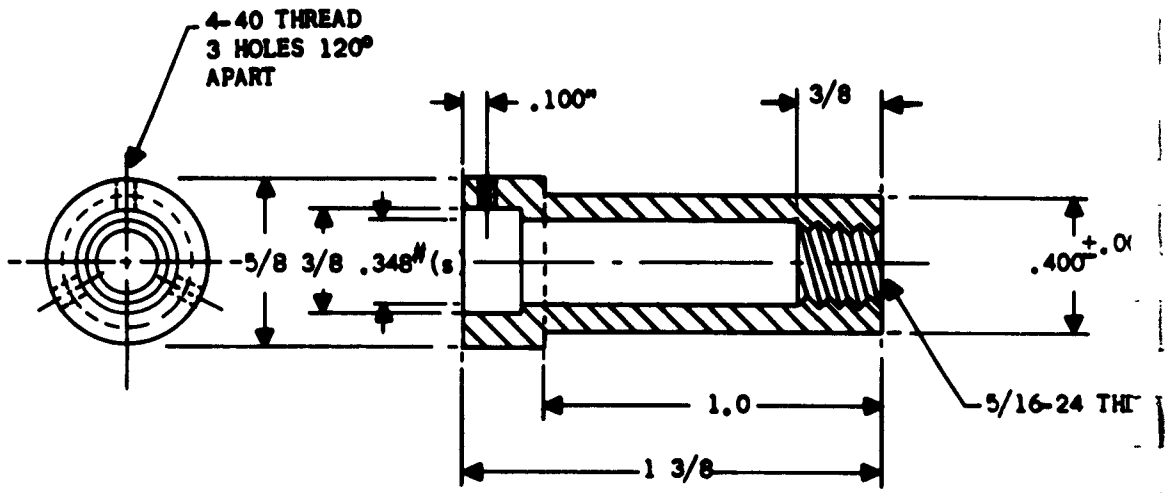

MATERIAL:
BRASS

FIGURE 15

SHORT ADAPTOR

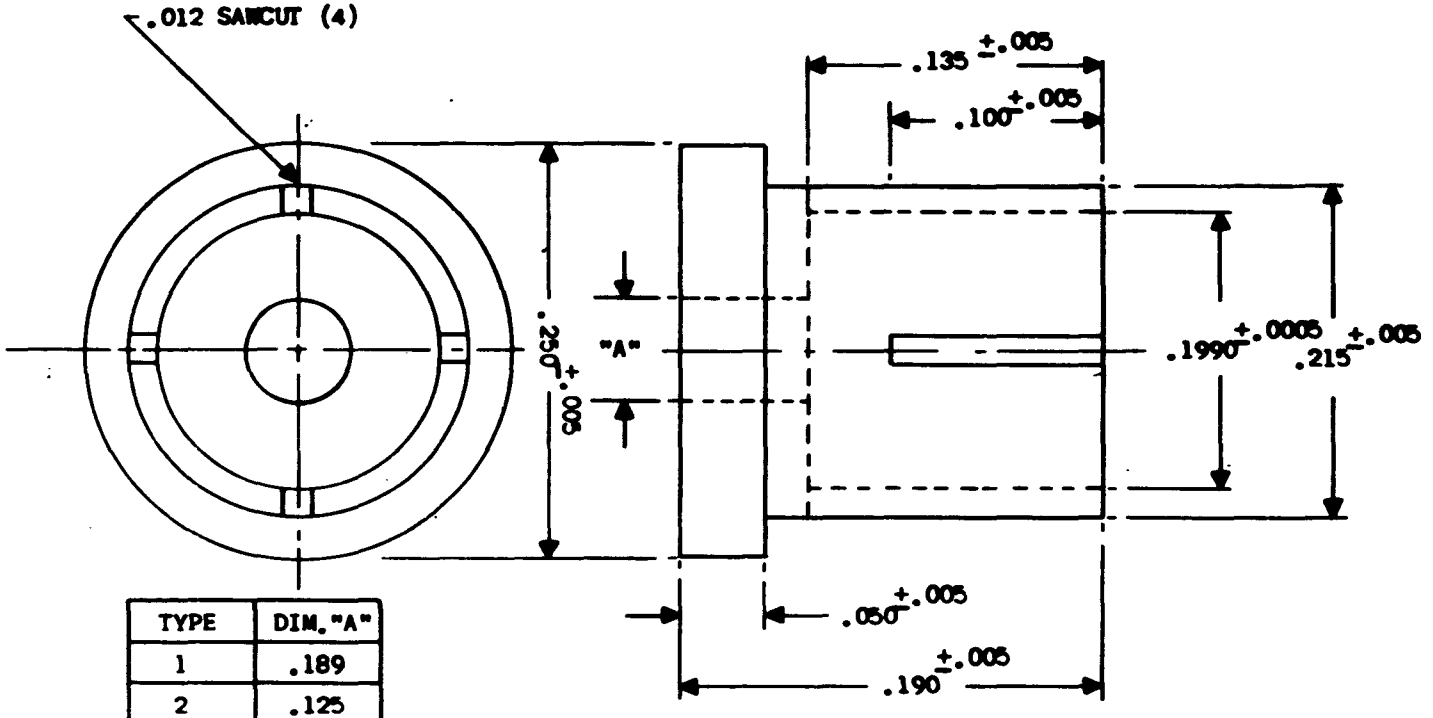

TYPE	DIM. "A"
1	.189
2	.125
3	.070
4	.090
5	.0625

MATERIAL:
BERYLLIUM COPPER

FIGURE 16

SHORT HOLDER

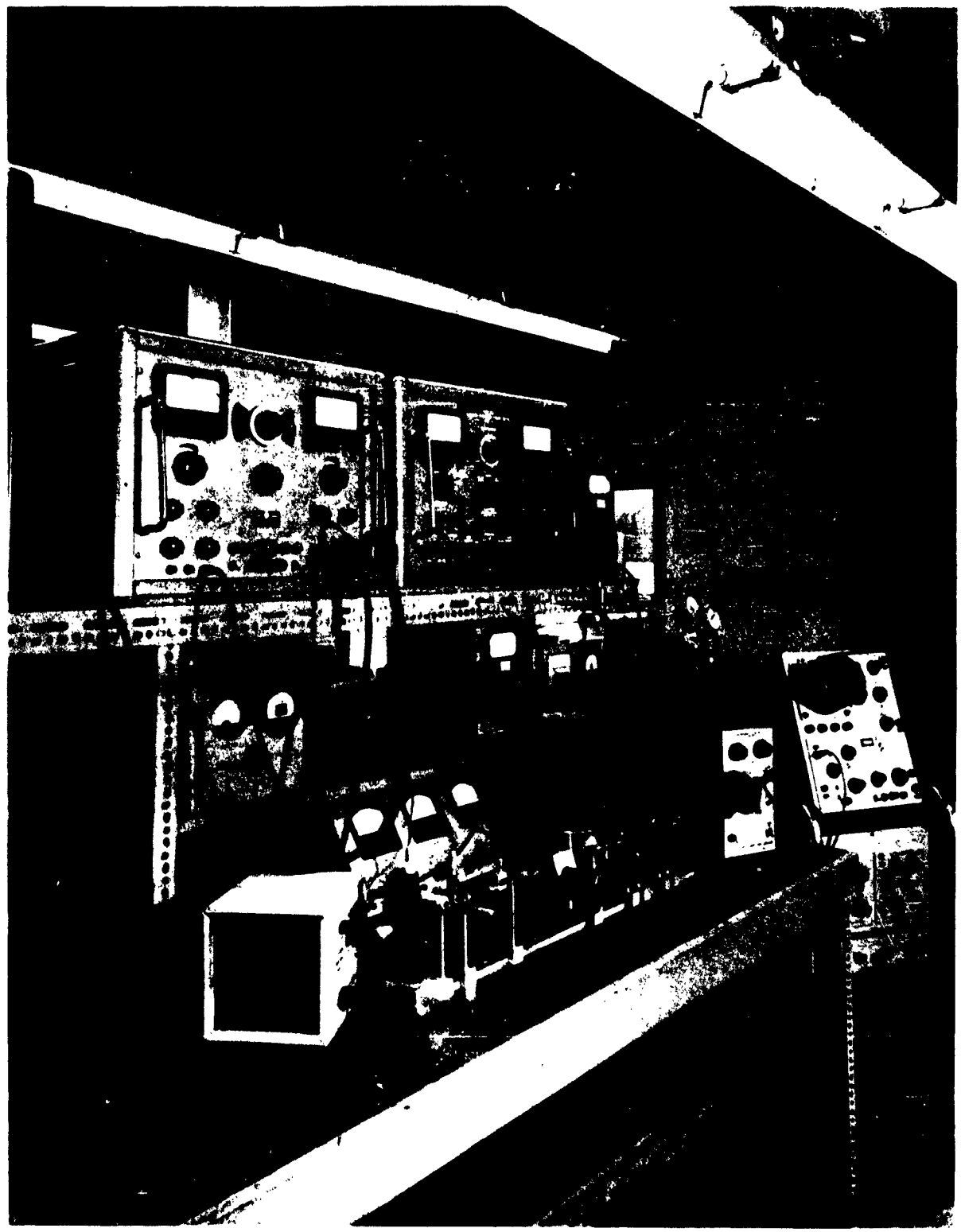

FIGURE 17

D-110

4 AND 2 MILLIMETER TEST EQUIPMENT

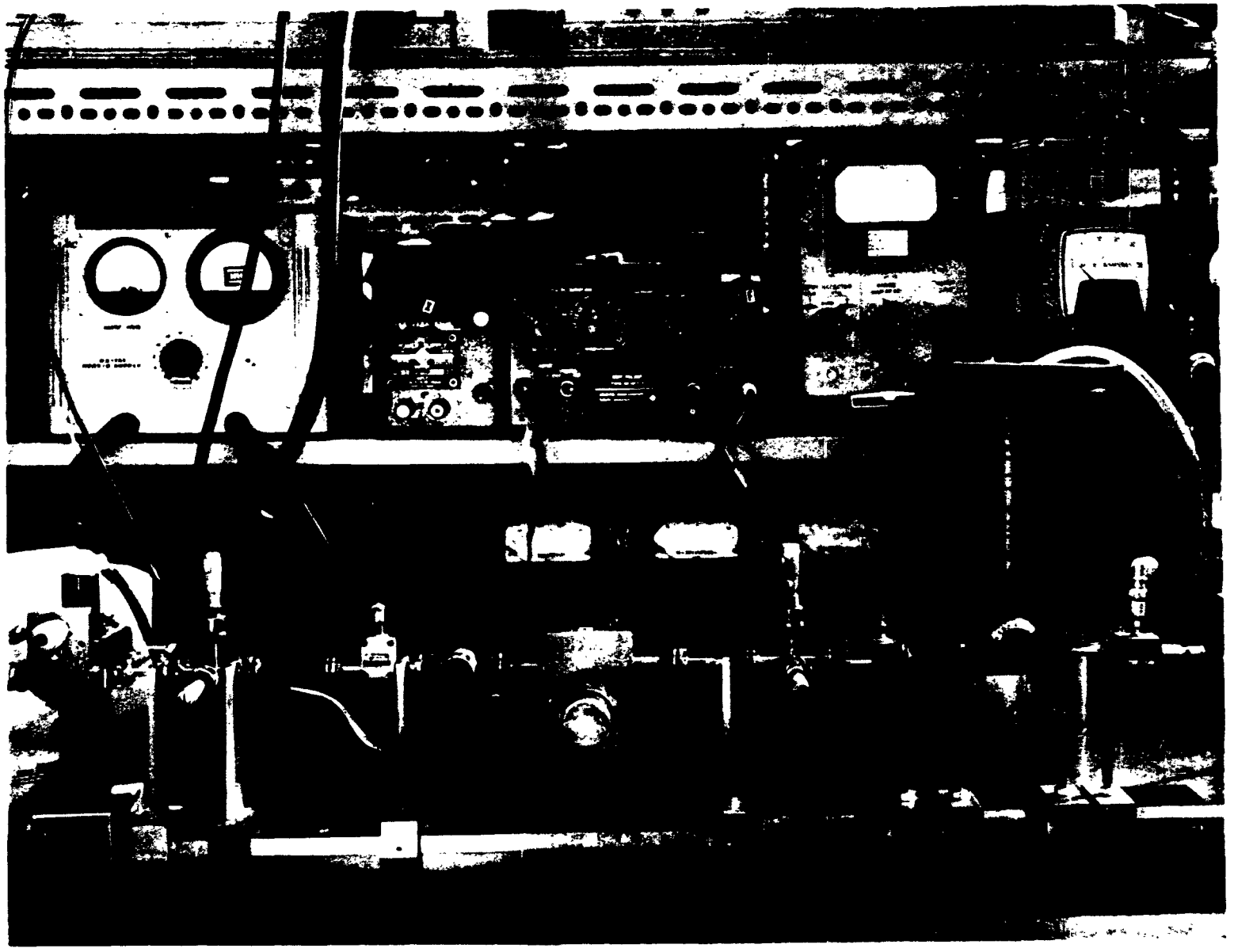

FIGURE 18

4 AND 2 MILLIMETER TEST KIT

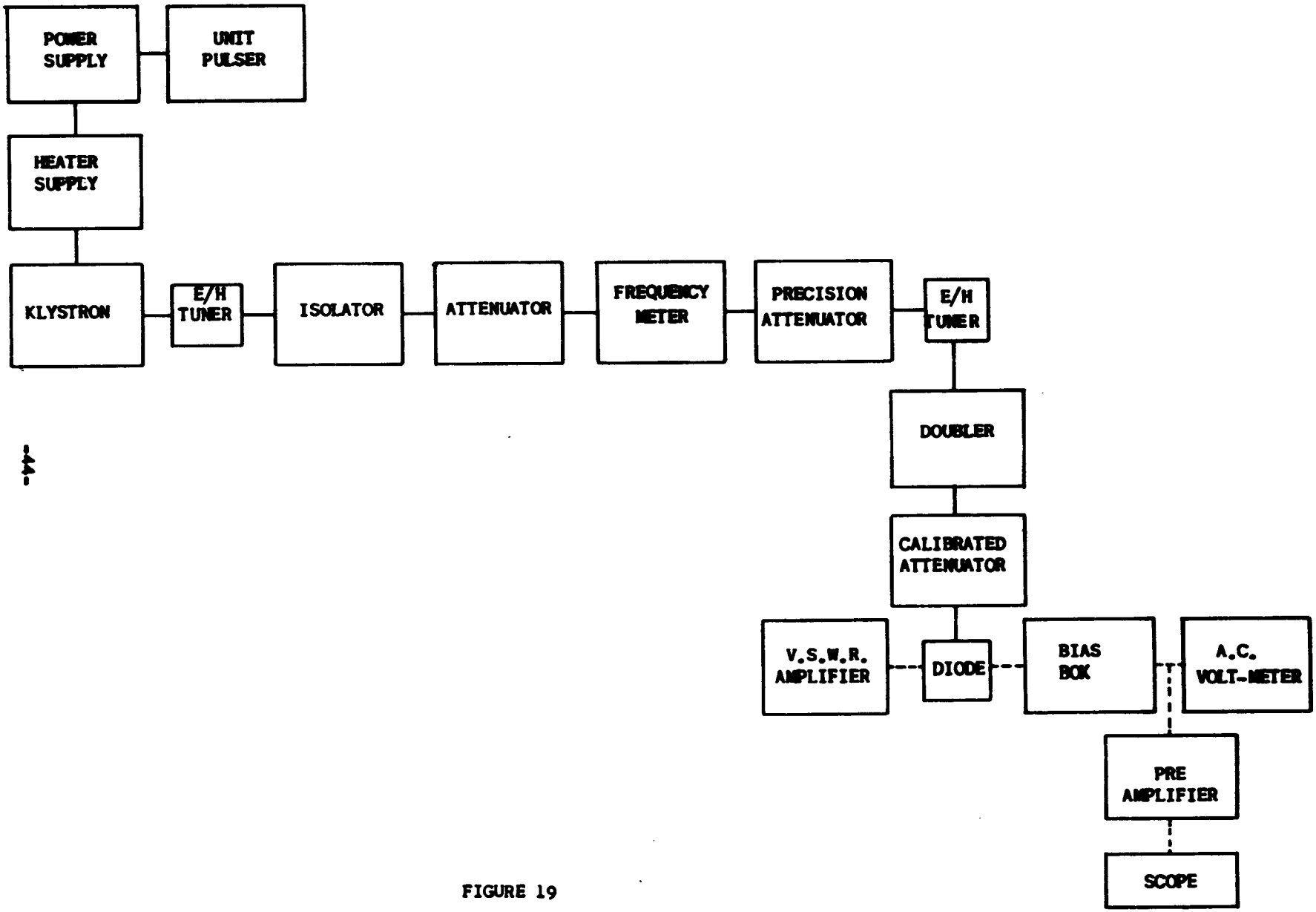

FIGURE 19

4 AND 2 MILLIMETER TEST KIT BLOCK DIAGRAM

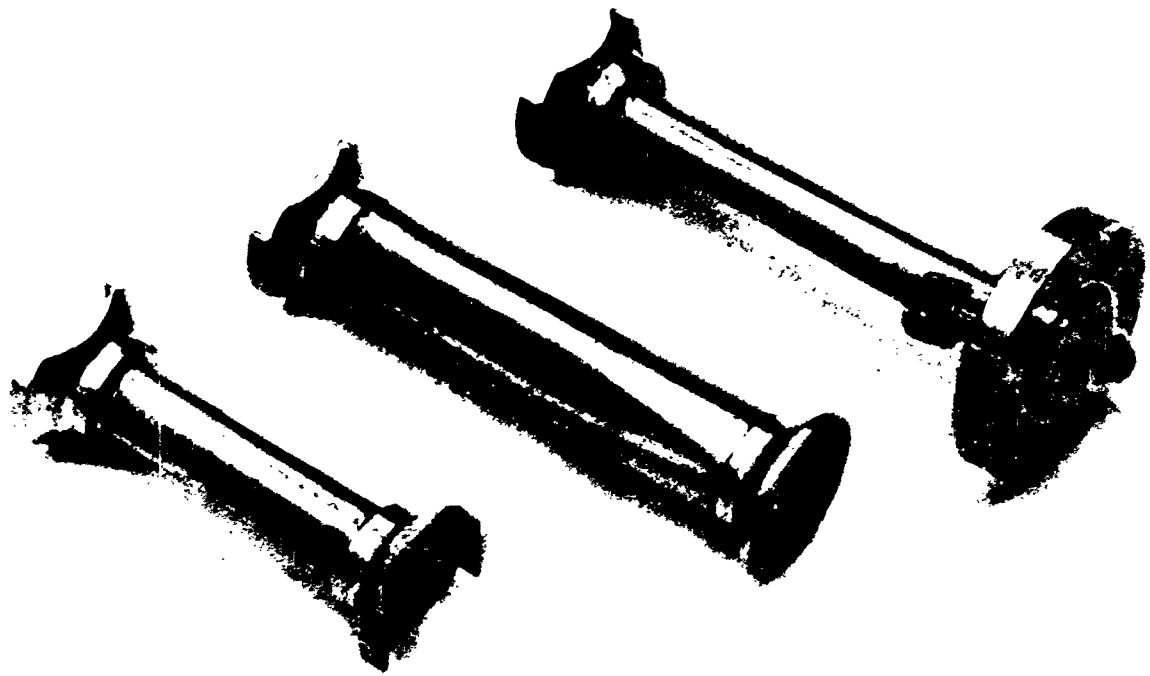

FIGURE 20

WAVEGUIDE TRANSISTIONS

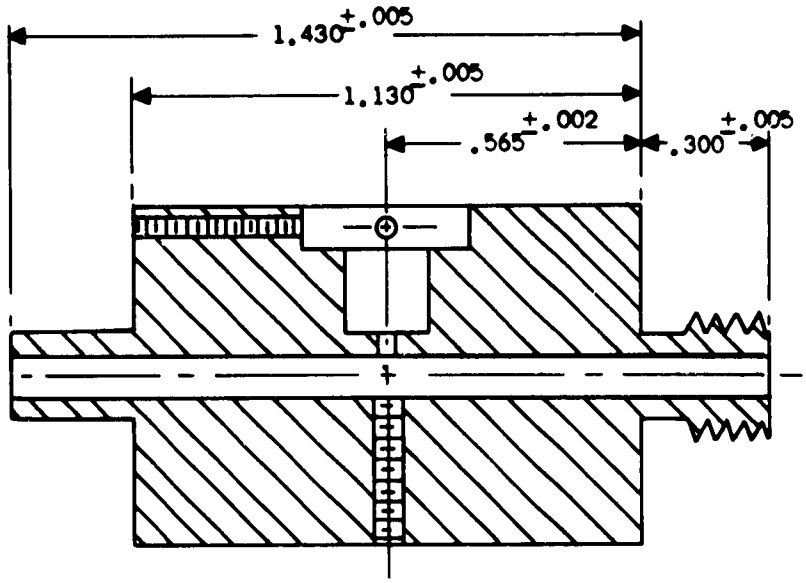

SECTION AA

MATERIAL:
BRASS

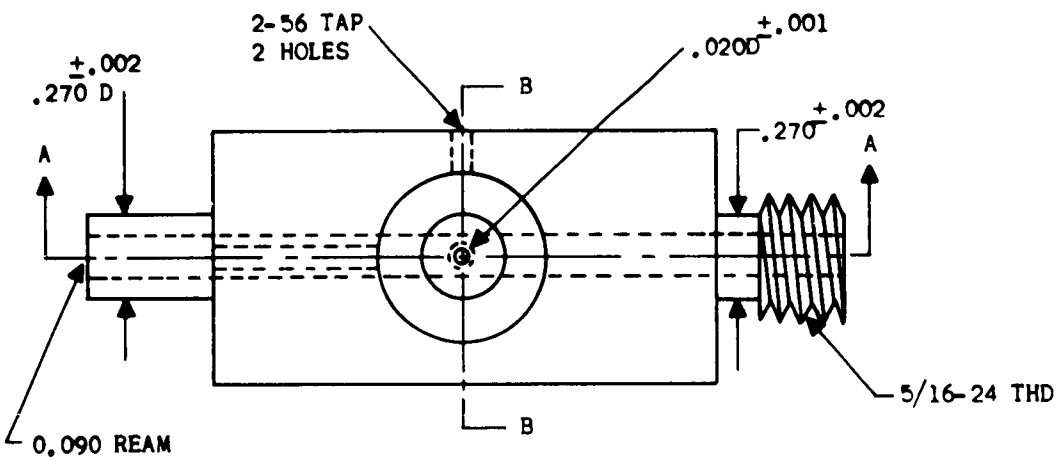

NOTE:
ALL DIAMETERS TO BE CONCENTRIC WITHIN ±.001

FIGURE 21

2 MILLIMETER DETECTOR MOUNT (1st)

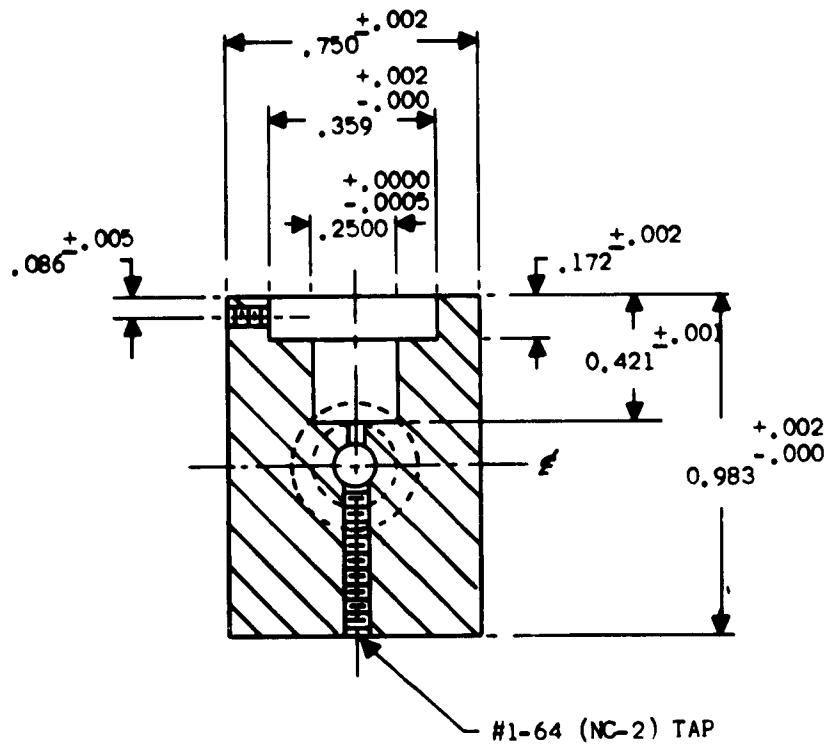

SECTION BB

1 114

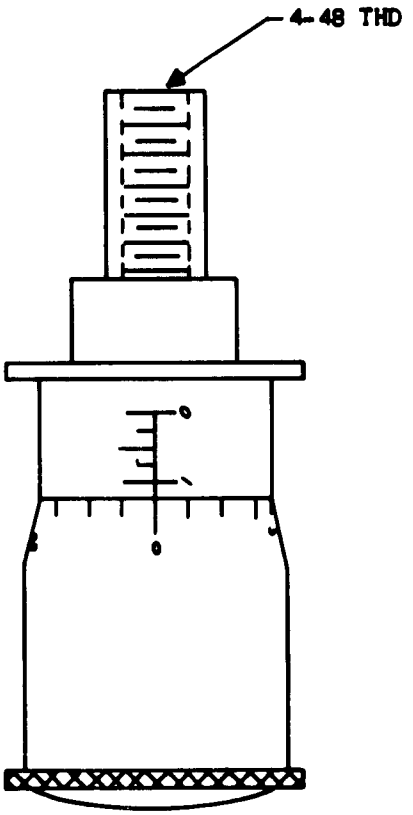

FIGURE 22

MICROMETER DRIVE

	140	100
A	.0254	.0460
B	.165D	.165D
C	.0770D	.0770D
D	.0750D	.0750D
E	.0350D	.0350D

MATERIAL:
BRASS

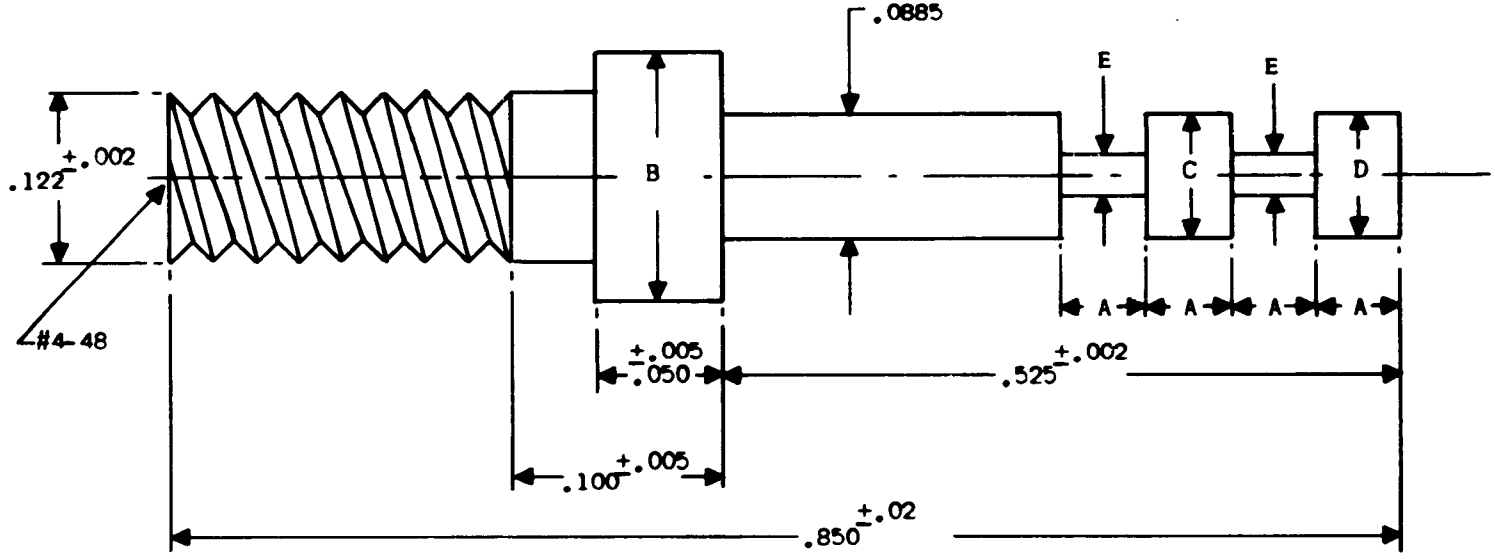

FIGURE 23

2 MILLIMETER DUMB BELL SHORT

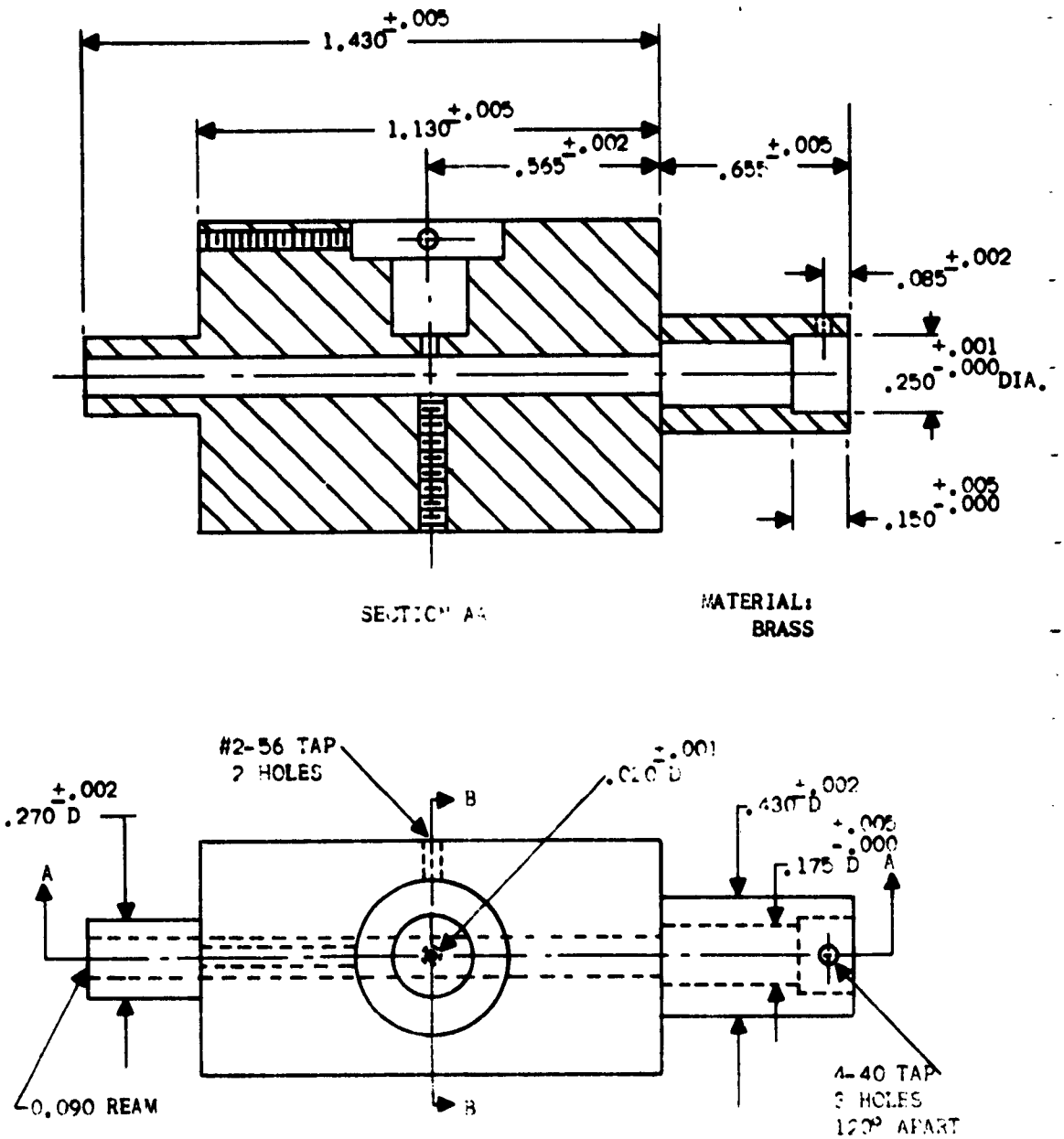

NOTE:
ALL DIAMETERS TO BE CONCENTRIC WITHIN ±.001

FIGURE 24

2 MILLIMETER DETECTOR MOUNT (2nd)

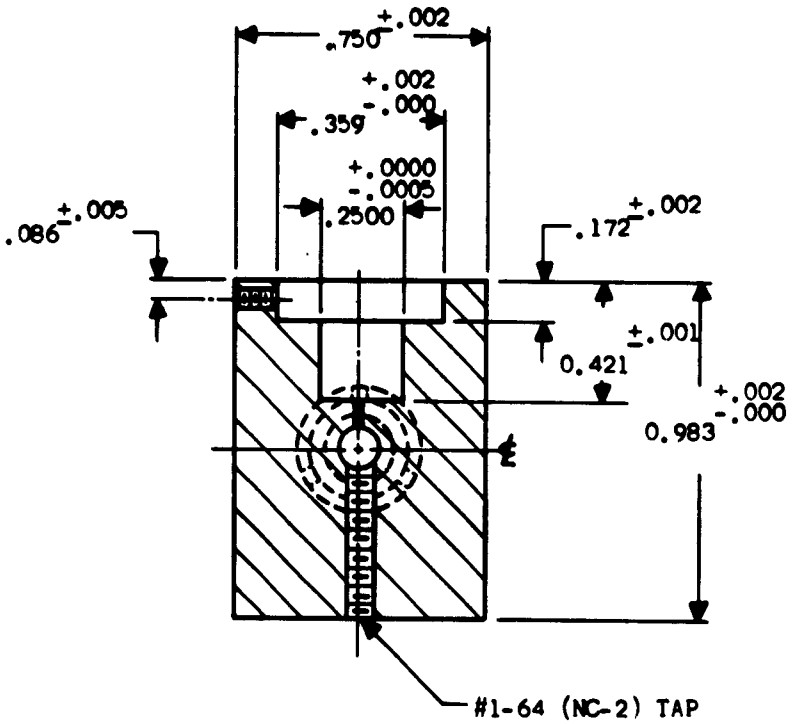
.750 +.002
+.002
.359 -.000
+.0000
-.0005
.2500
.086 ±.005
.172 ±.002
±.001
0.421
+.002
0.983 -.000
#1-64 (NC-2) TAP

SECTION BB

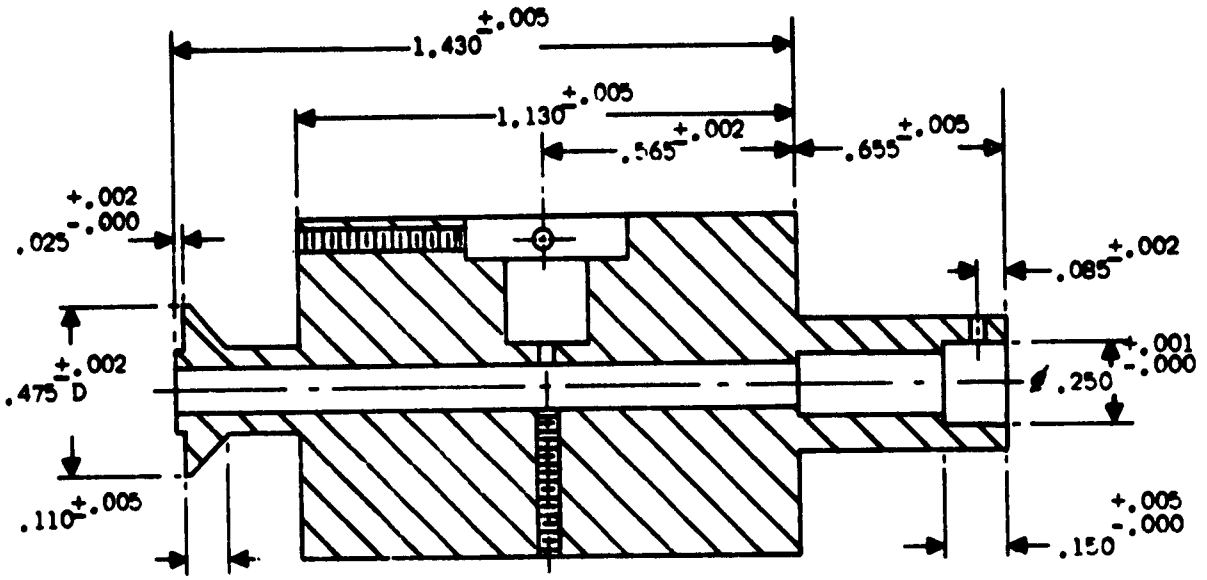

SECTION AA

MATERIAL:
BRASS

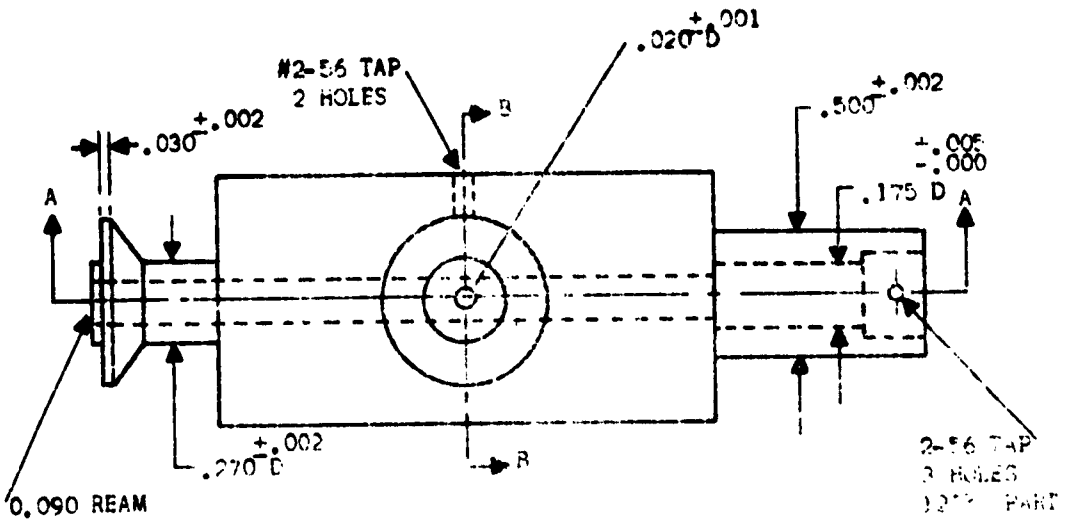

NOTE:
ALL DIAMETERS TO BE CONCENTRIC WITHIN ±.001

FIGURE 25A

FINAL 2 MILLIMETER DETECTOR MOUNT

FIGURE 25B

2 MILLIMETER VIDEO DETECTOR

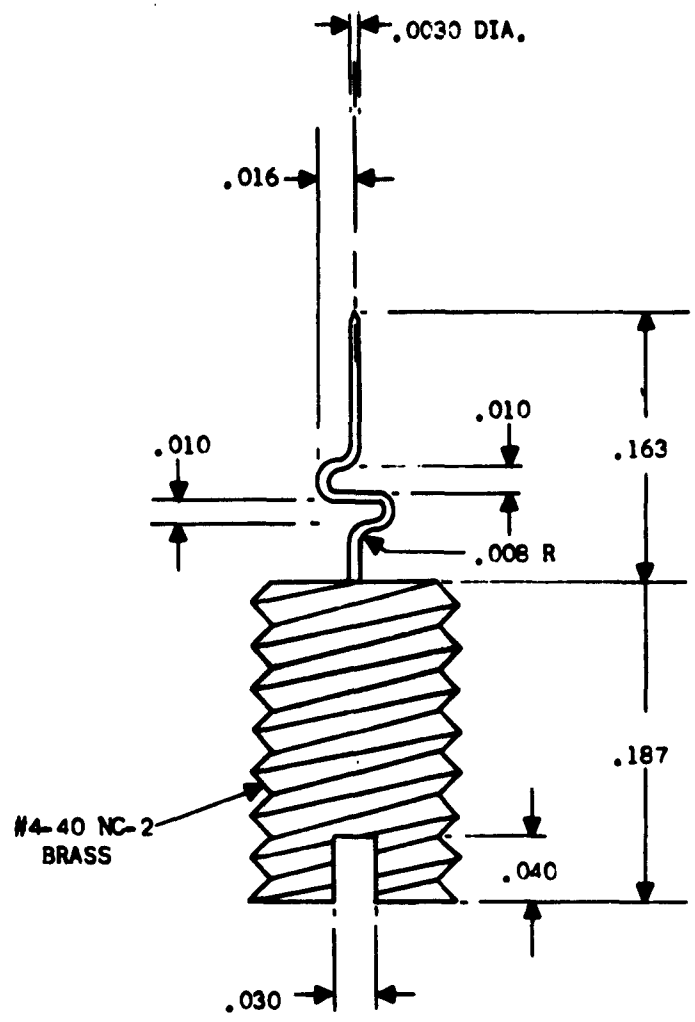

NOTES:

1. CONCENTRICITY -.012 T.I.R. (WHISKER TO SCREW)
2. ALIGNMENT OF TOP & BOTTOM LEGS -.010 T.I.R.

FIGURE 26

SHORT AMPLITUDE "S"-BEND WHISKER AND SCREW SUB-ASSEMBLY

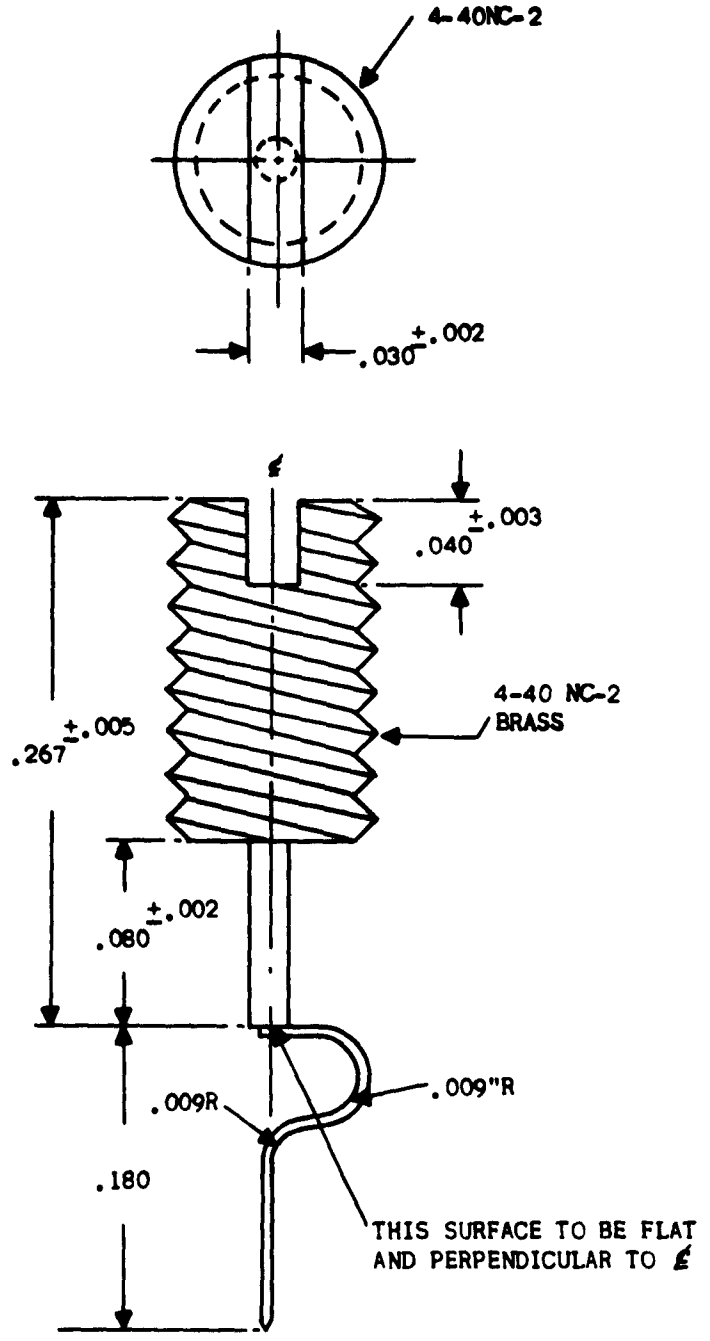

FIGURE 27

0.0015" "C"-BEND WHISKER AND SCREW SUB-ASSEMBLY

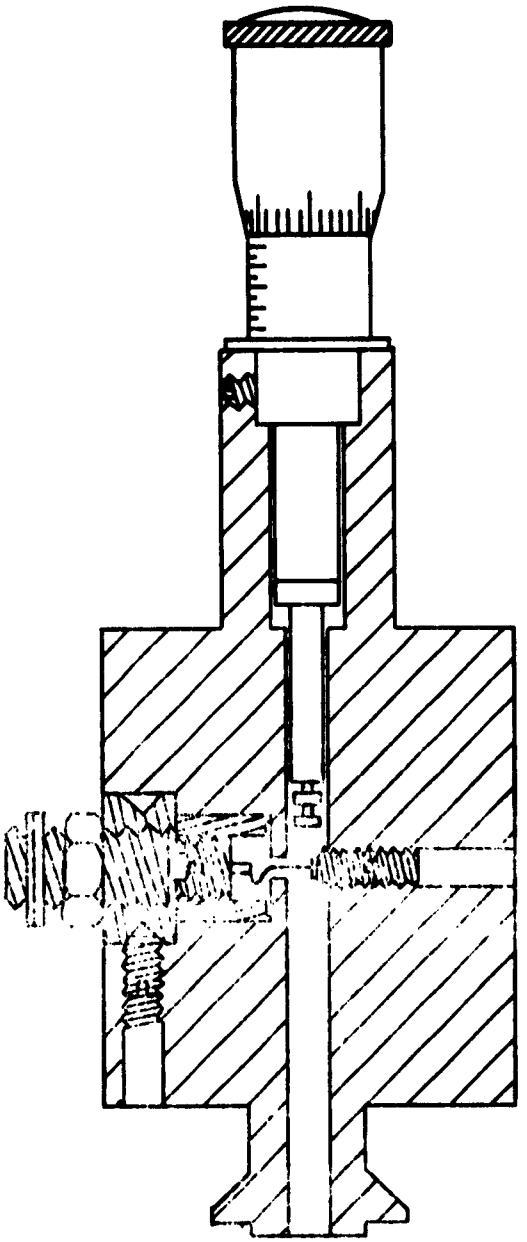

FIGURE 28

2 MILLIMETER DIODE ASSEMBLY

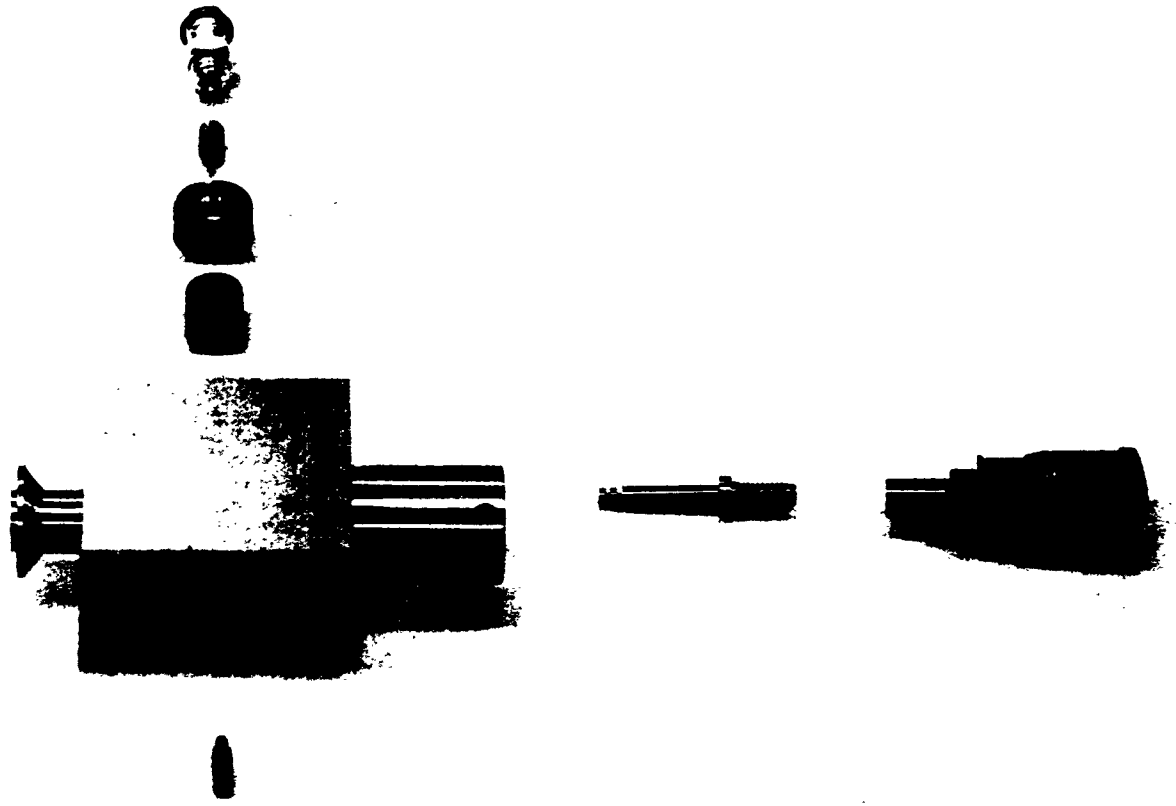

FIGURE 29

EXPLODED VIEW 2 MILLIMETER DETECTOR

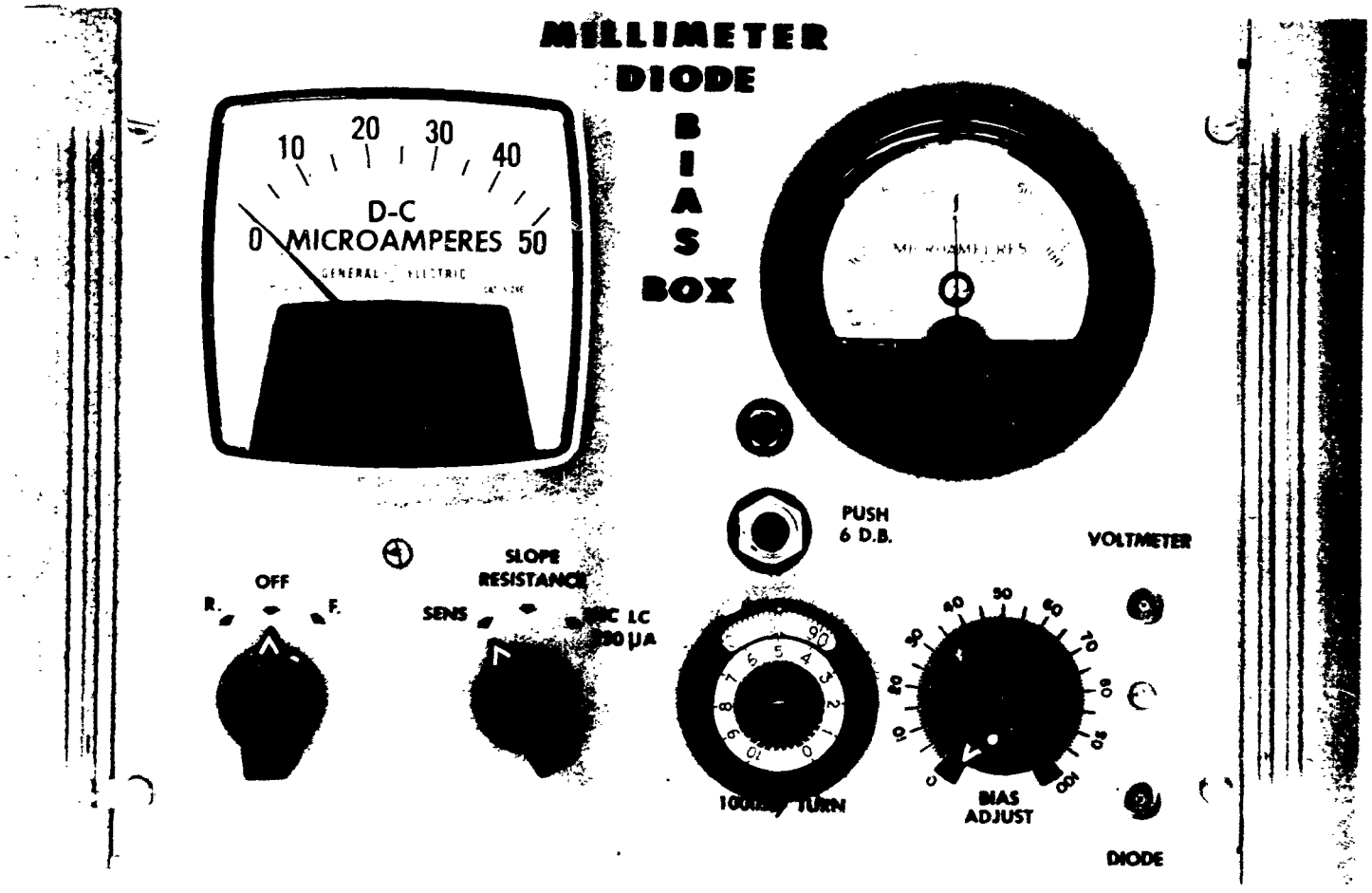

FIGURE 30

FIGURE OF MERIT TEST KIT

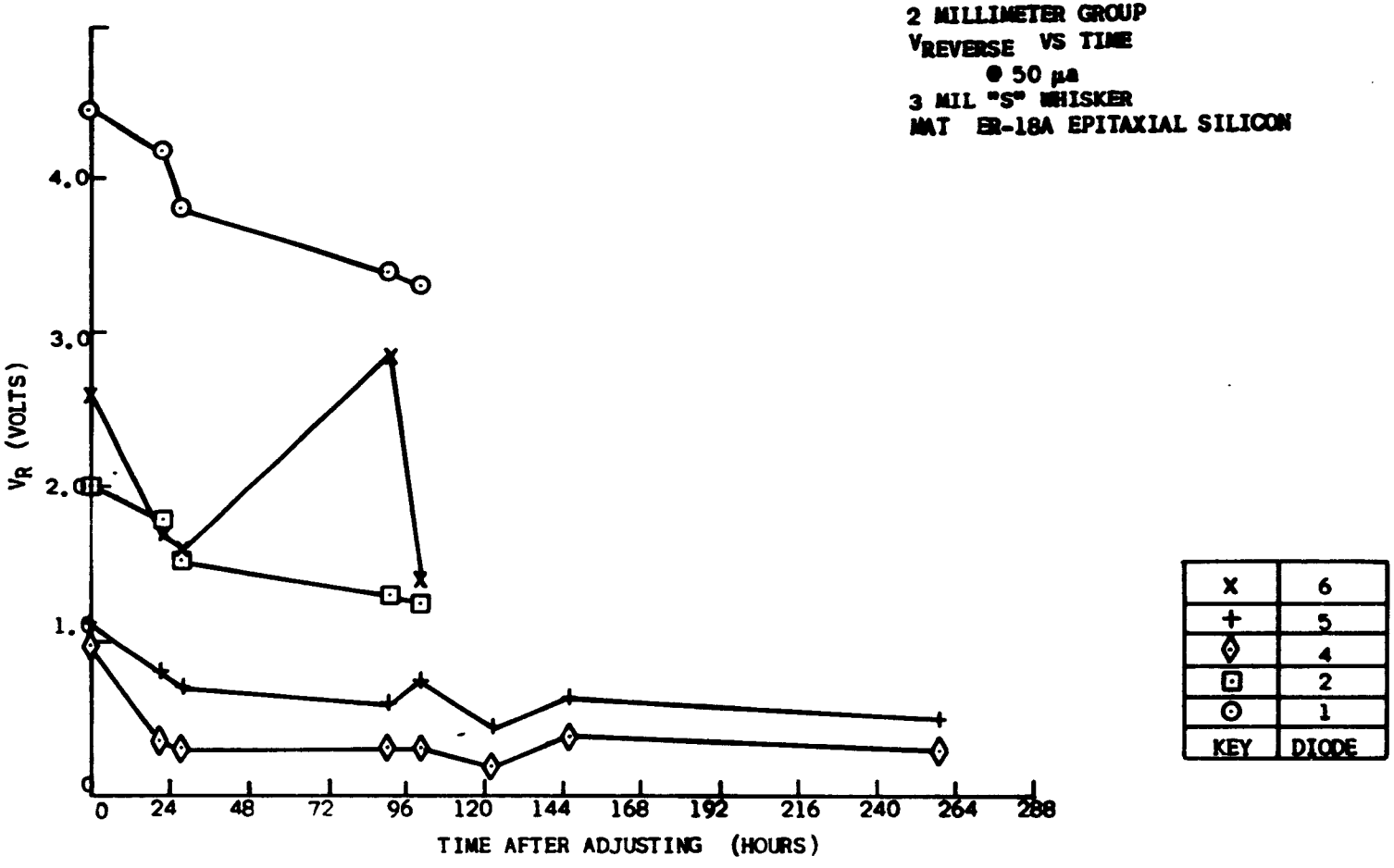

FIGURE 31

2 MILLIMETER DIODE STABILITY GRAPHS

2 MILLIMETER GROUP
$V_{FORWARD}$ Vs TIME

● 50 μa
3 MIL "S" WHISKER
MAT ER-18A EPITAXIAL SILICON

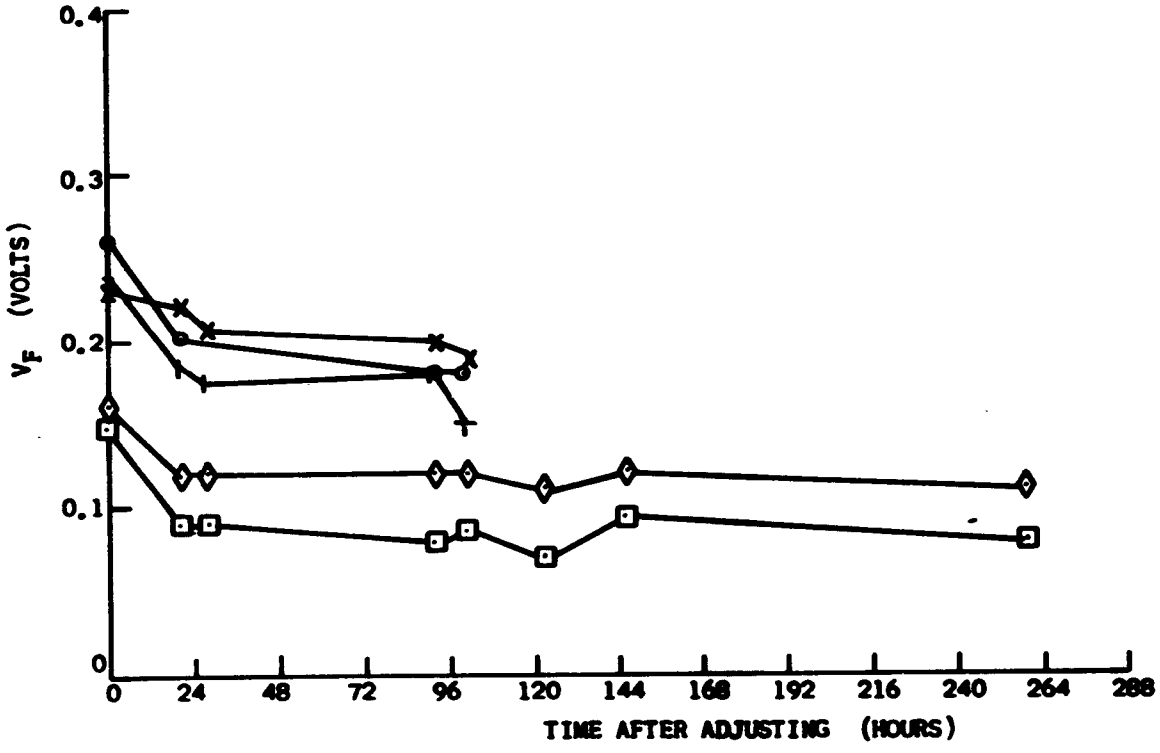

KEY	DIODE
+	6
◊	5
⊡	4
X	2
●	1

2 MILLIMETER GROUP
$V_{REVERSE}$ Vs TIME
@50 μa
3 MIL "S" WHISKER
MAT AL.-DOPED SILICON

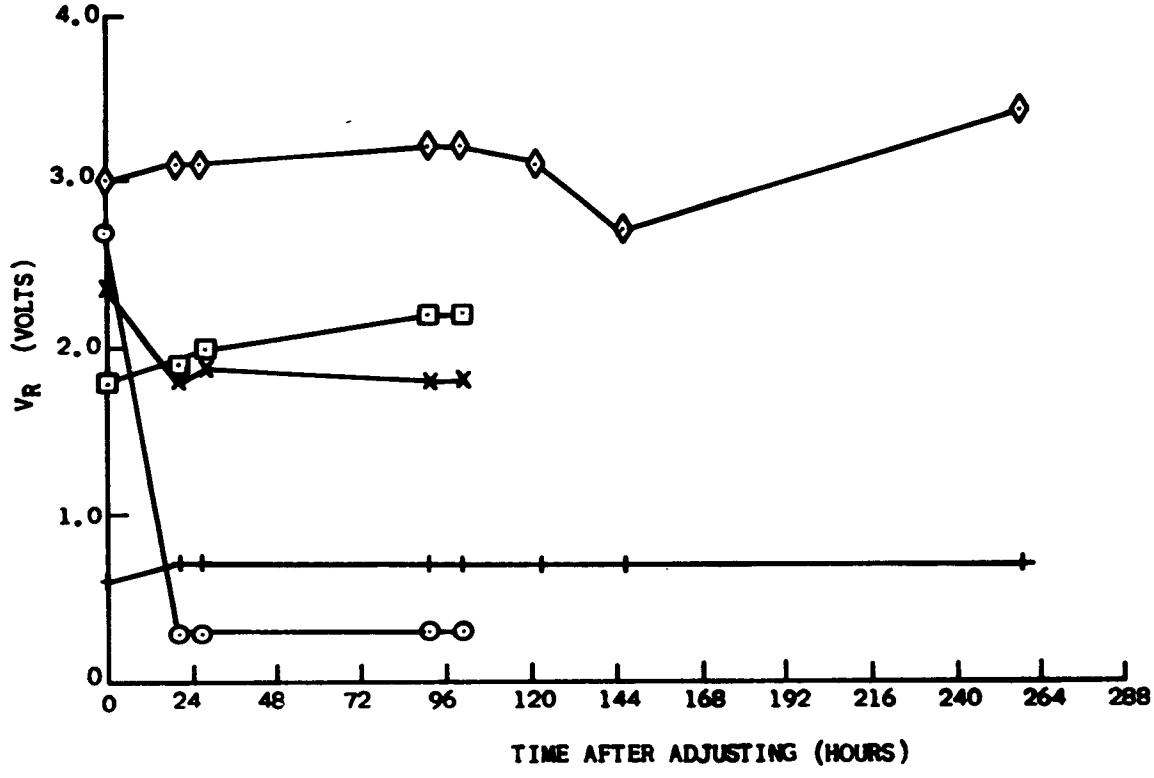

KEY	DIODE
X	5A
◇	4A
⊡	3A
+	2A
⊙	1A

2 MILLIMETER GROUP
$V_{FORWARD}$ Vs TIME
@50 μa
AL-DOPED SILICON
3 MIL "S"

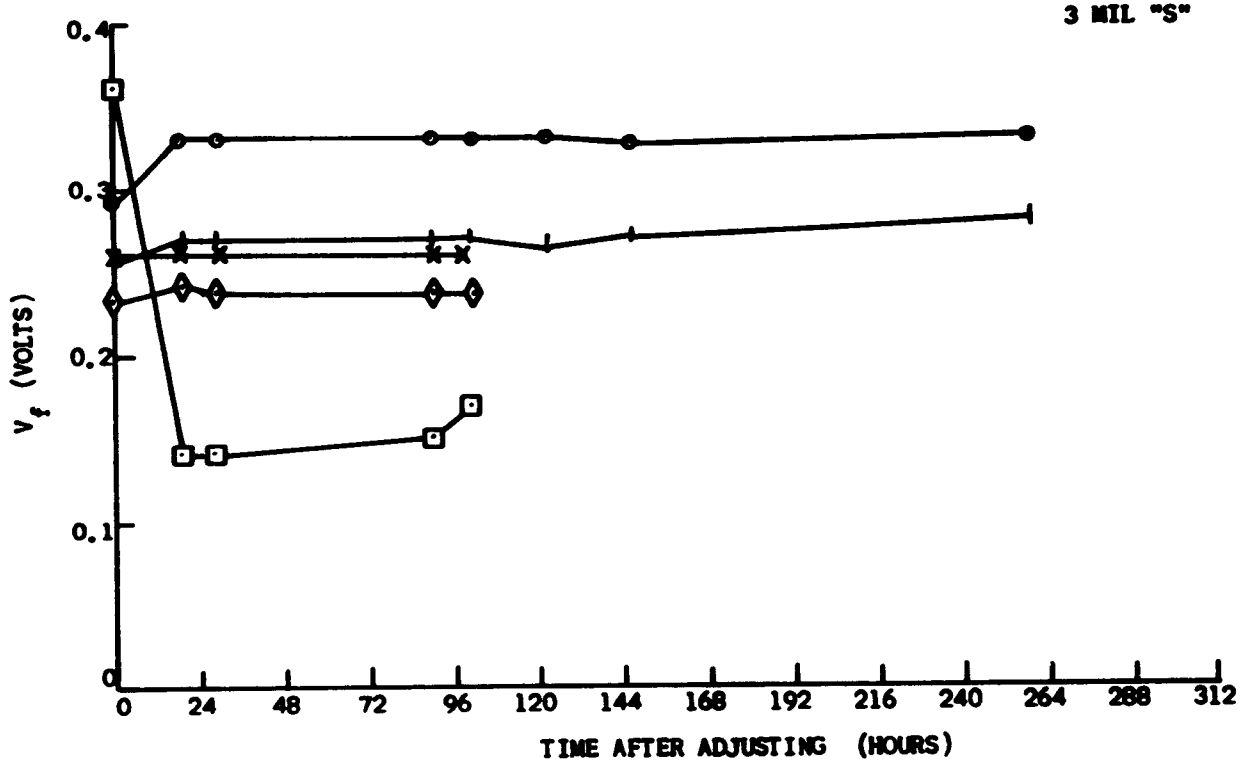

KEY	DIODE
◇	5A
+	4A
X	3A
●	2A
⊡	1A

2 MILLIMETER GROUP
$V_{REVERSE}$ VS TIME
@50 μa
BORON DOPED SILICON
3 MIL "S"

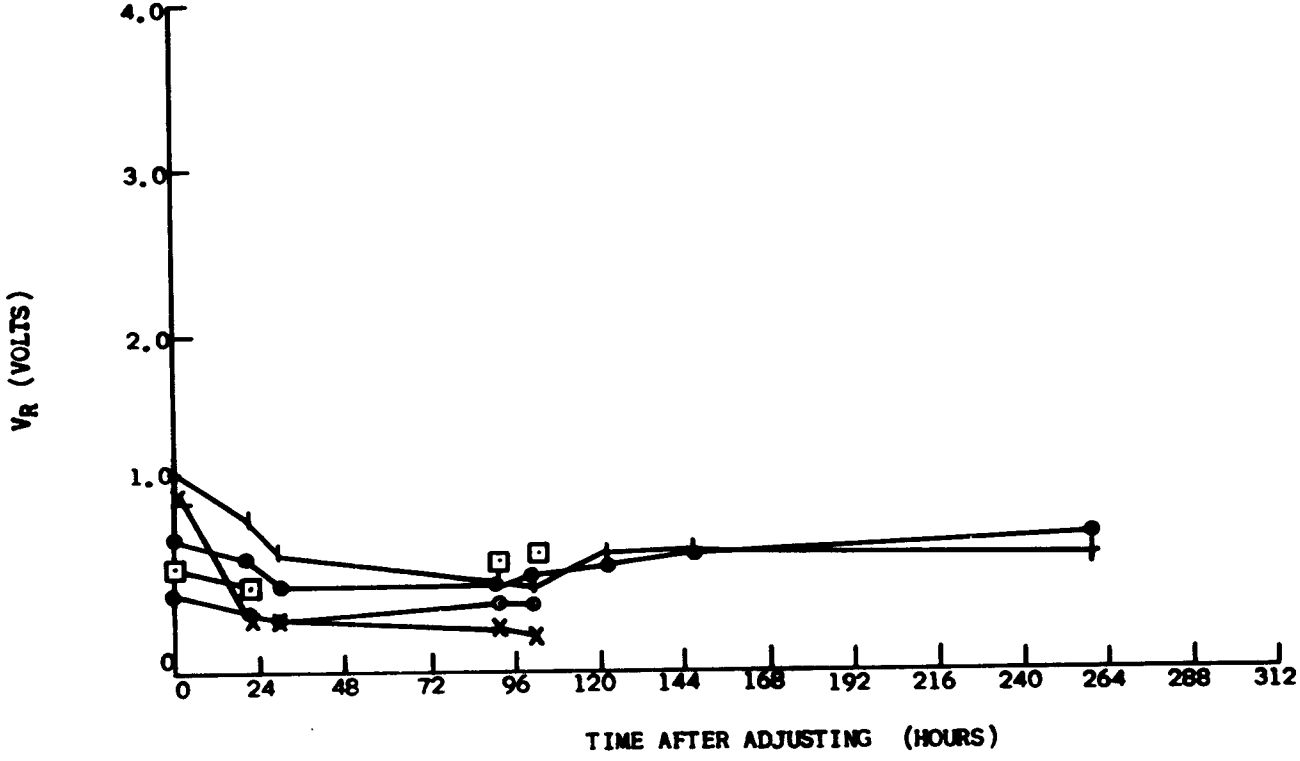

KEY	DIODE
o	5b
+	4b
x	3b
□	2b
●	1

2 MILLIMETER GROUP
$V_{FORWARD}$ Vs TIME
@50 μs
3 MIL "S" WHISKER
MAT: BORON DOPED SILICON

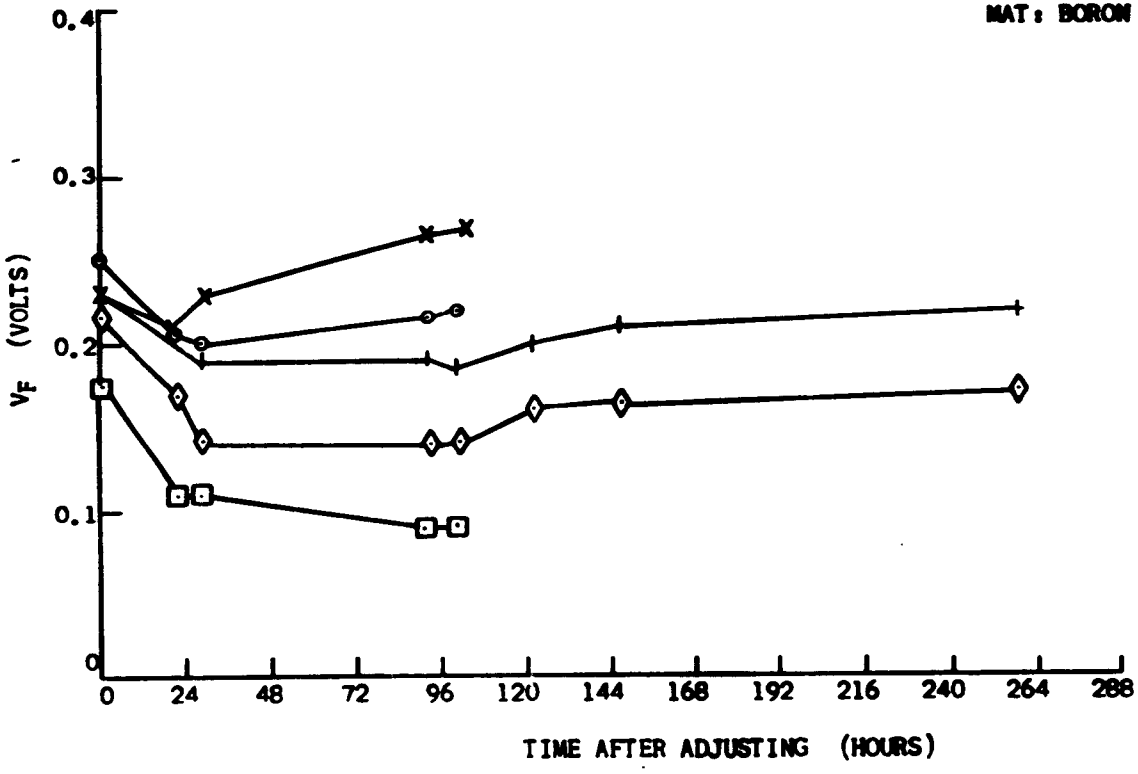

KEY	DIODE
+	5B
◇	4B
⊡	3B
X	2B
●	1B

2 MILLIMETER GROUP
$V_{REVERSE}$ Vs TIME
@50 μa
1 1/2 MIL WHISKER
MAT ME3880 BORON DOPED SILICON

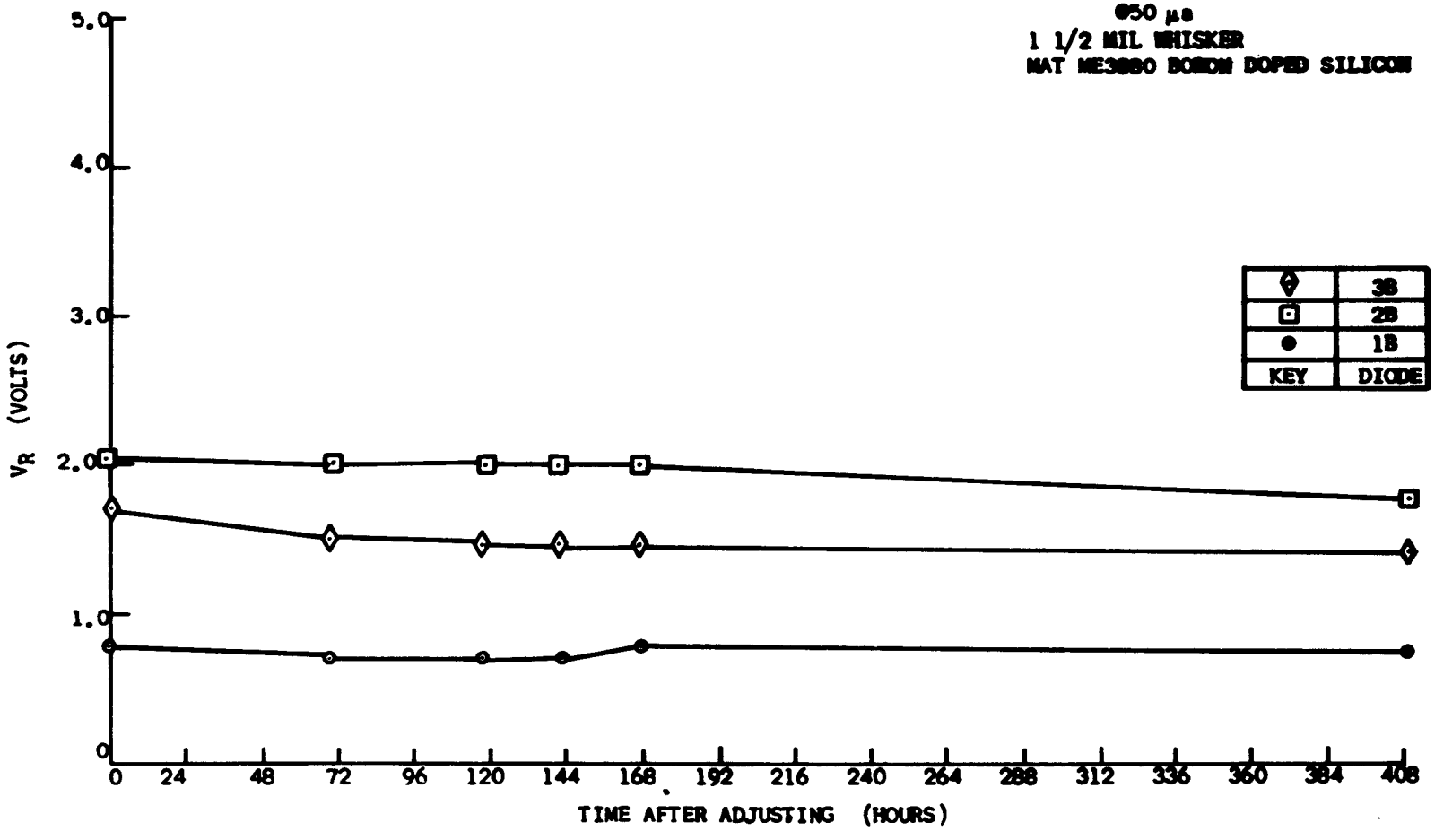

2 MILLIMETER GROUP
$V_{FORWARD}$ Vs TIME
@50 μa
1 1/2 MIL WHISKER
MAT ME3880 BORON DOPED SILICON

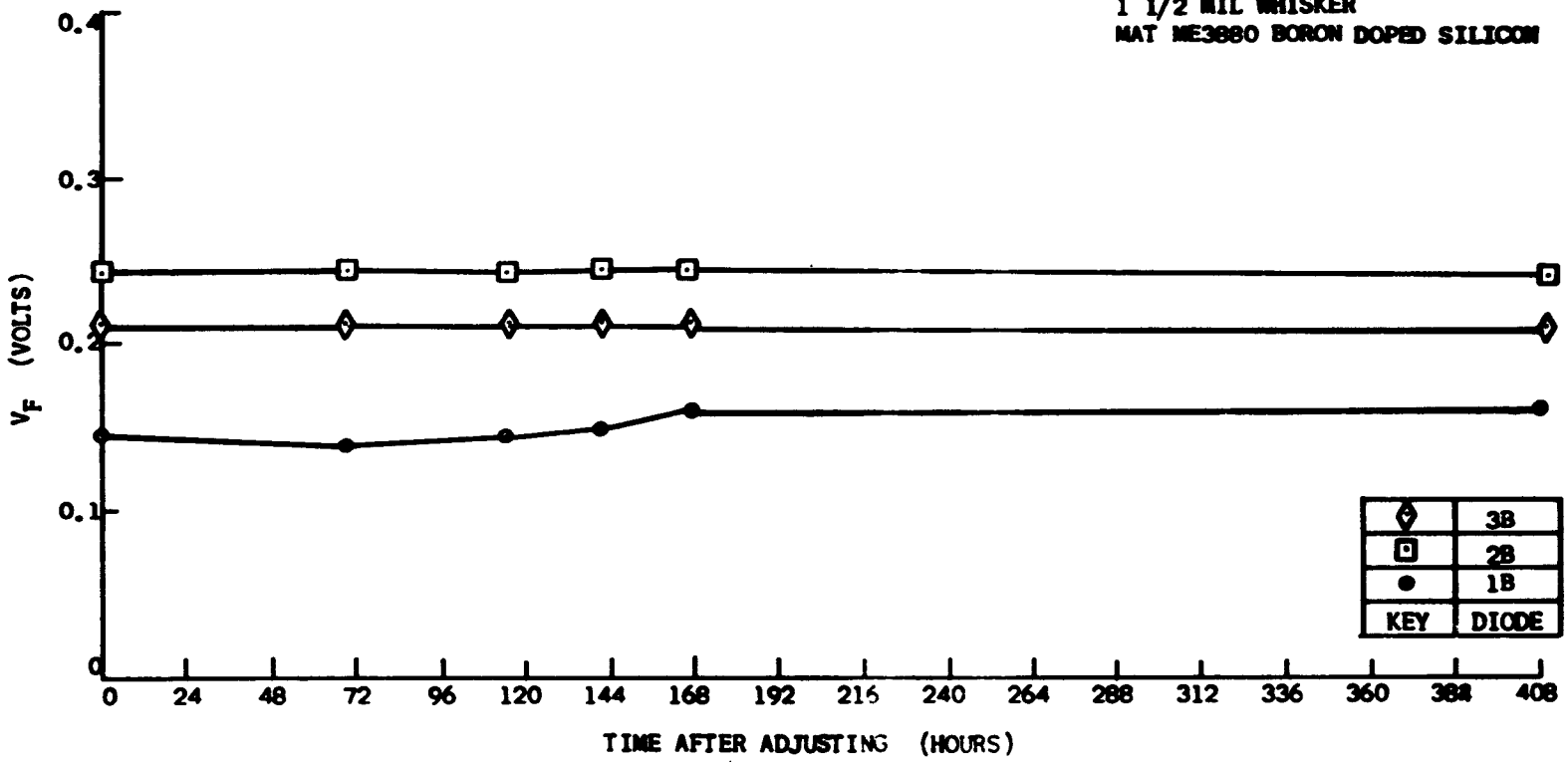

2 MILLIMETER GROUP
$V_{REVERSE}$ Vs TIME
@50 μa

1 1/2 MIL WHISKER
MAT M1394 ALUMINUM DOPED SILICON

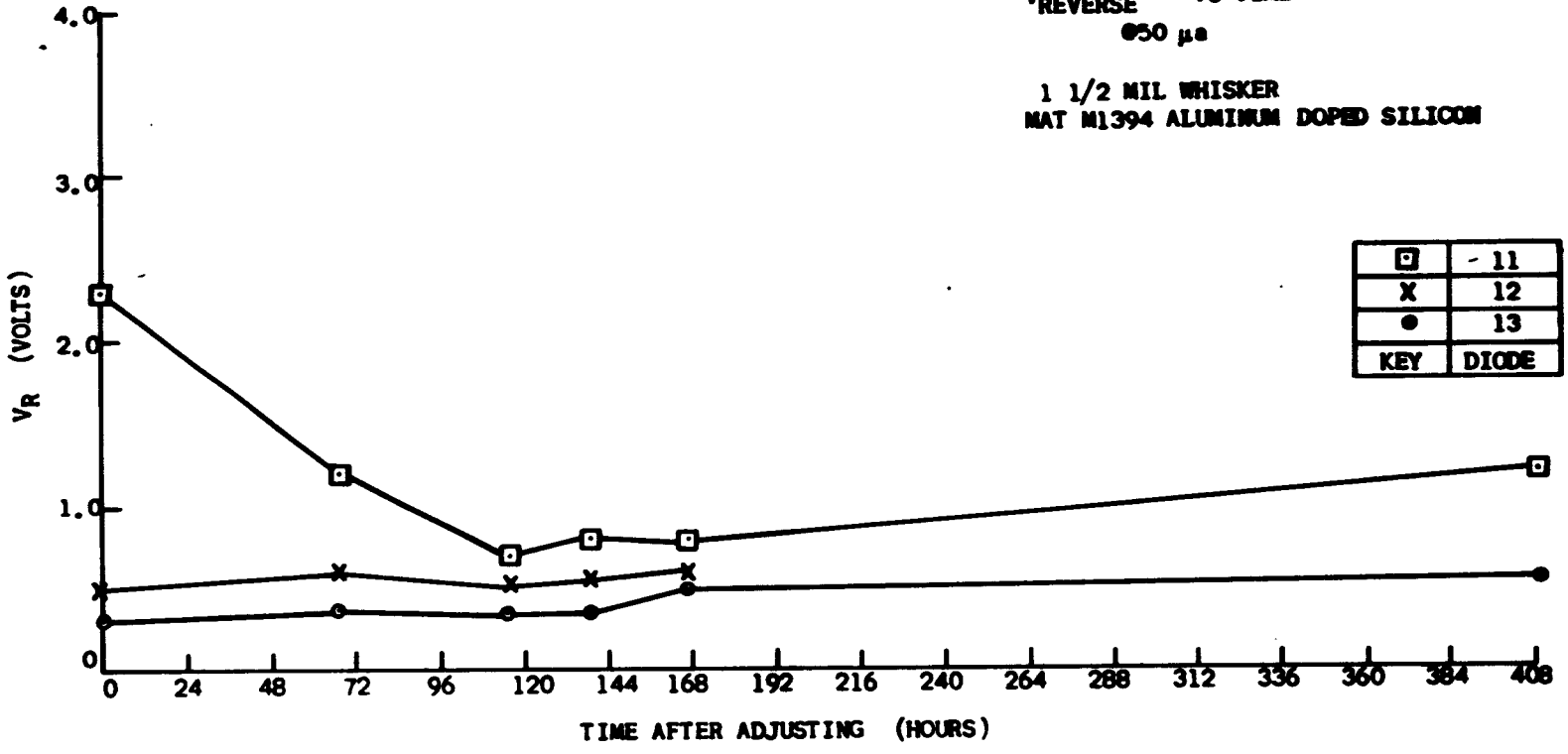

2 MILLIMETER GROUP
$V_{FORWARD}$ Vs TIME
@50 μa

1 1/2 MIL WHISKER
MAT M1394 ALUMINUM DOPED SILICON

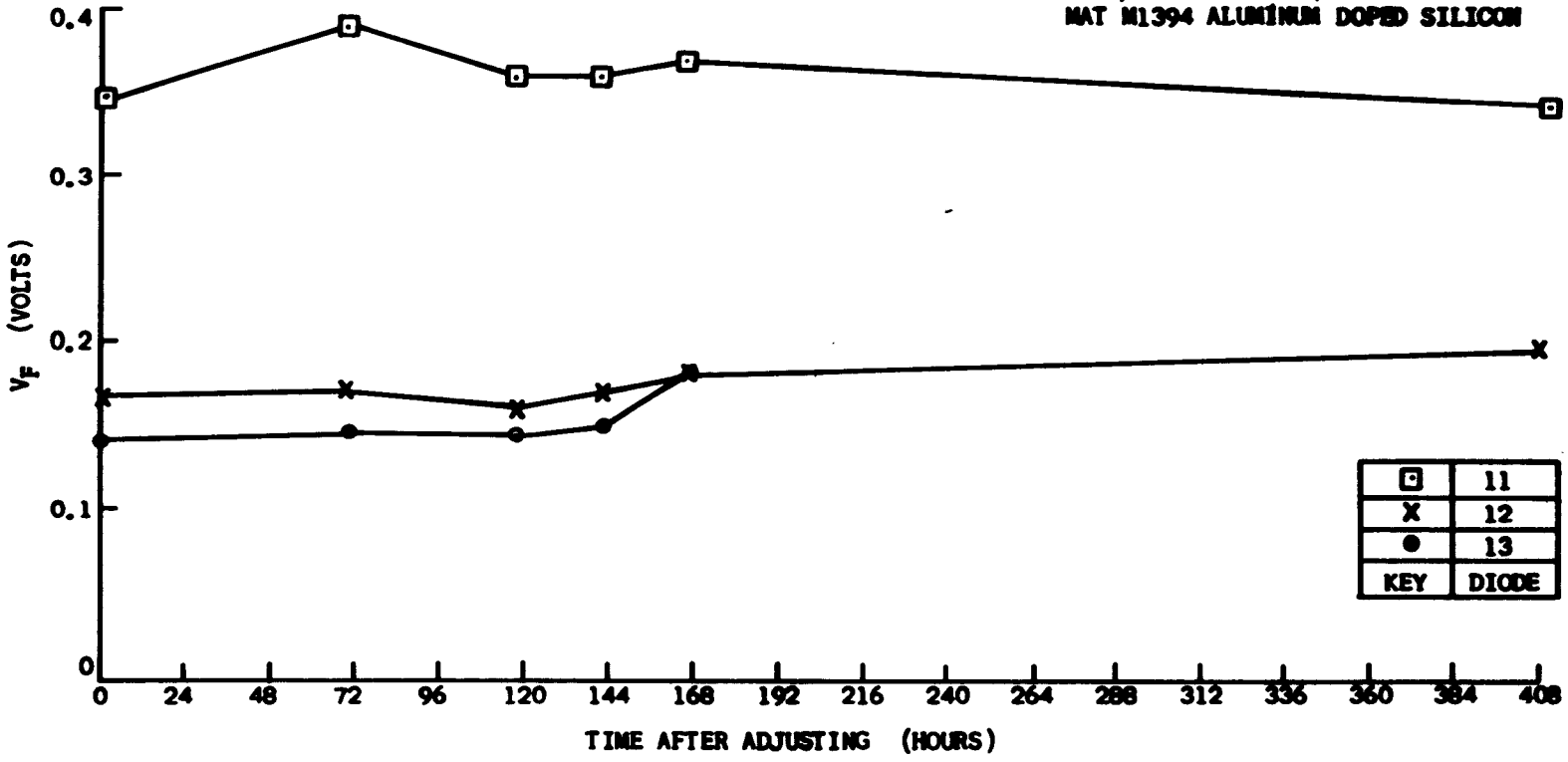

2 MILLIMETER GROUP
$V_{REVERSE}$ Vs TIME
● 50 μa
1½ MIL WHISKER
MAT ER-18A EPITAXIAL SILICON

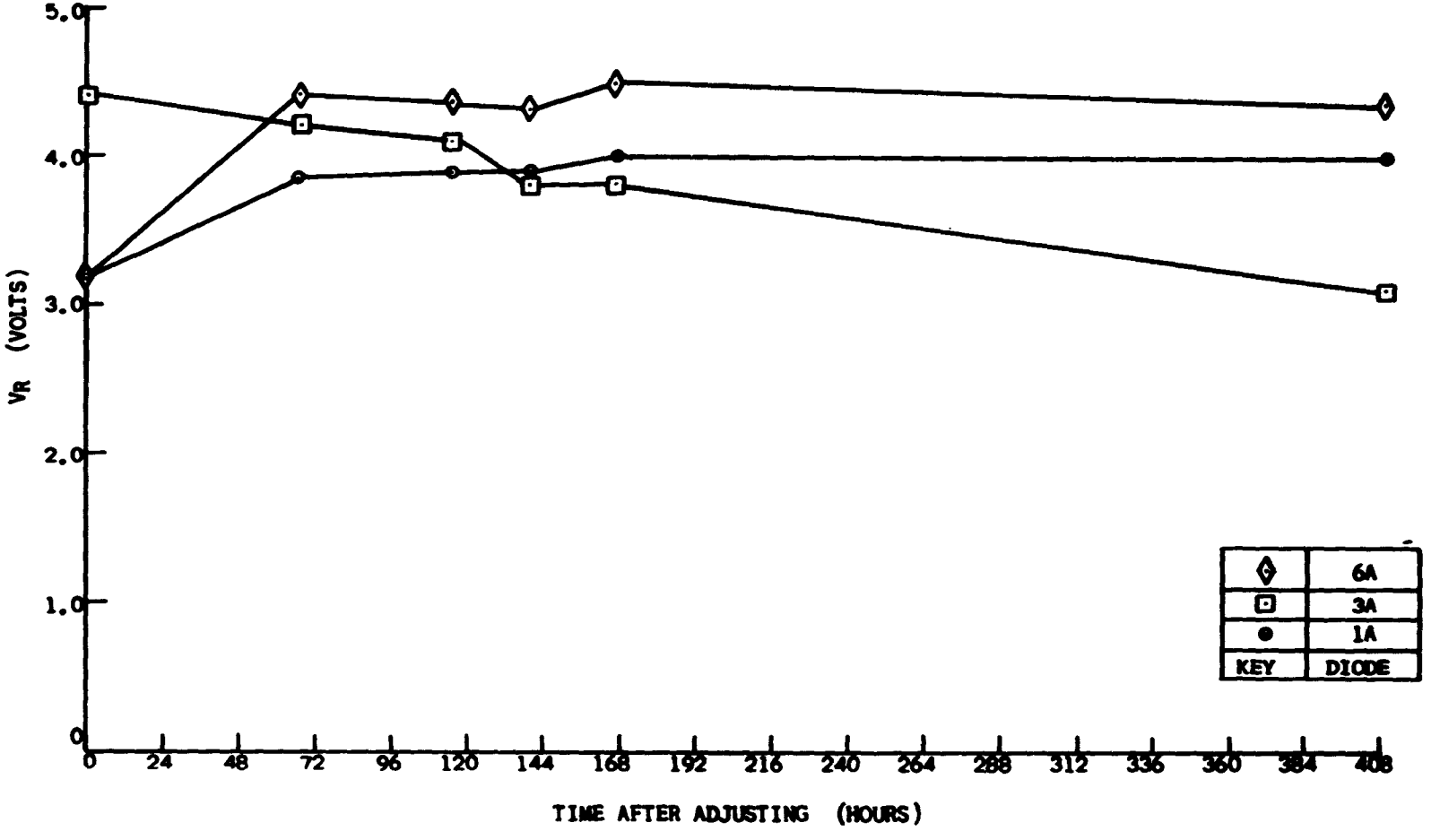

2 MILLIMETER GROUP
$V_{FORWARD}$ vs TIME
@50 μa
1 1/2 MIL WHISKER
MAT ER-18-A EPITAXIAL SILICON

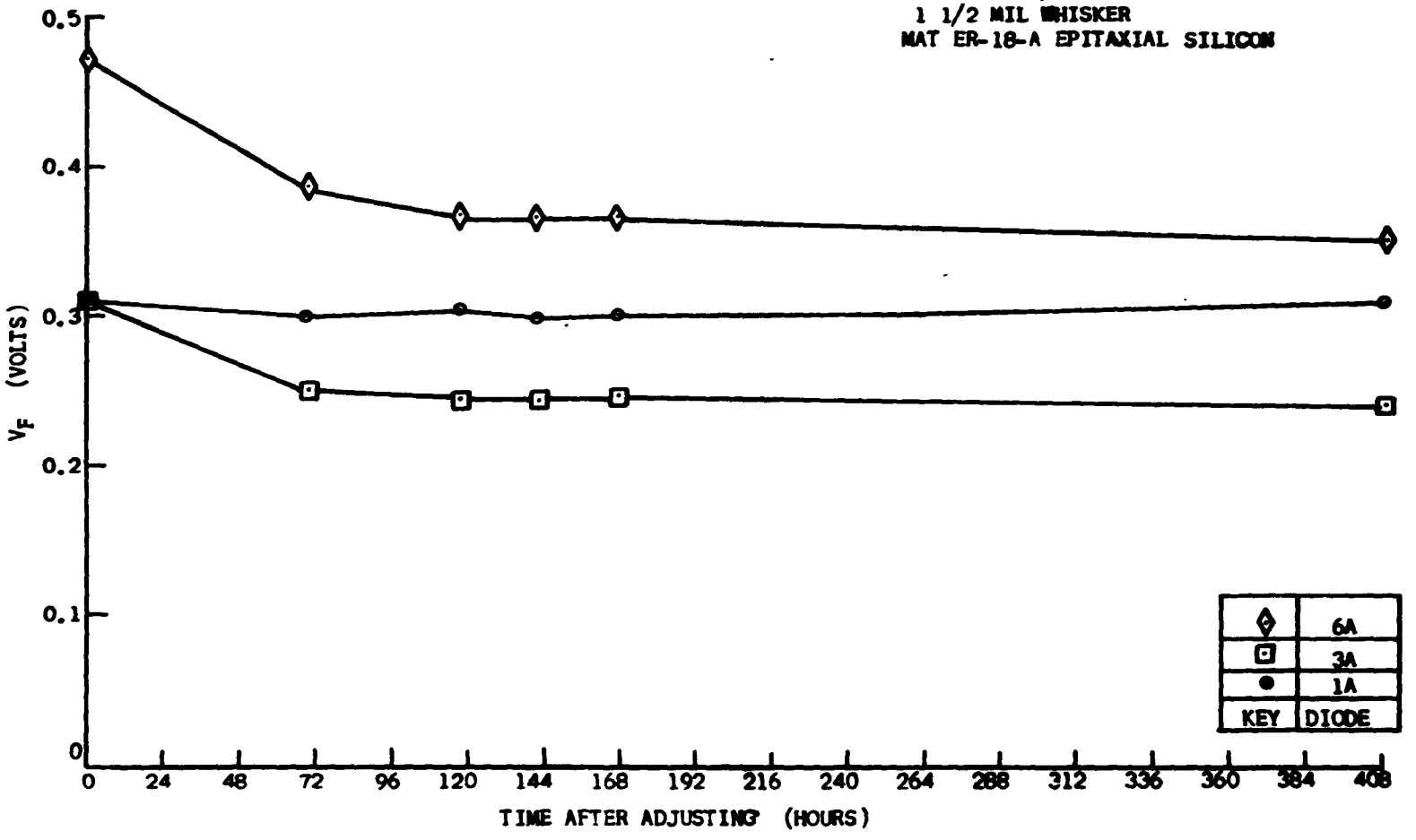

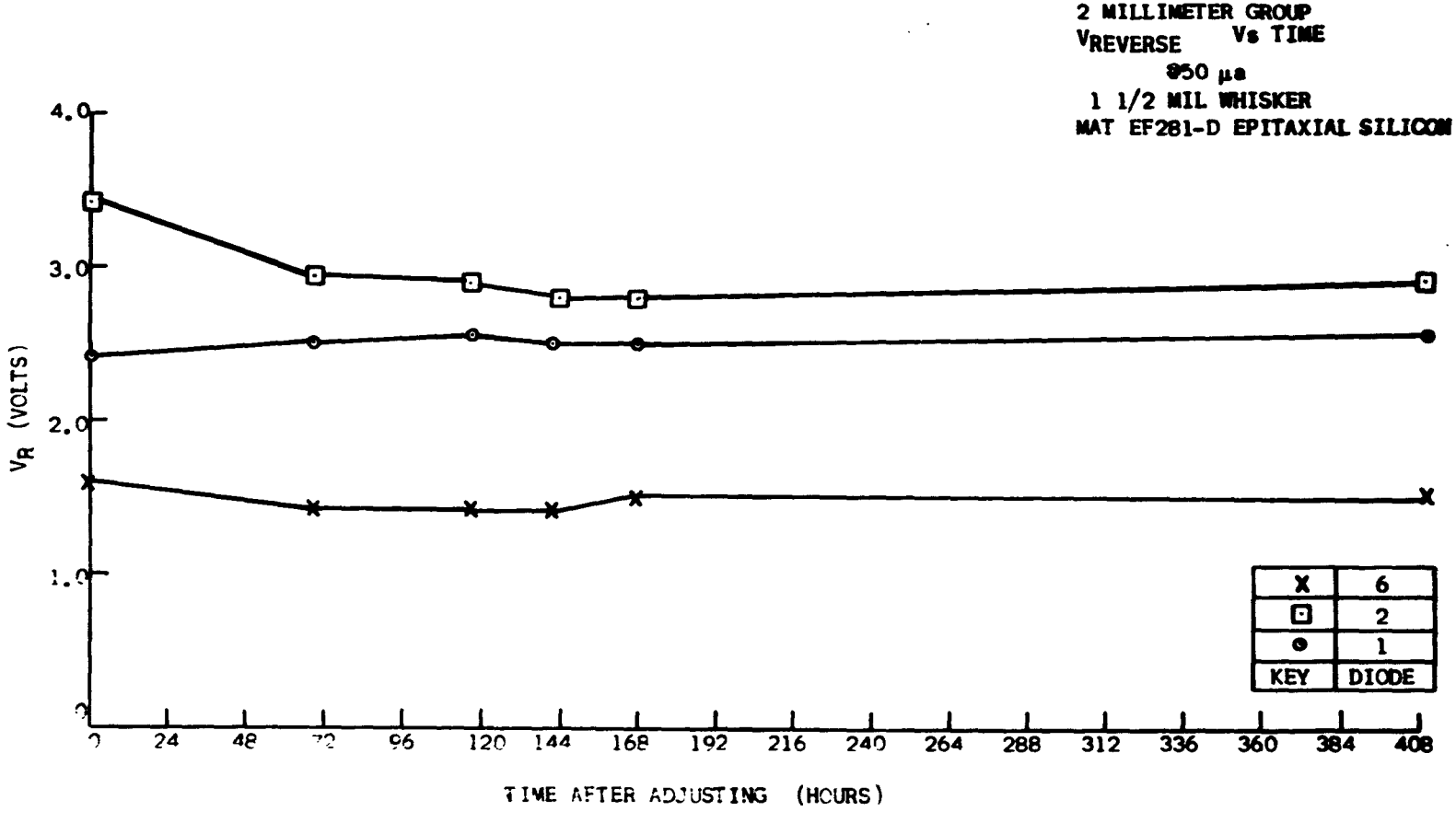
2 MILLIMETER GROUP
VREVERSE Vs TIME
950 µa
1 1/2 MIL WHISKER
MAT EF281-D EPITAXIAL SILICON
4.0
3.0
2.0
1.0
VR (VOLTS)
0
24
48
72
96
120
144
168
192
216
240
264
288
312
336
360
384
408
TIME AFTER ADJUSTING (HOURS)
X 6
2
1
KEY DIODE

2 MILLIMETER GROUP
$V_{FORWARD}$ Vs TIME
950 μa
1 1/2 MIL WHISKER
MAT EF281-D EPITAXIAL SILICON

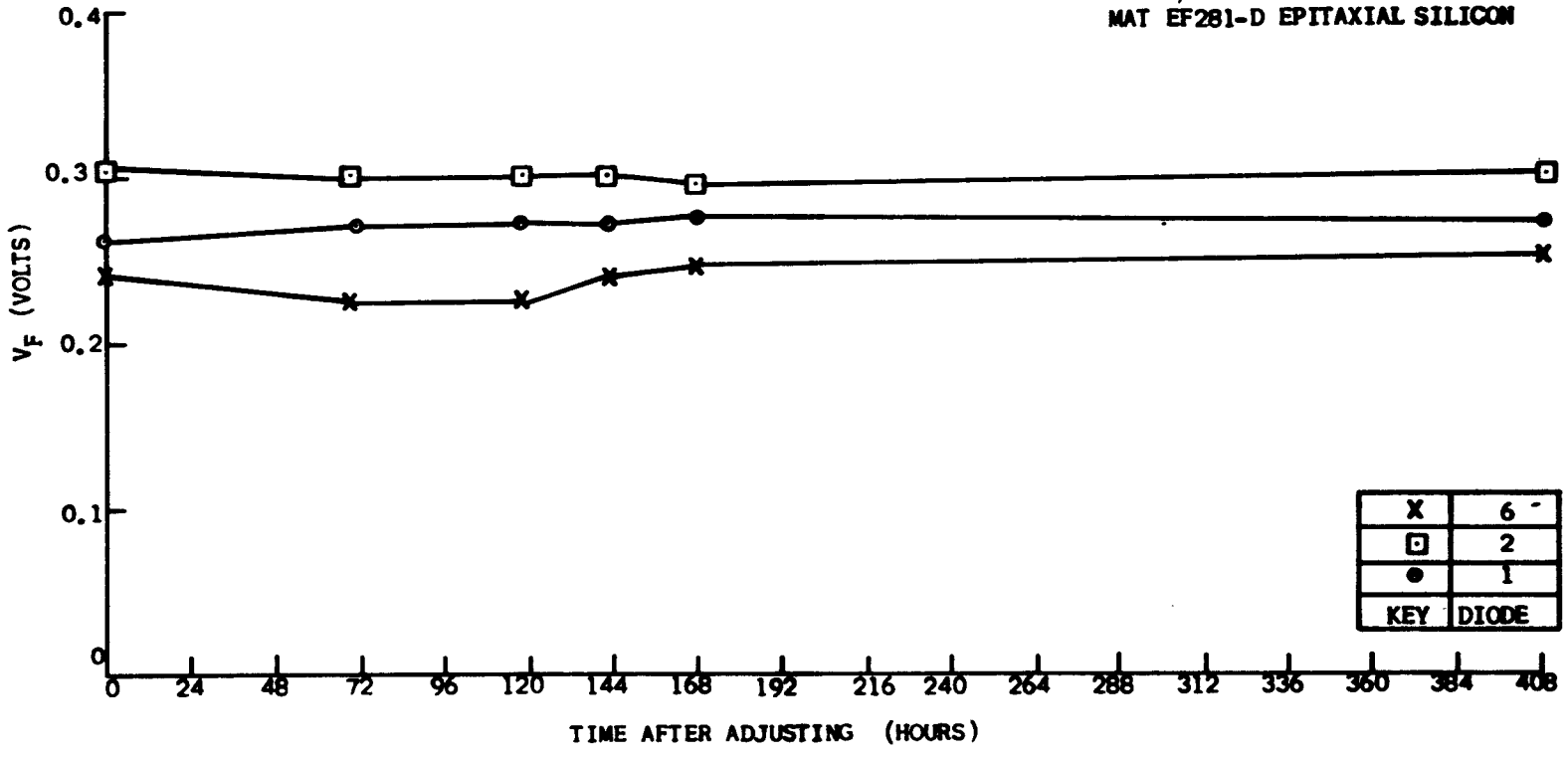

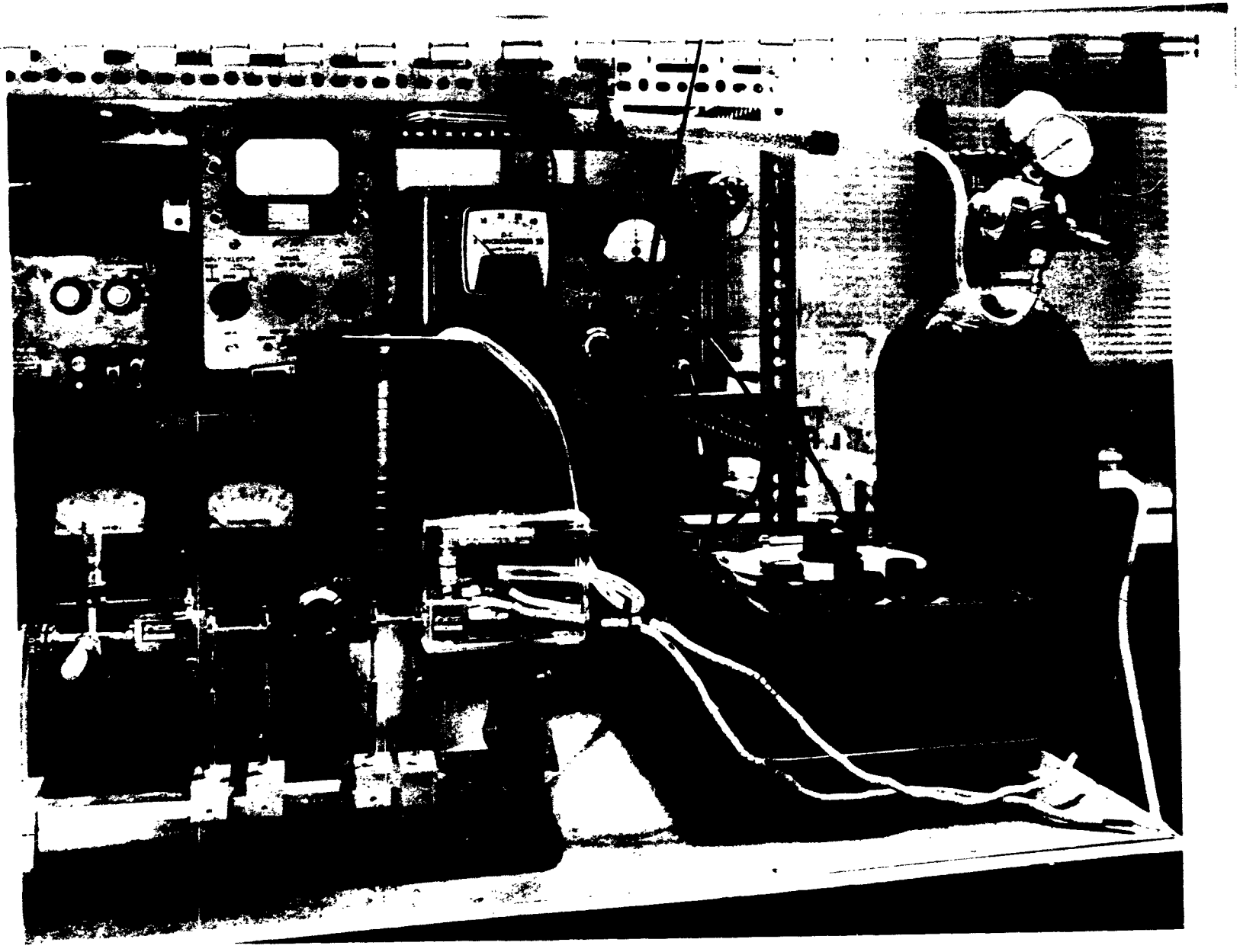

FIGURE 32

LOW TEMPERATURE TEST EQUIPMENT

FIGURE OF MERIT vs TEMPERATURE
2 MILLIMETER DETECTOR
DIODES #5 & 2A 140 Gc @ 42.3 μ WATTS (20μa) BIAS

$$FM = \frac{MVec \times 10^3}{(Rs + 1200)^{0.5}(42.3)}$$

DIODES #6A & 13 140 Gc @ 31.0 μ WATTS (20 μa) BIAS

$$FM = \frac{MVec \times 10^3}{(Rs + 1200)^{0.5}(31.0)}$$

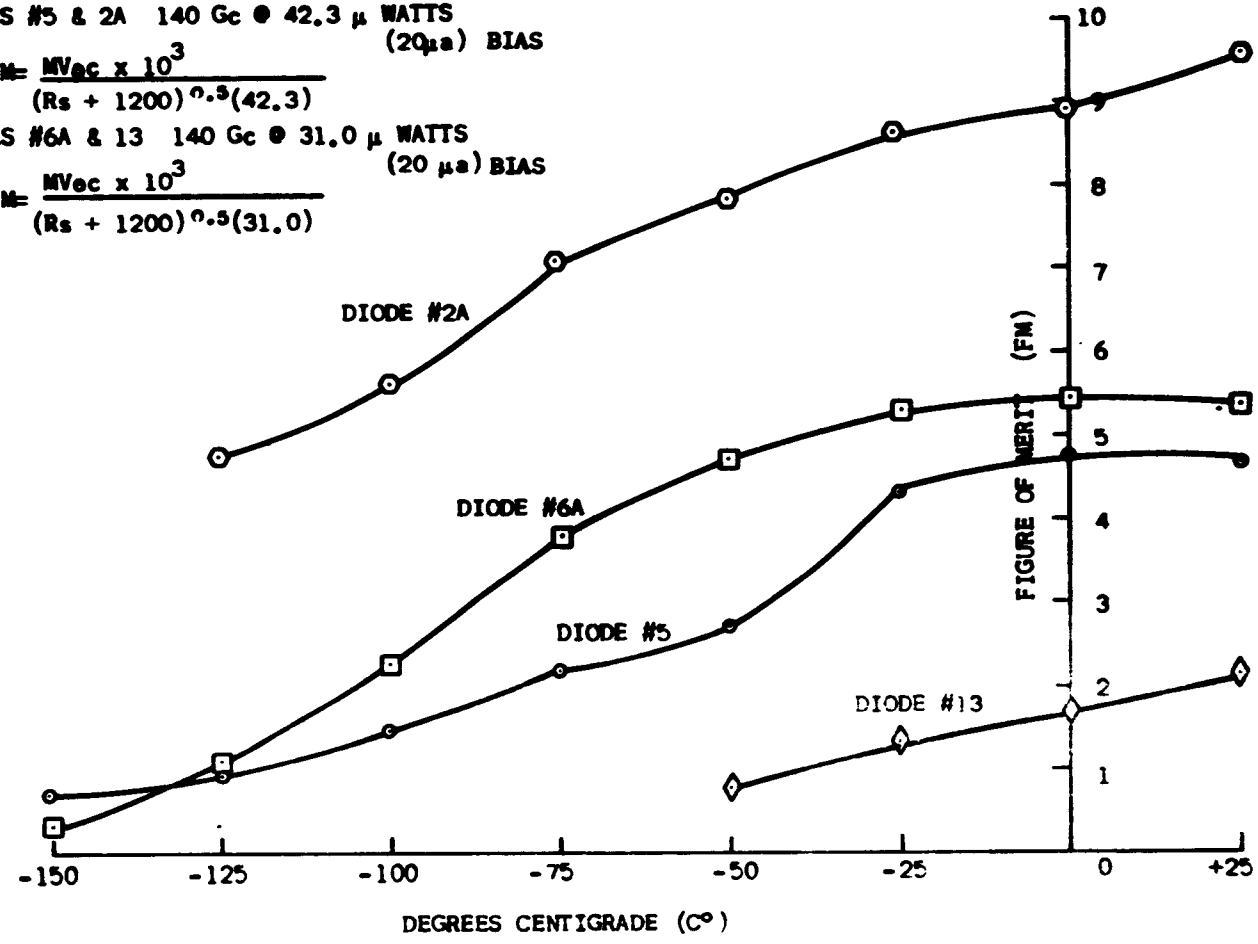

FIGURE 33

LOW TEMPERATURE FIGURE OF MERIT GRAPHS

FIGURE OF MERIT vs TEMPERATURE
2 MILLIMETER DETECTOR
140 Gc @ 42.3 μ WATTS, O-BIAS

$$FM = \frac{MVoc \times 10^3}{(Rs + 1200)^{0.5}\ (42.3)} \qquad FM = \frac{MVoc \times 10^3}{(Rs \times 1200)^{0.5}\ (31.0)}$$

DIODE #5 2A @42.3 μ WATTS
DIODE #6A 13 @31.0 μ WATTS

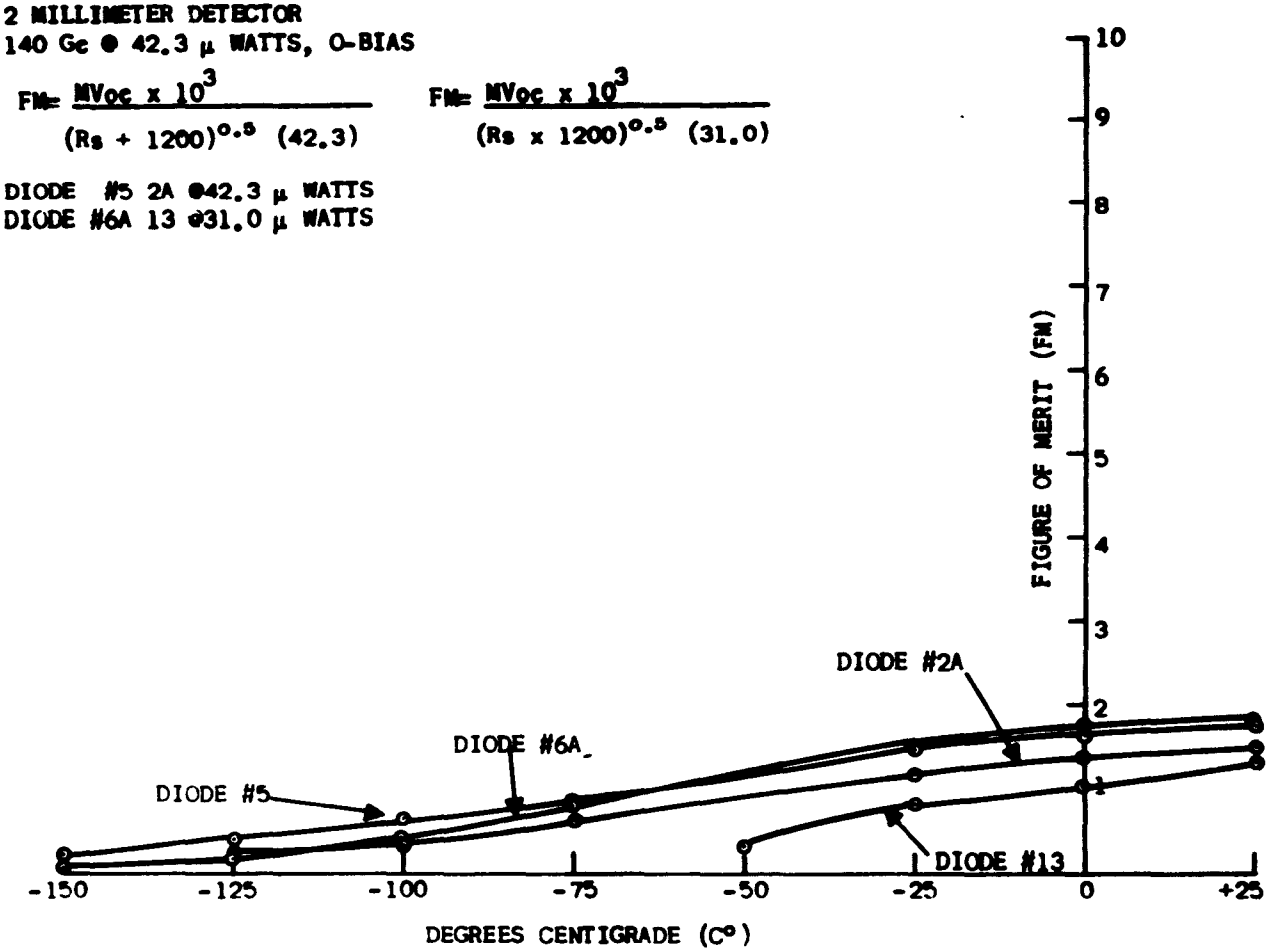

FIGURE OF MERIT vs TEMPERATURE
2 MILLIMETER DETECTOR
140 Gc @ 42.3 & 31.0 μ WATTS 10 μa

$$FM = \frac{MVoc \times 10^3}{(Rs + 1200)^{0.5}(42.3)} \qquad FM = \frac{MVoc \times 10^3}{(Rs + 1200)^{0.5}(31.0)}$$

DIODE #5 2A @ 42.3 μ WATTS
DIODE #6A 13 @ 31.0 μ WATTS

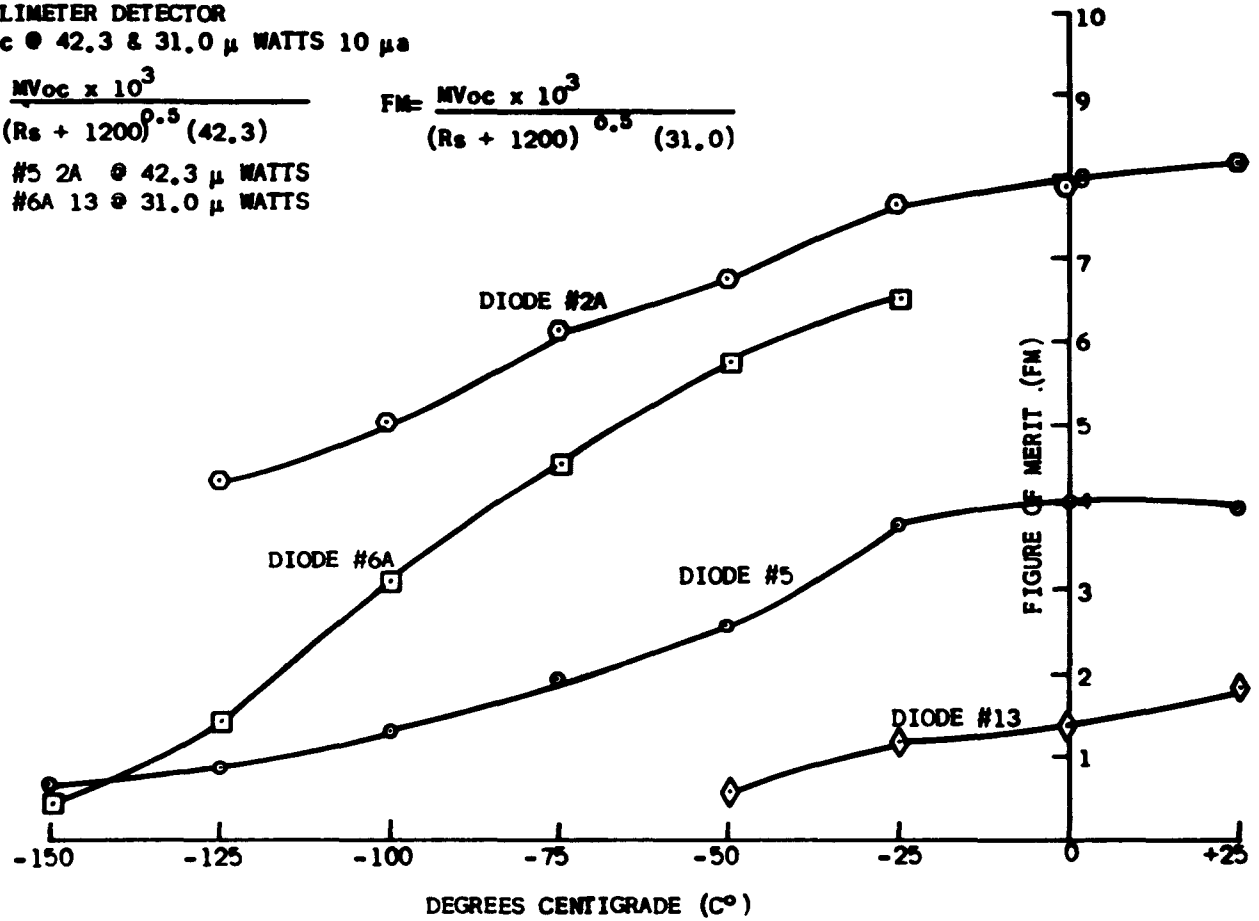

FIGURE OF MERIT vs TEMPERATURE
2 MILLIMETER DETECTOR
140 Gc @ 42.3 μ WATTS, O-BIAS

$$FM = \frac{MVoc \times 10^3}{(Rs + 1200)^{0.5} (42.3)}$$

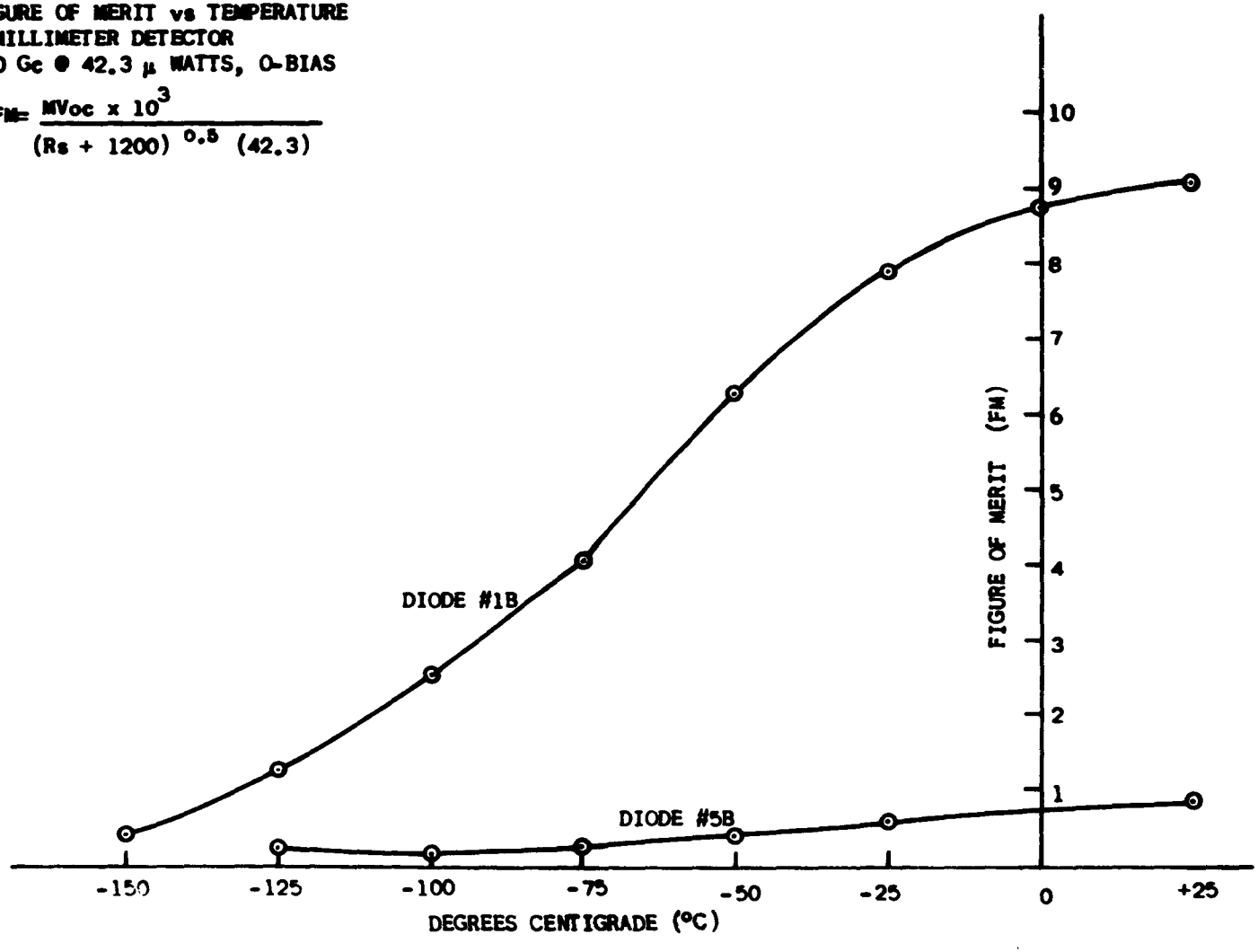

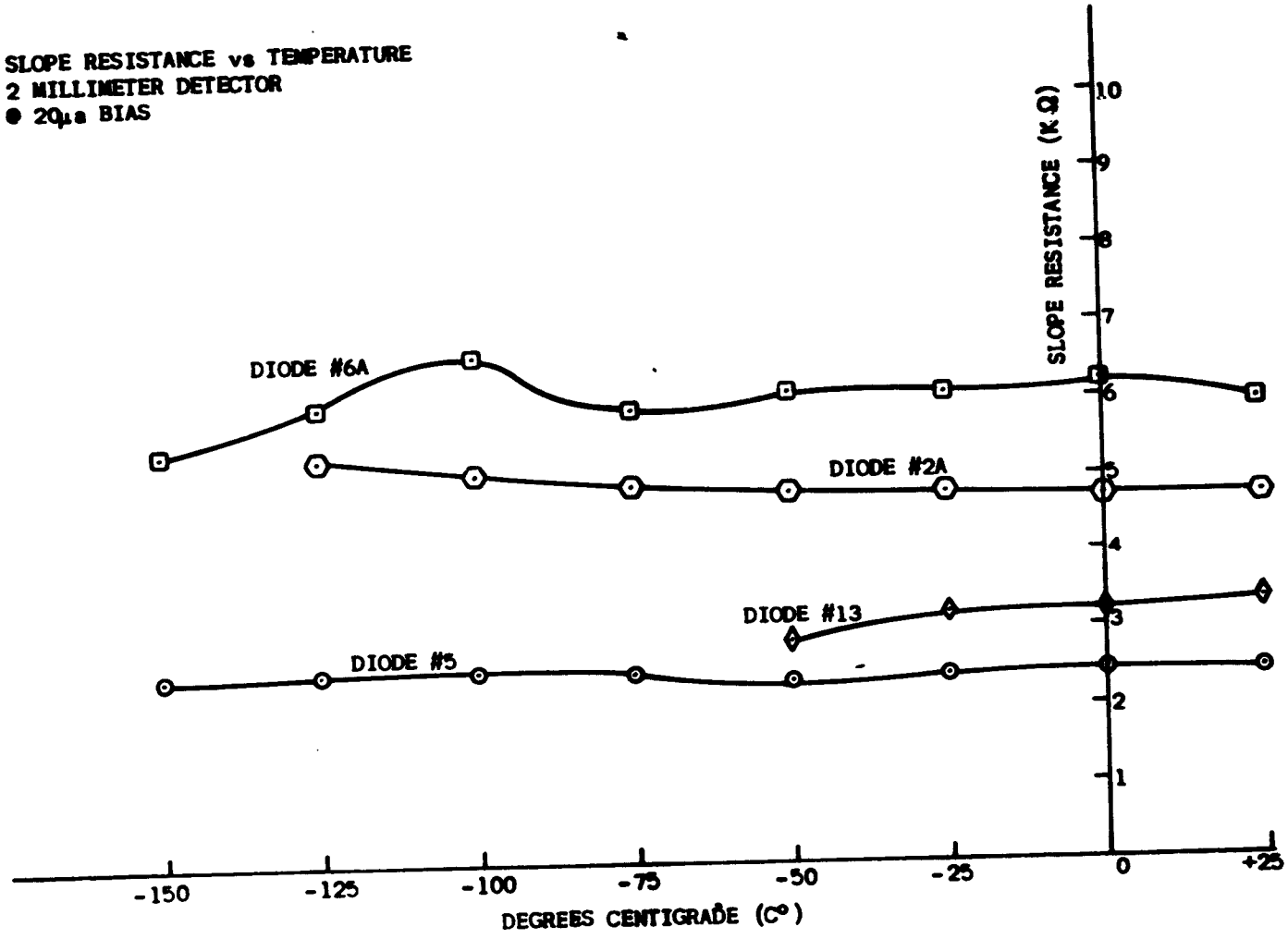
SLOPE RESISTANCE vs TEMPERATURE
2 MILLIMETER DETECTOR
● 20μa BIAS
SLOPE RESISTANCE (KΩ)
10
9
8
7
6
5
4
3
2
1
DIODE #6A
DIODE #2A
DIODE #13
DIODE #5
-150
-125
-100
-75
-50
-25
0
+25
DEGREES CENTIGRADE (C°)

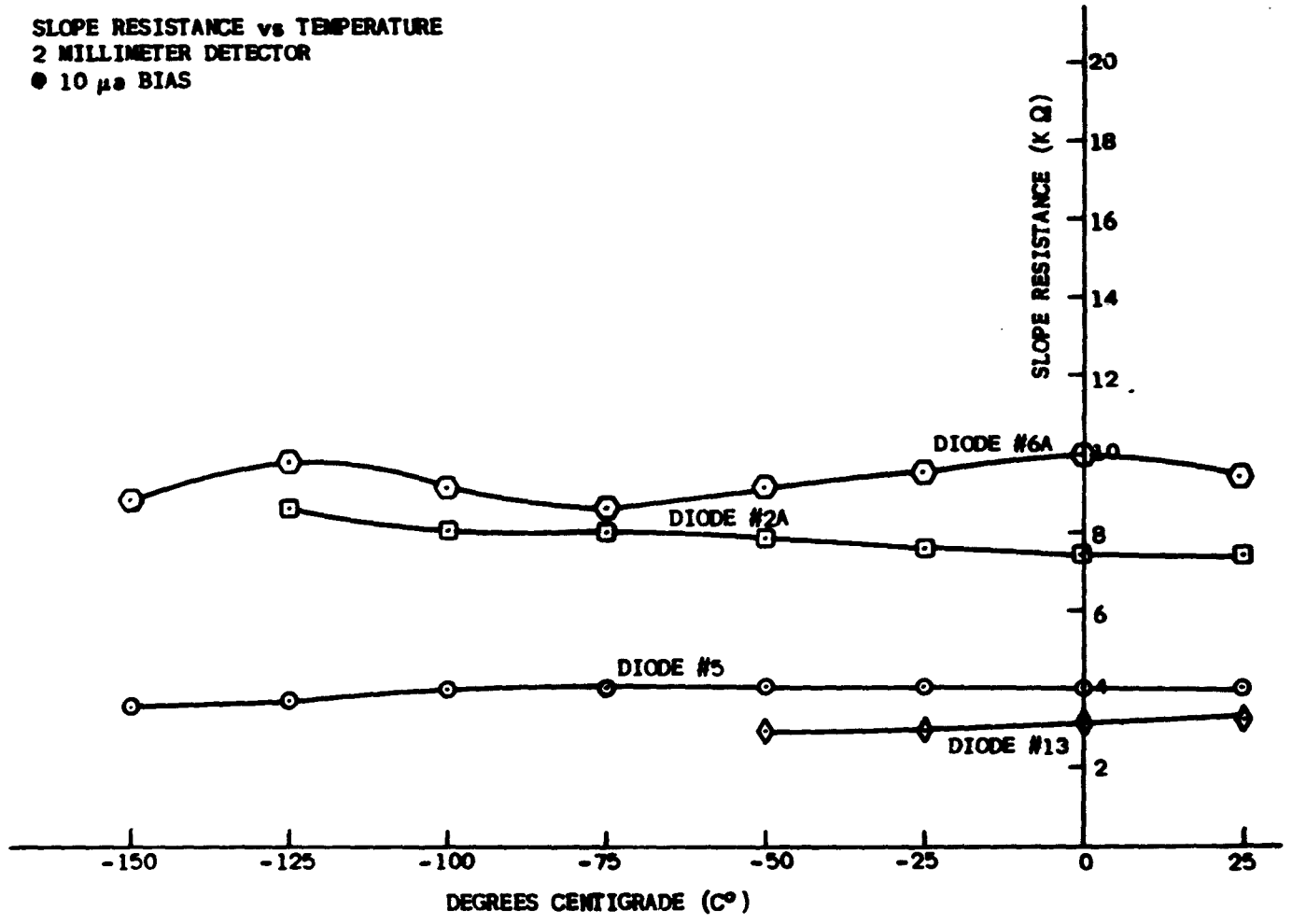
SLOPE RESISTANCE vs TEMPERATURE
2 MILLIMETER DETECTOR
● 10 μa BIAS
SLOPE RESISTANCE (K Ω)
20
18
16
14
12
10
8
6
4
2
DIODE #6A
DIODE #2A
DIODE #5
DIODE #13
-150
-125
-100
-75
-50
-25
0
25
DEGREES CENTIGRADE (C°)

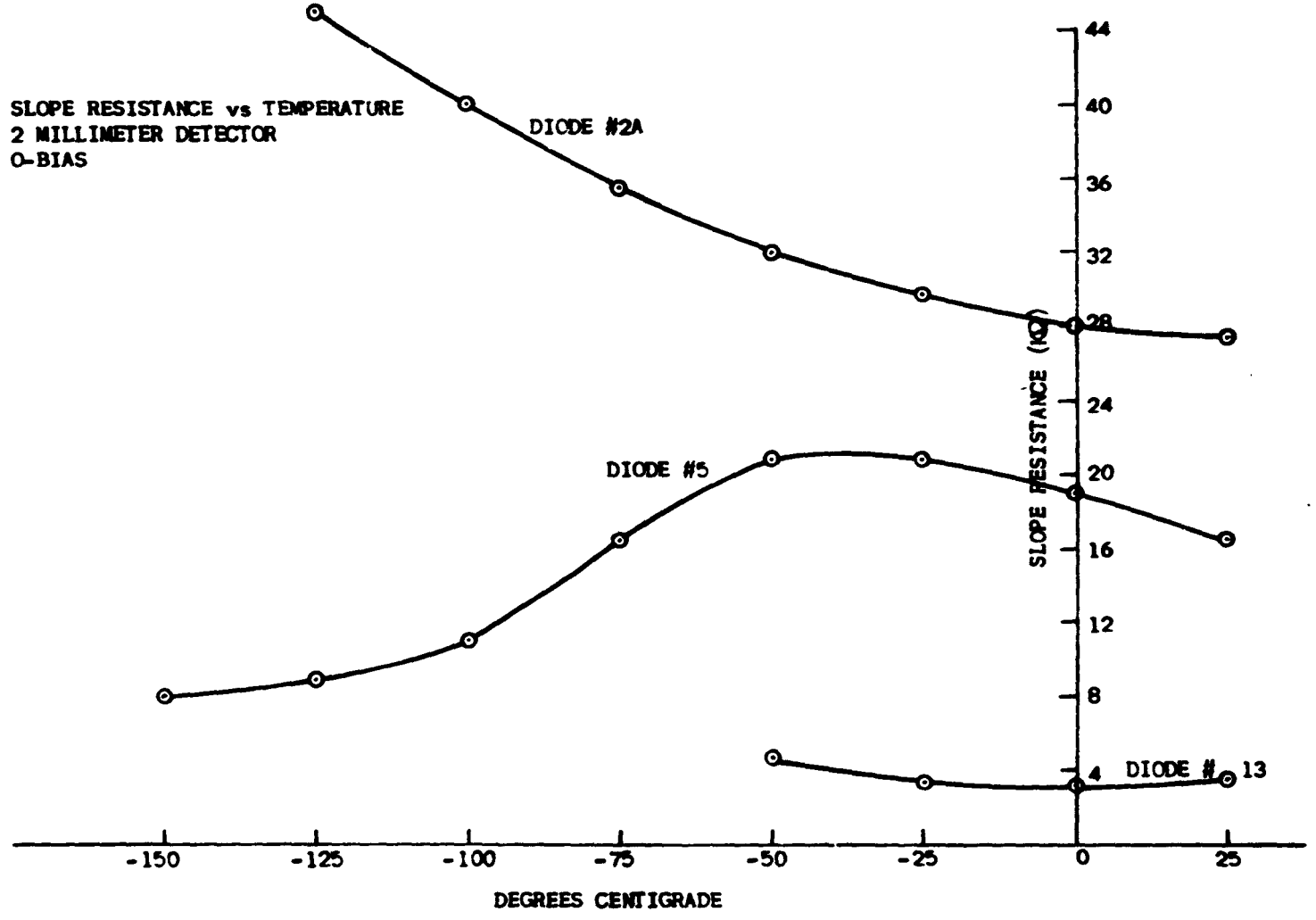
SLOPE RESISTANCE vs TEMPERATURE
2 MILLIMETER DETECTOR
0-BIAS
DIODE #2A
DIODE #5
DIODE # 13
SLOPE RESISTANCE (KΩ)
44
40
36
32
28
24
20
16
12
8
4
-150
-125
-100
-75
-50
-25
0
25
DEGREES CENTIGRADE

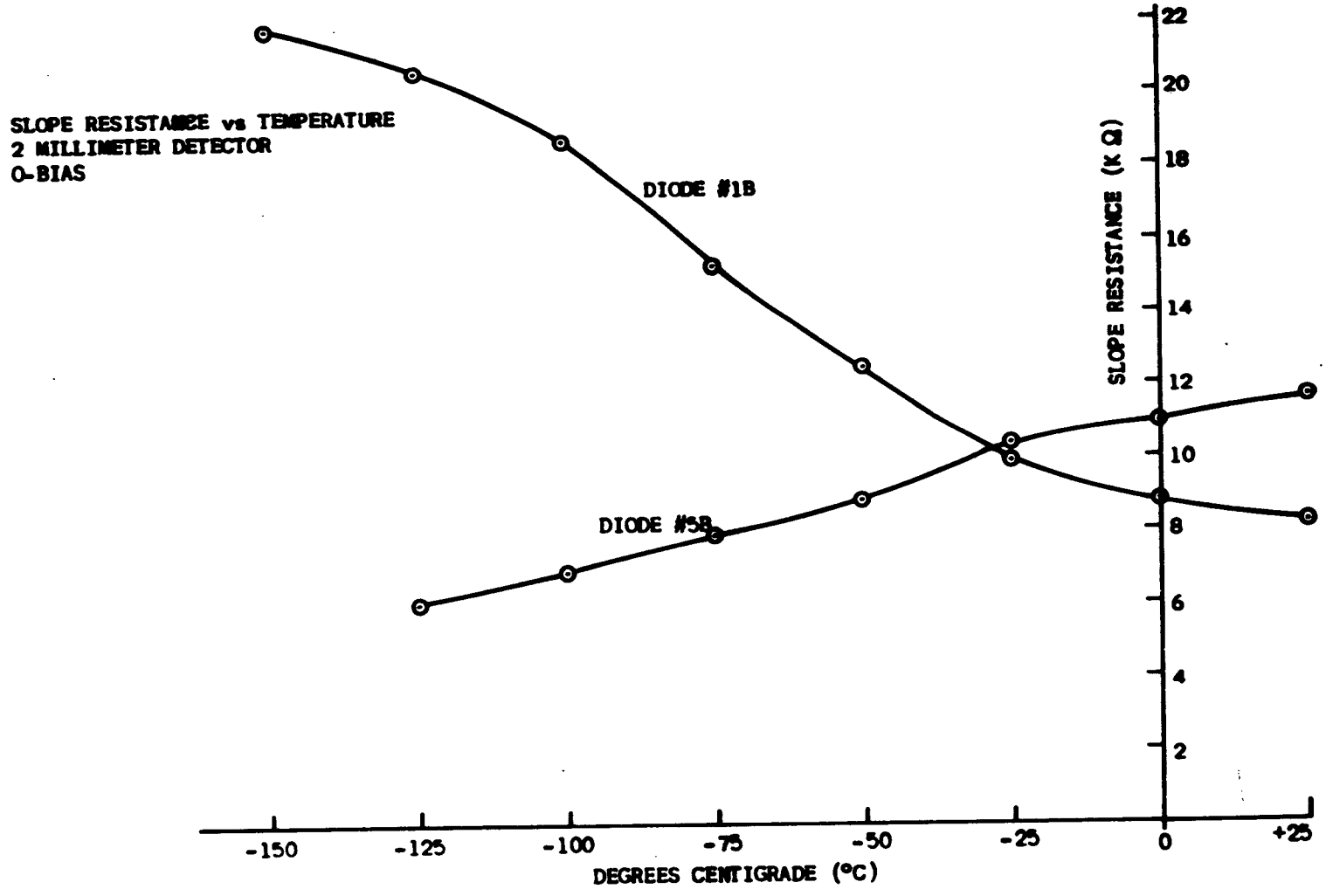
SLOPE RESISTANCE vs TEMPERATURE
2 MILLIMETER DETECTOR
0-BIAS
DIODE #1B
DIODE #5B
SLOPE RESISTANCE (K Ω)
22
20
18
16
14
12
10
8
6
4
2
-150
-125
-100
-75
-50
-25
0
+25
DEGREES CENTIGRADE (°C)

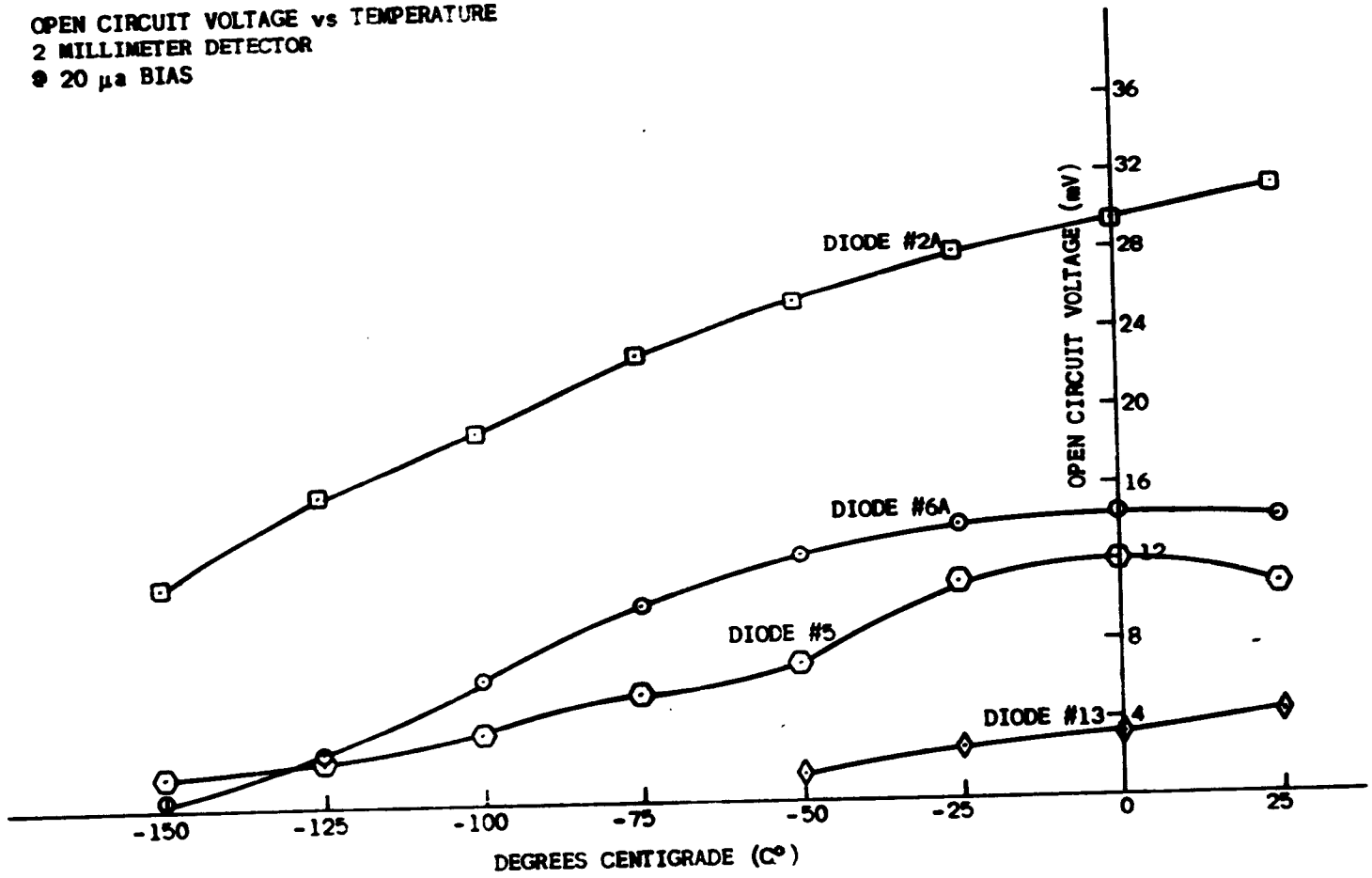
OPEN CIRCUIT VOLTAGE vs TEMPERATURE
2 MILLIMETER DETECTOR
@ 20 μa BIAS
DIODE #2A
DIODE #6A
DIODE #5
DIODE #13
OPEN CIRCUIT VOLTAGE (mV)
36
32
28
24
20
16
12
8
4
-150
-125
-100
-75
-50
-25
0
25
DEGREES CENTIGRADE (C°)

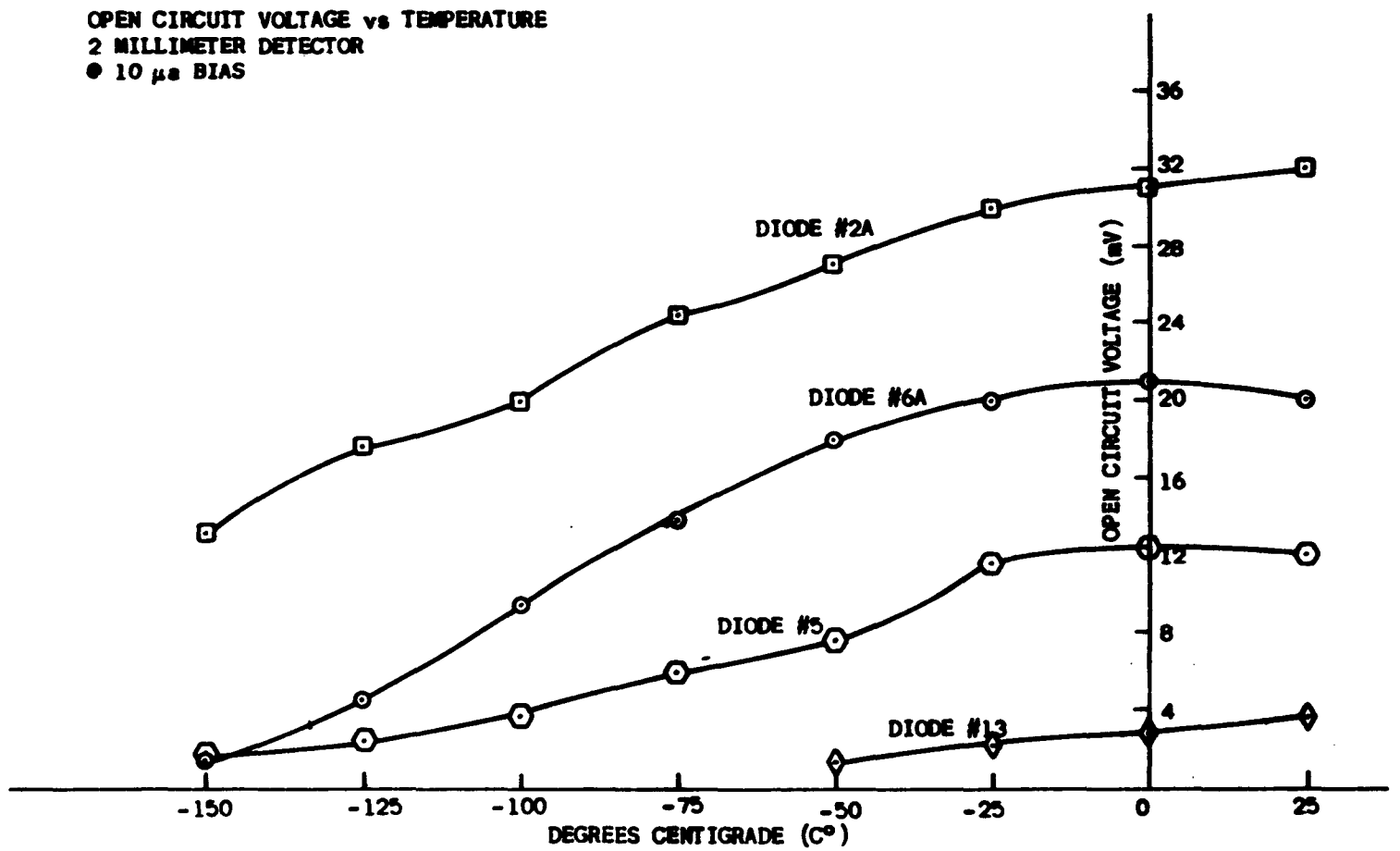
OPEN CIRCUIT VOLTAGE vs TEMPERATURE
2 MILLIMETER DETECTOR
● 10 μa BIAS
DIODE #2A
DIODE #6A
DIODE #5
DIODE #13
OPEN CIRCUIT VOLTAGE (mV)
36
32
28
24
20
16
12
8
4
-150
-125
-100
-75
-50
-25
0
25
DEGREES CENTIGRADE (C°)

OPEN CIRCUIT VOLTAGE vs TEMPERATURE
2 MILLIMETER DETECTOR
0-BIAS

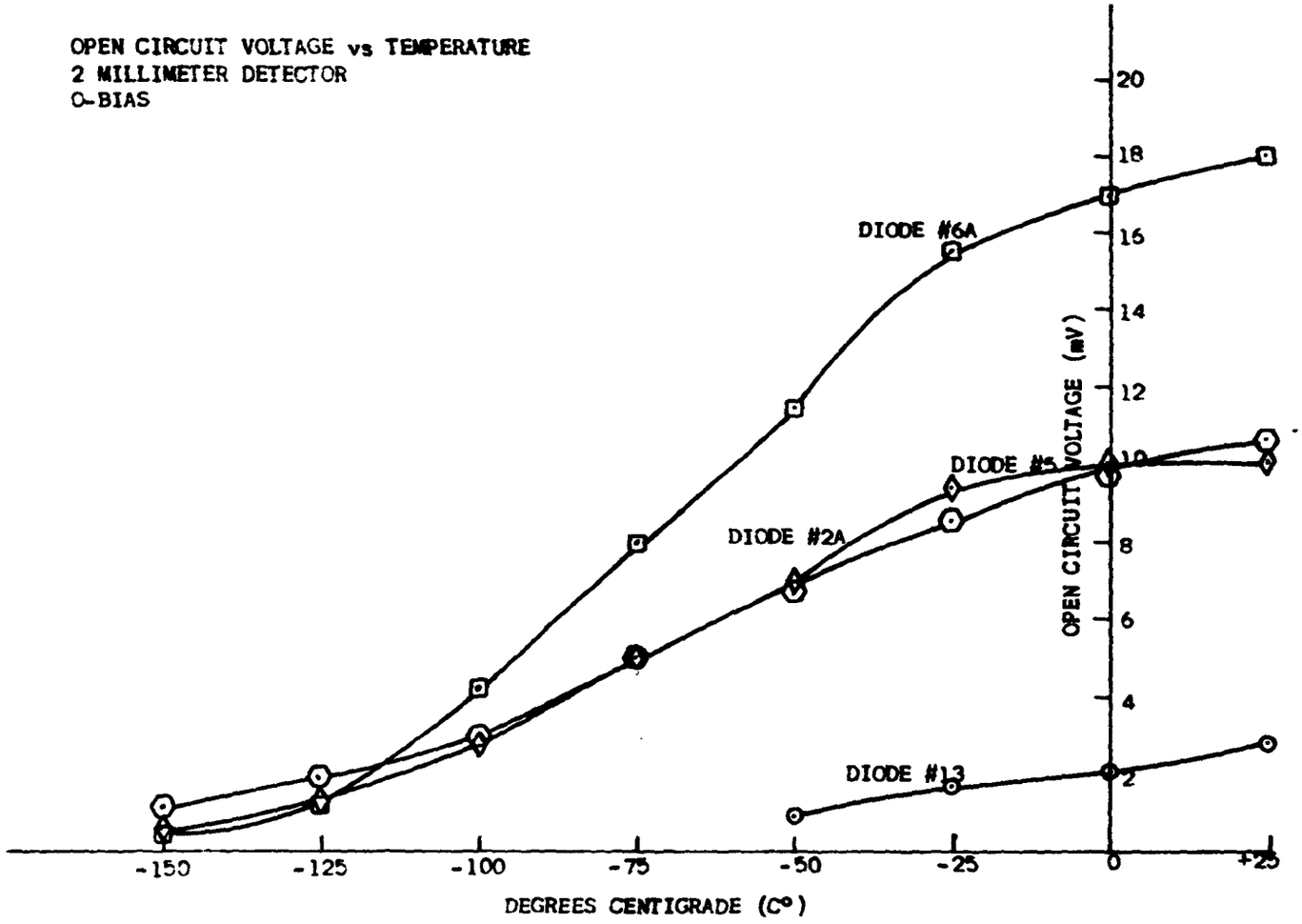

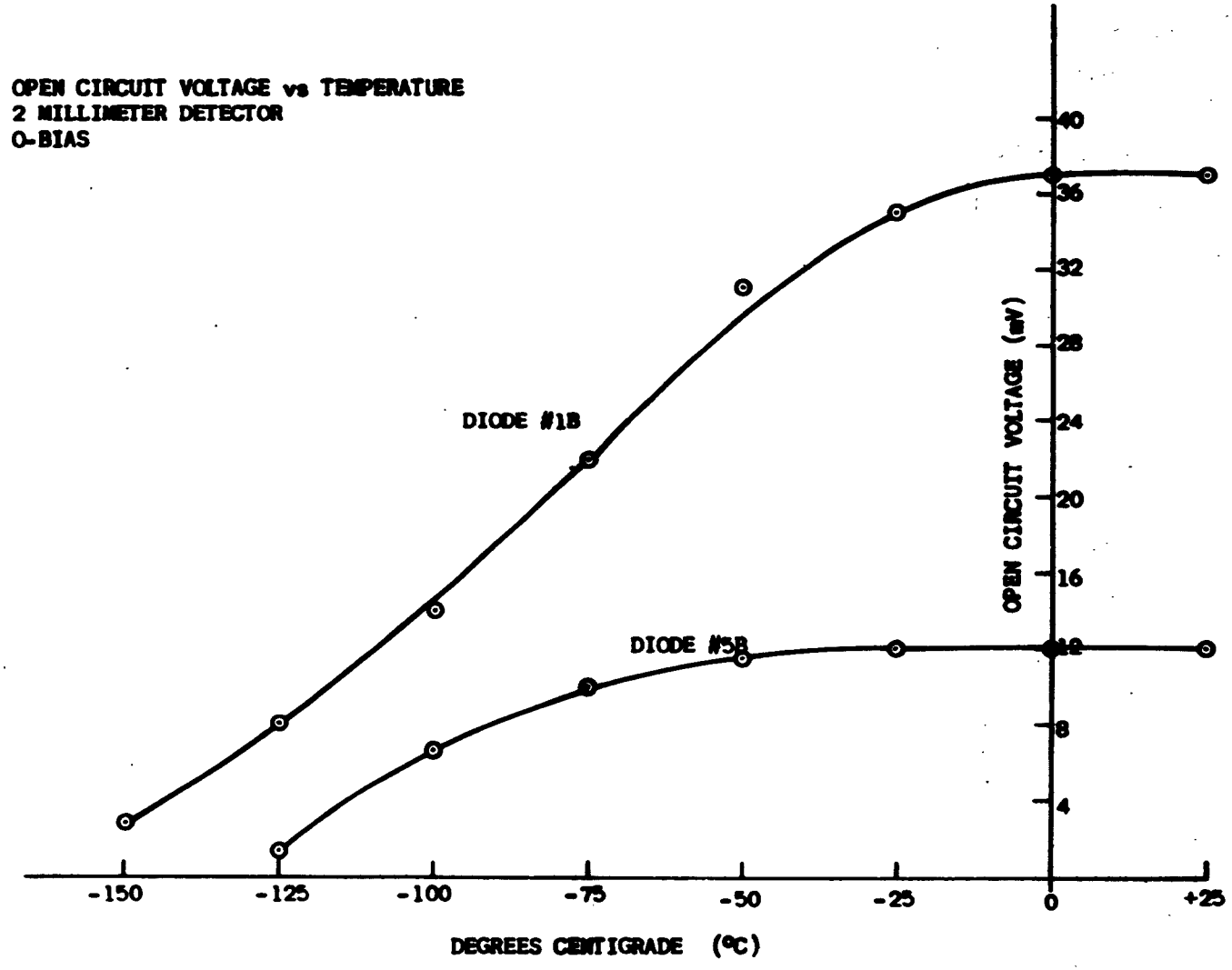
OPEN CIRCUIT VOLTAGE vs TEMPERATURE
2 MILLIMETER DETECTOR
0-BIAS
DIODE #1B
DIODE #5B
OPEN CIRCUIT VOLTAGE (mV)
40
36
32
28
24
20
16
12
8
4
-150
-125
-100
-75
-50
-25
0
+25
DEGREES CENTIGRADE (°C)

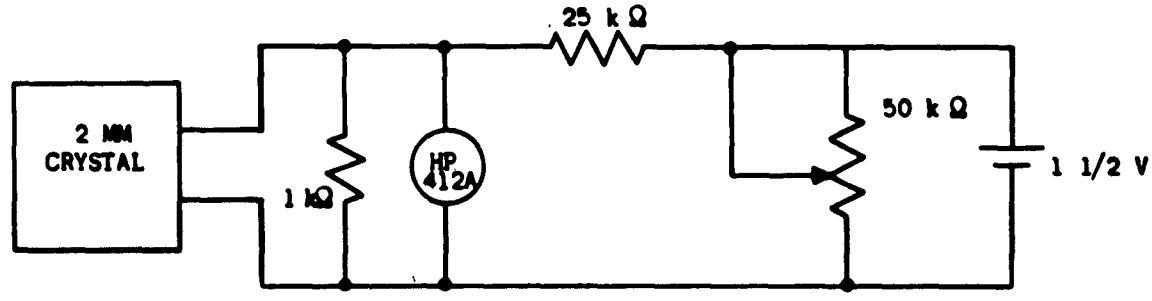

FIGURE 34

INCREMENTAL CONVERSION LOSS SCHEMATIC

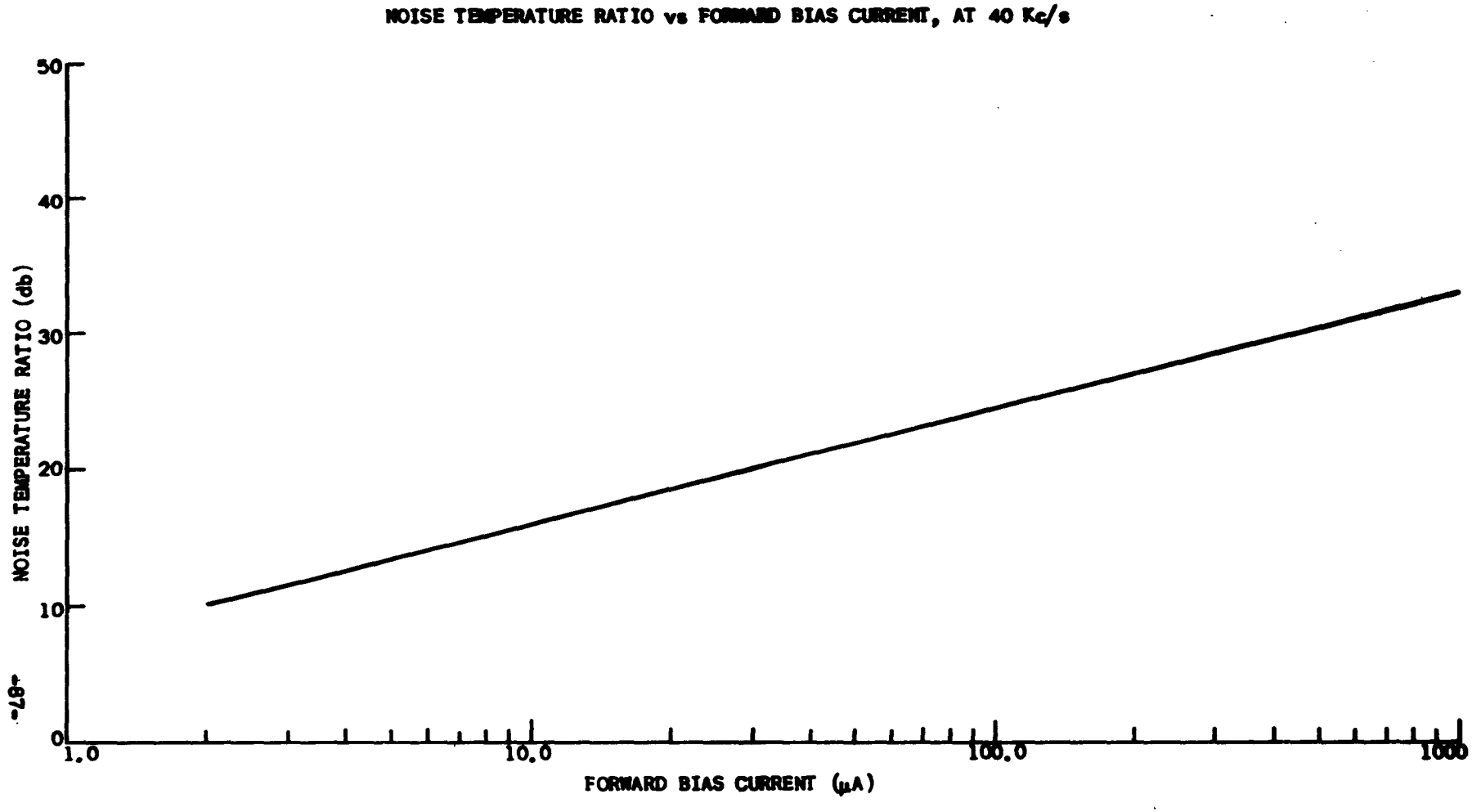

FIGURE 35

NOISE TEMPERATURE vs BIAS GRAPH

NOISE TEMPERATURE RATIO vs FREQUENCY

CODE NO.	FORWARD BIAS CURRENT
1	540 μA
2	185 μA
3	70 μA
4	35 μA
5	12 μA
6	4 μA

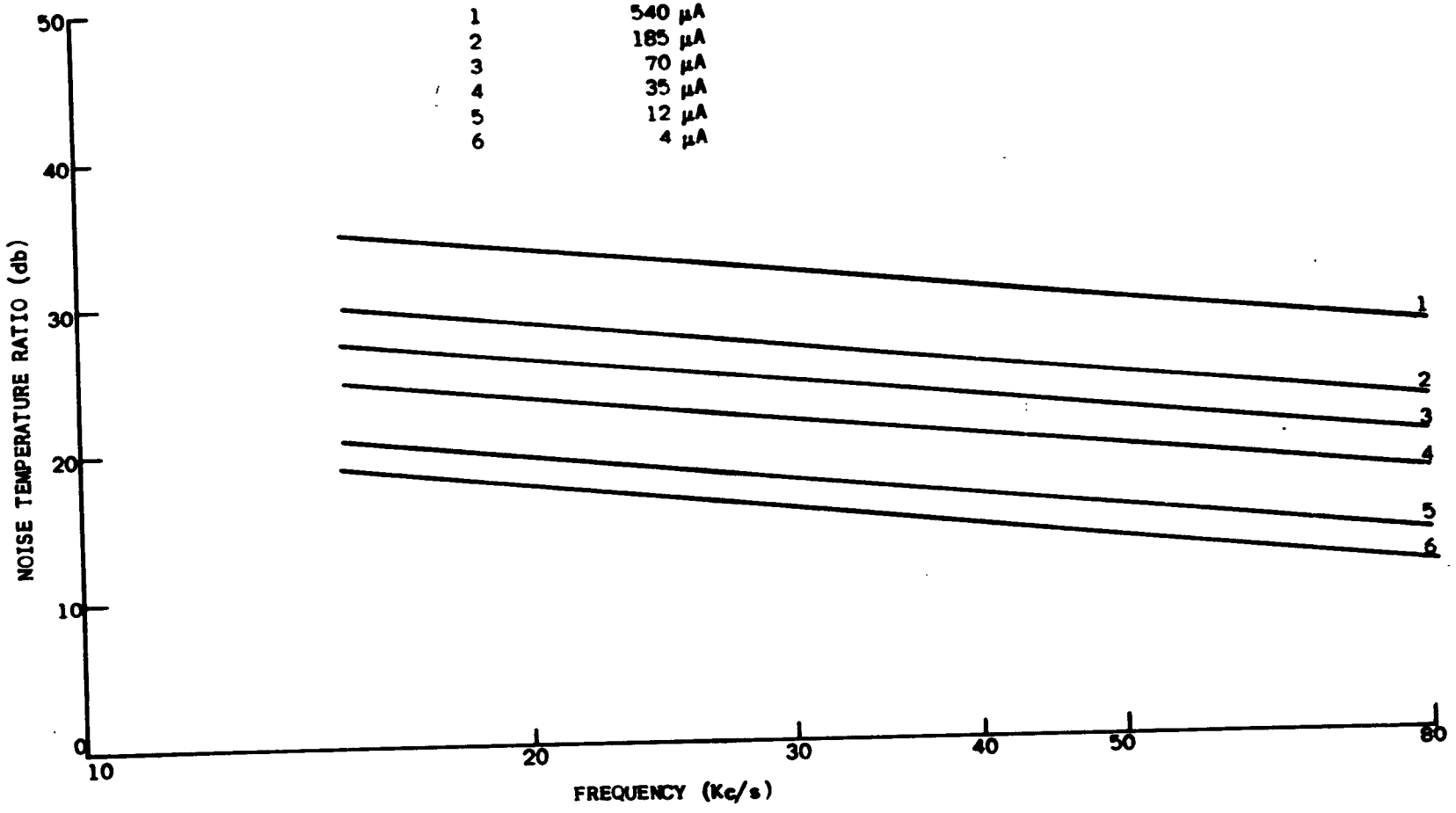

FIGURE 36

NOISE TEMPERATURE vs FREQUENCY GRAPH

HARMONIC GENERATOR				140 kMc DETECTOR			
Diode Number	Diode Type	Silicon	Input Power (mw)	Detector Number	Silicon	Guide Size	Output db Above Noise
1	MA-435	Al-doped	115	4	Al-doped	.090"	16
2	MA-4146	Epitax.	12.5	4	"	"	43
3	"	"	1.0	1	Epitax.	.0625"	8
"	"	"	1.0	2	"	.070"	10
"	"	"	1.0	3	Al-doped	.070"	16
"	"	"	1.0	4	"	.090"	19
"	"	"	1.0	5	Epitax.	"	5
4	"	"	12.5	4	Al-doped	"	41
"	"	"	12.5	5	Epitax.	"	34

3 1/2 mil "S"-bend whisker used in above units

TABLE 1

DYNAMIC RANGE OF 2 MILLIMETER DIODES

DYNAMIC RANGE (db)				OPEN C'KT VOLTAGE (mv)			
Power Level / Diode Number	1 μ watt	10 μ watt	100 μ watt	Power Level / Diode Number	1 μ watt	10 μ watt	100 μ watt
0	31.6	41.3	47.5	0	4.4	36	195
1	26.5	37.0	44.0	1	2.05	18.3	100
2	27.5	38.1	45.0	2	2.00	17.7	80
4	27.3	37.3	44.1	4	2.42	23.9	125
5	25.5	36.0	43.5	5	1.24	12.3	82
6	25.5	35.5	43.2	6	.90	9.5	55
7	25.3	34.3	40.5	7	6.00	49	207

Epitaxial Si + 3 1/2 mil "S"-bend whisker Freq. 135.4 ± 1 kMc

TABLE II

CALIBRATION DATA FOR 2-MILLIMETER VIDEO DETECTOR STANDARDS

Diode Number	R_V (kΩ)	Figure of Merit
0	91	14.5
1	>100	6.4
2	47	9.2
4	>100	7.6
5	40	6.1
6	29	5.2
7	>100	18.8

TABLE III

SLOPE RESISTANCE AND CALCULATED

FIGURE OF MERIT OF 2-MILLIMETER STANDARDS

Diode No.	Bias μA	R_V kΩ	γ X10^{-3}	F.M.
2	0	3.46	2.0	29.3
	20	2.4	2.21	36.9
	25	2.0	2.14	37.9
	30	1.7	2.07	38.4
	35	1.6	2.04	37.8
	40	1.4	1.97	38.7
	45	1.3	1.93	38.6
	50	1.2	1.895	38.8
4	0	< 1.0	2.18	46.5
	20	3.1	2.25	34.3
	25	3.0	2.17	33.5
	30	2.9	2.11	33.0
	35	2.84	2.07	32.6
	40	2.77	2.00	31.7
	45	2.70	1.89	30.3
	50	2.65	1.83	29.5
5	0	21.46	3.09	20.6
	20	4.3	2.42	32.7
	25	3.65	2.21	31.8
	30	3.30	2.07	30.9
	35	3.0	1.89	29.3
	40	2.78	1.79	28.4
	45	2.60	1.65	26.9
	50	2.43	1.545	25.7
6	0	33.0	3.23	17.6
	20	3.55	2.60	37.7
	25	3.05	2.35	36.1
	30	2.70	2.17	34.7
	35	2.48	2.04	33.7
	40	2.30	1.89	32.0
	45	2.15	1.79	31.0
	50	2.03	1.68	29.7

TABLE IV

BIASED FIGURE OF MERIT

Diode No.	Whisker	Silicon
1 2 3 4 5	.003" "S"-bend Tungsten	Epitaxial
1-A 2-A 3-A 4-A 5-A	.003" "S"-bend Tungsten	Al-doped Si
1-B 2-B 3-B 4-B 5-B	.003" "S"-bend Tungsten	Boron Doped Si

AFTER APPROXIMATELY 100 HOURS ALL BUT DIODES
4, 5, 2A, 4A, 4B and 5B WERE READJUSTED AS FOLLOWS

1 2 6	.0015" "C"-bend Tungsten	Epitaxial Si From Generator
1-A 3-A 6-A	.0015" "C"-bend Tungsten	Epitaxial
1-B 2-B 3-B	.0015" "C"-bend Tungsten	Boron Doped Si
11 12 13	.0015" "C"-bend Tungsten	Al-doped Si

TABLE V

2-MILLIMETER DETECTOR MAKEUP

Diode No.	R_V 0 μa	R_V 10 μa	R_V 20 μa	$\gamma_{@0}$	$\gamma_{@10}$	$\gamma_{@20}$
1	>110.0k	4.4 k	2.4 k	2.8	4.85	4.0
2	>110.0k	5.5 k	3.2 k	2.9	4.2	3.5
4	2.1k	1.8 k	1.5 k	.5	.55	.58
5	5.0k	3.0 k	2.1 k	.45	.48	.48
6	31.0k	6.0 k	3.2 k	1.4	2.4	2.2
1-A	>110.0k	5.9 k	3.1 k	.46	.64	.56
2-A	29.2k	8.0 k	4.9 k	.46	.9	.85
3-A	27.0k	5.5 k	3.5 k	.78	.71	.59
4-A	>110.0k	4.7 k	2.65k	.30	.48	.45
1-B	10.0k	4.3 k	2.55k	2.0	3.55	3.9
2-B	104.0k	4.4 k	2.4 k	.85	1.58	1.3
4-B	8.0k	4.24k	2.8 k	1.35	1.51	1.50
5-B	20.1k	5.5 k	3.1 k	.43	.60	.56
11	30.0k	8.2 k	4.9 k	8.2	7.3	5.6
13	12.4k	5.6 k	3.5 k	.68	1.28	1.28

TABLE VI

DATA FOR CALCULATION OF FIGURE OF MERIT UNDER BIAS

Diode No.	F.M. 0 μa	F.M. 10 μa	F.M. 20 μa
1	8.4	37.3	66.7
2	8.7	5.13	51.5
4	8.72	10.2	11.5
5	5.72	7.41	8.38
6	7.81	28.3	33.2
1-A	1.378	7.57	8.55
2-A	2.64	9.40	10.9
3-A	4.65	8.69	8.6
4-A	.889	6.17	7.25
1-B	18.91	47.8	58.01
2-B	2.62	21.15	31.75
4-B	14.1	20.5	22.82
5-B	2.9	7.34	8.55
11	46.5	75.4	71.6
13	5.83	15.45	18.7

TABLE VII

FIGURE OF MERIT WITH BIAS

Diode No.	Temp. °C	R_V 0 Bias	R_V 10 μa Bias	R_V 20 μa Bias	γ 0 Bias	γ 10 μa Bias	γ 20 μa Bias	
1B	+25	8.2			37.0			
	0	8.8			37.0			Power
	-25	9.9			35.0			Level
	-50	12.5			31.0			42.3μW
	-75	15.3			22.0			
	-100	18.7			15.0			
	-125	20.7			8.0			
	-150	21.8			2.7			
5B	+25	11.6			4.0			
	-25	10.4			2.7			Power
	-50	8.8			1.8			Level
	-75	7.9			1.1			42.3μW
	-100	6.9			.75			
	-125	6.0			.75			
2A	+25	27.5	7.4	4.7	10.6	32.0	31.0	
	0	28.0	7.4	4.7	9.8	31.0	29.6	Power
	-25	30.0	7.6	4.8	8.6	30.0	28.0	Level
	-50	32.0	7.8	4.8	6.8	27.0	25.4	31.0μW
	-75	35.5	8.0	4.9	5.0	24.4	23.0	
	-100	40.0	8.0	5.1	3.0	20.0	19.0	
	-125	45.0	8.5	5.3	2.0	17.8	16.0	
6A	+25	> 100K	9.4	5.9	18.0	20.0	14.0	
	0	> 100K	9.9	6.2	17.0	21.0	14.5	
	-25	> 100K	9.5	6.05	15.5	20.0	14.0	Power
	-50	> 100K	9.1	6.1	11.5	18.0	12.5	Level
	-75	> 100K	8.6	5.9	8.0	14.0	10.0	31.0μW
	-100	> 100K	9.05	6.6	4.2	9.6	6.3	
	-125	> 100K	9.8	6.0	1.3	4.6	2.8	
	-150	> 100K	8.8	5.4	.45	1.4	.82	
5	+25	16.5	4.0	2.4	10.0	12.0	11.8	
	0	19.0	4.0	2.4	10.0	12.4	12.0	
	-25	21.0	4.1	2.4	9.4	11.6	11.0	Power
	-50	21.0	4.0	2.35	7.0	7.8	7.0	Level
	-75	16.5	4.0	2.45	5.0	6.0	5.6	31.0μW
	-100	11.0	4.0	2.45	2.8	3.9	3.7	
	-125	8.9	3.7	2.47	1.34	2.5	2.3	
	-150	8.0	3.6	2.45	.6	1.90	1.84	
13	+25	3.4	3.3	3.35	2.8	3.7	4.4	
	0	3.1	3.19	3.21	2.1	2.8	3.4	
	-25	3.21	2.99	3.2	1.7	2.4	2.7	
	-50	4.6	2.99	2.85	.9	1.2	1.6	
	-75							
	-100	DIODE OPENED						
	-125							
	-150							

TABLE VIII

BELOW-AMBIENT FIGURE OF MERIT DATA

Diode No.	Temp. °C	F.M. 0 Bias	F.M. 10 μa Bias	F.M. 20 μa Bias
1B	+25	9.04		
	0	8.75		
	-25	7.9		
	-50	6.3		
	-75	4.07		
	-100	2.52		
	-125	1.28		
	-150	.42		
5B	+25	.836		
	-25	.591		
	-50	.423		
	-75	.27		
	-100	.195		
	-125	.206		
2A	+25	1.49	8.17	9.56
	0	1.37	7.91	8.95
	-25	1.15	7.66	8.65
	-50	.88	6.73	7.84
	-75	.62	6.09	7.09
	-100	.342	5.0	5.64
	-125	.22	4.27	4.77
6A	+25	1.83	6.5	5.35
	0	1.72	6.5	5.45
	-25	1.57	6.5	5.3
	-50	1.17	5.75	4.73
	-75	.807	4.5	3.81
	-100	.426	3.1	2.29
	-125	.131	1.41	1.08
	-150	.045	.452	.326
5	+25	1.78	3.95	4.65
	0	1.66	4.025	4.74
	-25	1.49	3.77	4.34
	-50	1.11	2.56	2.76
	-75	.89	1.97	2.21
	-100	.602	1.28	1.46
	-125	.361	.845	.906
	-150	.148	.642	.727
13	+25	1.33	1.76	2.09
	0	1.03	1.37	1.665
	-25	.834	1.17	1.275
	-50	.381	.588	.785

TABLE IX

BELOW AMBIENT FIGURE OF MERIT

Diode No.	T.S.S. 0 Bias	T.S.S. 10 μa Bias	T.S.S. 20 μa Bias
1	29.0	30.0	31.0
2	31.0	32.0	32.0
4	25.4	28.2	28.2
5	24.0	26.8	27.0
11	33.5	> 35.0	> 35.0
1A	32.2	34.2	35.0
2A	23.4	31.0	31.5
3A	29.5	33.0	33.0
4A	21.2	22.5	23.0
1B	28.7	30.0	30.0
4B	31.0	31.0	31.0
5B	26.0	26.0	26.0

TABLE X

TANGENTIAL SIGNAL SENSITIVITY

DIODE 1B

$$Lc = \frac{gb}{2Po\left(\frac{\Delta I}{\Delta P}\right)^2}$$

$$gb = \frac{1}{500}$$

$P = 16 \times 10^{-6}$ watts $\qquad Po = 24 \times 10^{-6}$ watts

$\Delta P = 16 \times 10^{-6}$ watts

$\Delta I = .22 \times 10^{-6}$ amps

$$Lc = \frac{1}{1{,}000(24 \times 10^{-6})\left(\frac{.22}{16}\right)^2} = -53.2 \text{ db}$$

After Readjust

$\Delta I = .36 \times 10^{-6}$ amps

$Lc = -49.2$ db

After Second Readjust

$\Delta I = .48 \times 10^{-6}$ amps

$Lc = -46.6$ db

TABLE XI

INCREMENTAL CONVERSION LOSS

APPENDIX I - 4 to 2 MILLIMETER HARMONIC GENERATOR

A. INTRODUCTION

This appendix describes the design and fabrication of a 4 to 2 millimeter harmonic generator. The generator is of the in-line form; the input and output waveguides lie along the same axis. The output waveguide, which is beyond cutoff for the fundamental frequency, acts as a tuning element for the fundamental frequency as well as a high-pass filter to obtain the output harmonic without fundamental. An E/H tuner is included in the fundamental waveguide as an additional, adjustable tuning element.

B. DESIGN

The input to the doubler is RG98/U rectangular waveguide. This guide has a $T.E._{10}$ -mode cutoff frequency of 39.9 kMc and propagates only the dominant mode at frequencies up to approximately 80 kMc. The output of the doubler is RG 138/U rectangular waveguide. This guide has a $T.E._{10}$ -mode cutoff frequency of 73.8 kMc and propagates only the dominant mode at frequencies up to approximately 148 kMc. If the fundamental frequency is to be 70 kMc and the crystal and whisker lie in the harmonic guide, the guide must be modified to lower its $T.E._{10}$ -mode cutoff frequency below 73.8 kMc. A standard practice in lowering the $T.E._{10}$ -mode frequency is to place a ridge in the center of the waveguide.[7] In this case the width of the ridge (A_2) is made equal to 1/2 the width of the RG138/U waveguide (A_1 = .080) i.e. $\frac{A_2}{A_1} = 0.5$. According to the chart on page 679, Ref.7, if the ratio of the guide height (b_1) to the guide height minus the ridge height ($b_2 = b_1 = a_3$) is set equal to 0.4, the $T.E._{10}$ -mode cutoff frequency is reduced to 49.2 kMc. This then will allow the fundamental frequency to enter the harmonic waveguide section containing the whisker and crystal.

A smooth tapered transistion must be made from the large rectangular input waveguide to the ridged smaller output or harmonic waveguide.[8] For maximum power transfer and minimum reflection the taper length should be five or more guide wavelengths for each factor of two in the ratio of the characteristic impedances to be matched.

The characteristic impedance of rectangular guide is

$$Z = \frac{754b}{a\sqrt{1 - \nu^2}}$$

where $\nu = \frac{fc}{f}$ and a is the width of the guide and b is the height.

For RG98/U

$$a = 0.148" \qquad fc = 39.9 \text{ kMc}$$
$$b = 0.074"$$

at 69.720 kMc

$$K = \frac{754\ (.074)}{.148\left(1 - \left(\frac{39.9}{69.72}\right)^2\right)^{1/2}} = 460$$

For the RG138/U ridged waveguide at 69.70 kMc

$$K = Z_\infty \frac{\lambda_g}{\lambda}$$

$$Z_\infty = 170, \quad K = 170\ \left(\frac{6.07}{4.3}\right) = 240\ \Omega$$

This is a ratio of characteristic impedances slightly less than 2 so a taper length of 5 guide wavelengths at 69.70 kMc in the ridged guide will be used.

$$5\lambda_g\ 69.7 = \frac{5\ (\ 4.3\ )}{\sqrt{1 - \left(\frac{4.3}{6.1}\right)^2}} = 1.195"$$

make it 1.20".

In the output guide the ridge must be tapered down to rectangular guide. This length will be made 5 guide wavelengths of 140 kMc in the ridged guide.

$$5\lambda_{g140} = \frac{5\ (2.15)}{\left[1 - \left(\frac{2.15}{6.1}\right)^2\right]^{1/2}} = .453"$$

make it 0.50".

C. FABRICATION

Figure #37 illustrates the design of the 4 to 2 millimeter harmonic generator. The body was machined in two halves to the specifications in Figures 38 and 39. The halves were placed together and secured with 4 #1-72 screws. A standard Philips claw flange was soldered to the output flange and the unit was then cleaned, degreased and gold plated.

The whisker used in this unit was the "S"-spring at 0.0035" diameter tungsten illustrated in Figure 5.

Silicon was prepared exactly the same as in the fabrication of the 4 millimeter wavelength detector with substrate resistivity of 0.0009 ohm-cm. The dice were soldered to crystal screws as illustrated in Figure 40. Before adjusting the silicon was etched to remove oxide from the epitaxial layer.

Figures 11 through 14 illustrate the additional parts of the diode needed for assembly. Upon assembly the whisker and screw subassembly were positioned in the diode to place the point contact approximately even with the surface of the ridge. All adjusting of the units was done by means of the silicon screw subassembly. The units were adjusted on the waveguide for a maximum dynamic range in combination with a circular guide 2-millimeter detector.

D. RESULTS

Table XII presents the conversion loss of the 4 to 2 millimeter detectors. As the sensitivities of the detectors increased it became possible to adjust the doublers more easily. The first whisker to silicon contact was readily detected and the E/H tuner in the fundamental guide was tuned before further adjusting was continued. This alternate adjusting, tuning procedure produced a very satisfactory diode.

E. CONCLUSIONS

The harmonic generator as described in this appendix is a sturdy unit that is compact and requires only simple tuning adjustments for maximum output. The ridged waveguide incorporated in this design is applicable to broad band use. Further study into whisker design and crystal materials will in the future lower the conversion loss of this diode to those of generators operating at lower frequencies.

APPENDIX II - CALIBRATED 2-MILLIMETER ATTENUATOR

A. INTRODUCTION

This appendix describes the design and fabrication of a 2-millimeter calibrated attenuator. The attenuator is the resistive card type with the card placed in the center of the guide at maximum E field. The circular card is mounted eccentrically and is lowered into or removed from the guide by means of simple rotation.

B. DESIGN

The attenuator was to be constructed in RG138/U rectangular waveguide to match the output of the harmonic generator described in Appendix I. To place the resistive card in the point of maximum E field in the waveguide a slot must be made in the top wall of the guide. If this slot is exactly in the center of the guide it will lie at a point of zero current and not effect the transmission properties of the guide. To prevent the slot of being a source of microwave power leakage, it is standard practice to make the slot width approximately 1/10 of the width of the guide. This rule may be followed providing this does not make the slot wider than the thickness of the guide walls. For RG138/U silver waveguide

Width = .080", height = .040"
Wall thickness = 0.030"
Slot width = $\frac{.080}{10}$ = 0.008"

A 0.005" thick 100 ohm/sq. mylar resistance card was decided upon. The card must protrude 0.070" into the guide from the top surface of the guide. This is the height of the guide (0.040") plus the wall thickness (0.030") and places the card just touching the bottom of the card. If the card is cut to a diameter of 1.0" a minimum slot length of 0.510" is required. The slot was made 0.075" long.

C. FABRICATION

The resistive card was cut to a diameter of 1.0" by clamping the card between a 1.0" circular brass disc and a cutting board. The disc is then traced with a razor blade to produce a perfectly smooth edge on the cut card. The card was mounted 0.070" off center on the shaft of a vernier dial. Lafayette Radio Stock #F-348. The center of the dial shaft was mounted 0.500" above the top surface of the waveguide. Figure 41 illustrates the design of the 2-millimeter attenuator.

The attenuator was calibrated by first setting the vernier dial to zero when the card was just even with the inside top surface of the waveguide. The dial was then rotated to introduce the card into the waveguide and its effect on the microwave power on the guide detected by the thermistor and read on a Hewlett Packard Power Bridge. Dial settings were recorded for various levels of attenuation.

D. RESULTS

Figure 42 presents the calibration curve of the attenuator. The insertion loss of the attenuator at zero setting is 0.5 db. The attenuator exhibited smooth action and fine repeatibility.

E. CONCLUSION

The attenuator described in this appendix is simple to construct. It was satisfactory in use in sensitivity measurements.

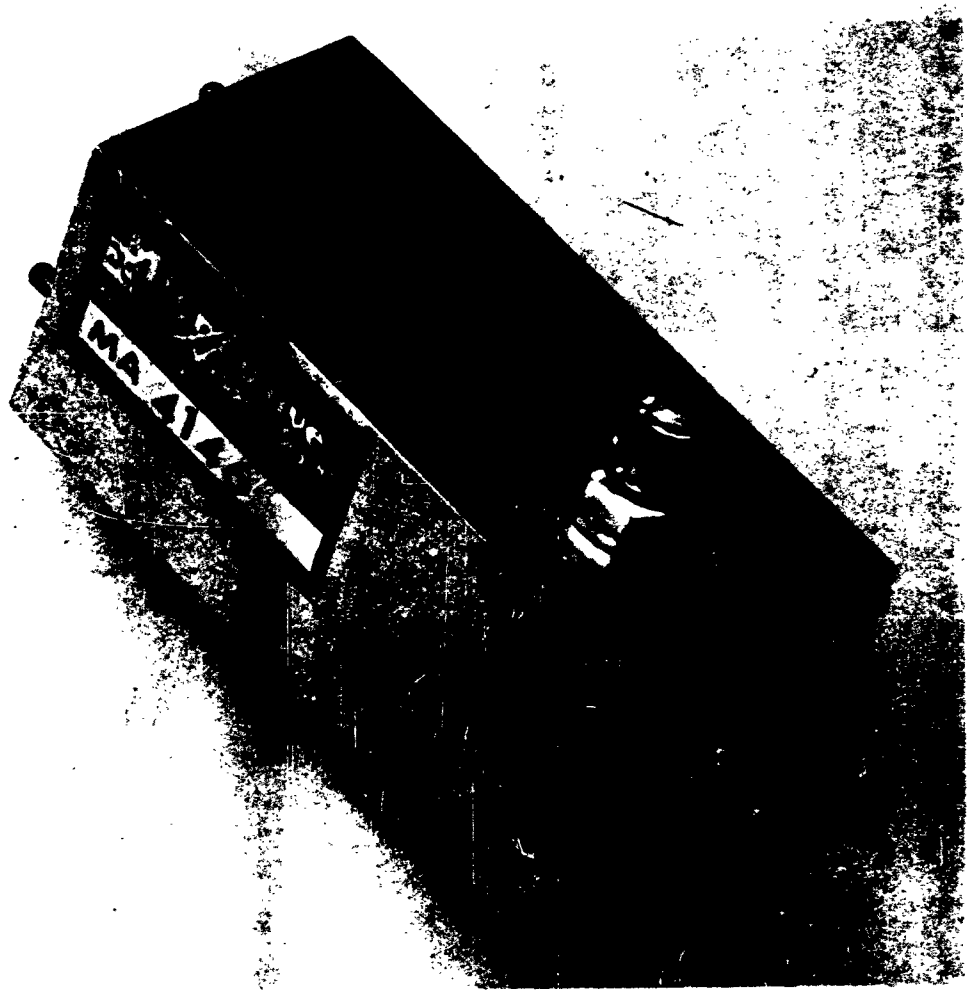

FIGURE 37

4 to 2 MILLIMETER HARMONIC GENERATOR

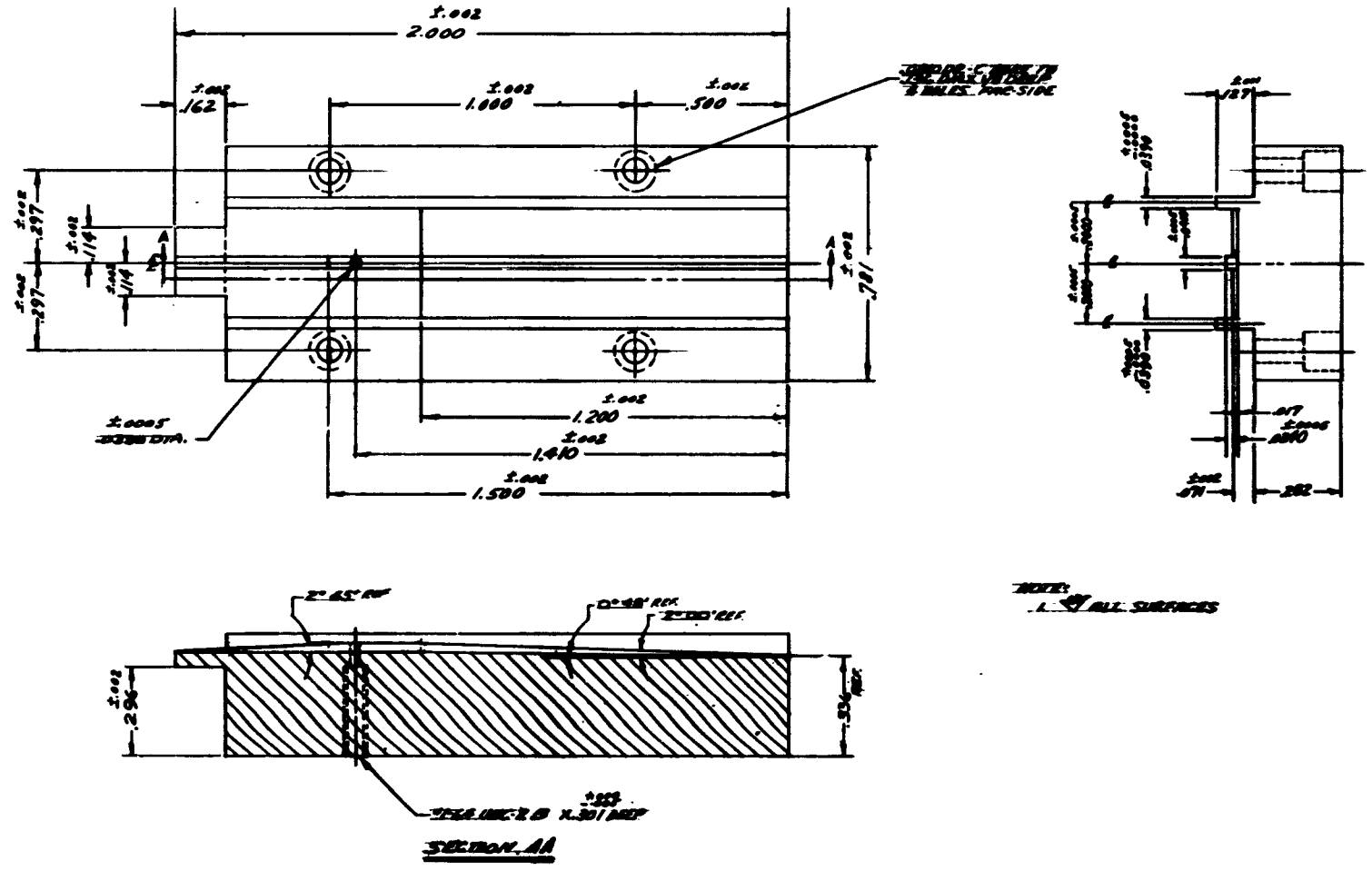

FIGURE 38

HARMONIC GENERATOR COVER

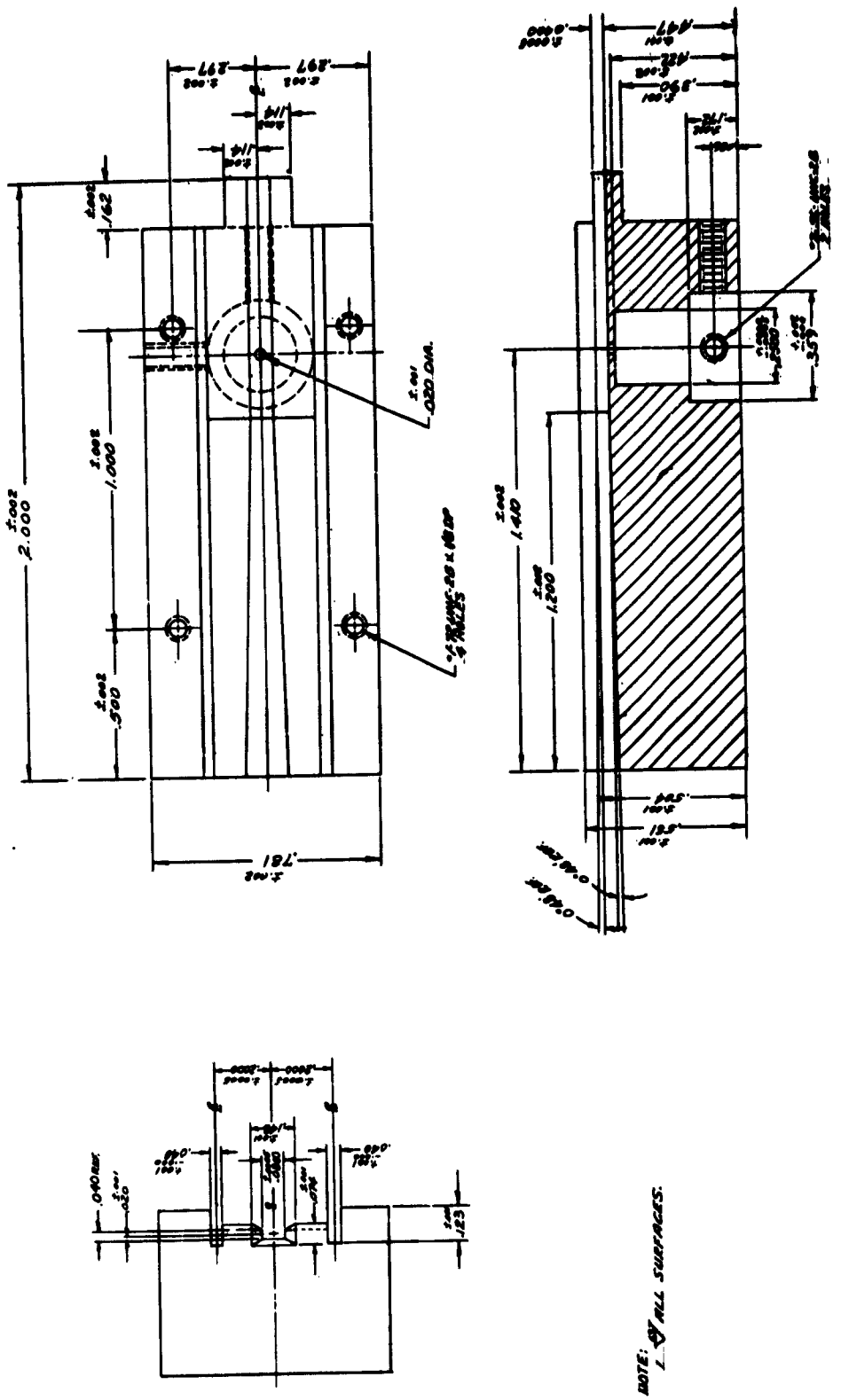

FIGURE 39
HARMONIC GENERATOR BODY

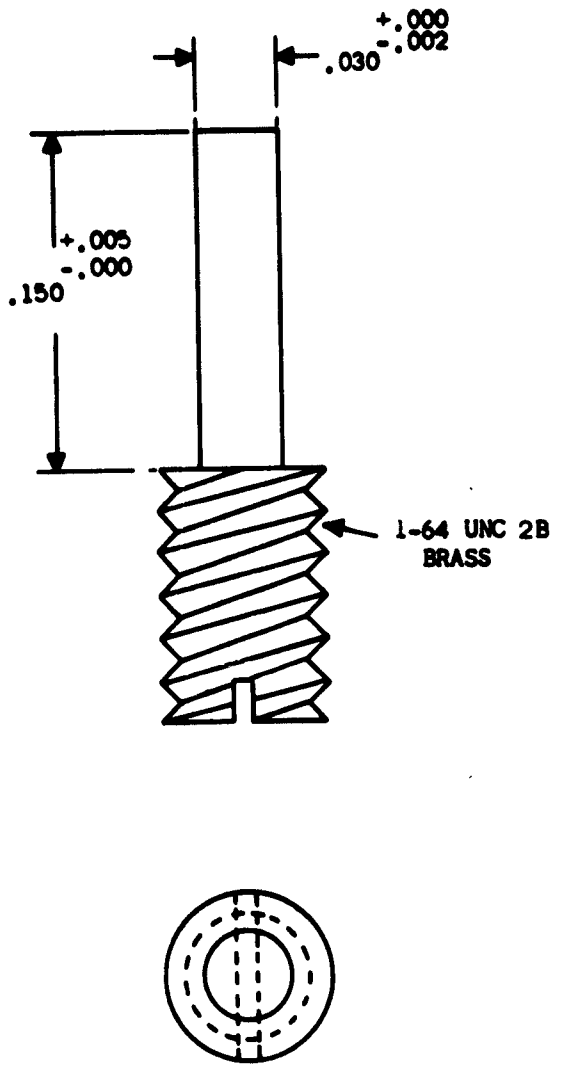

FIGURE 40

SILICON SCREW

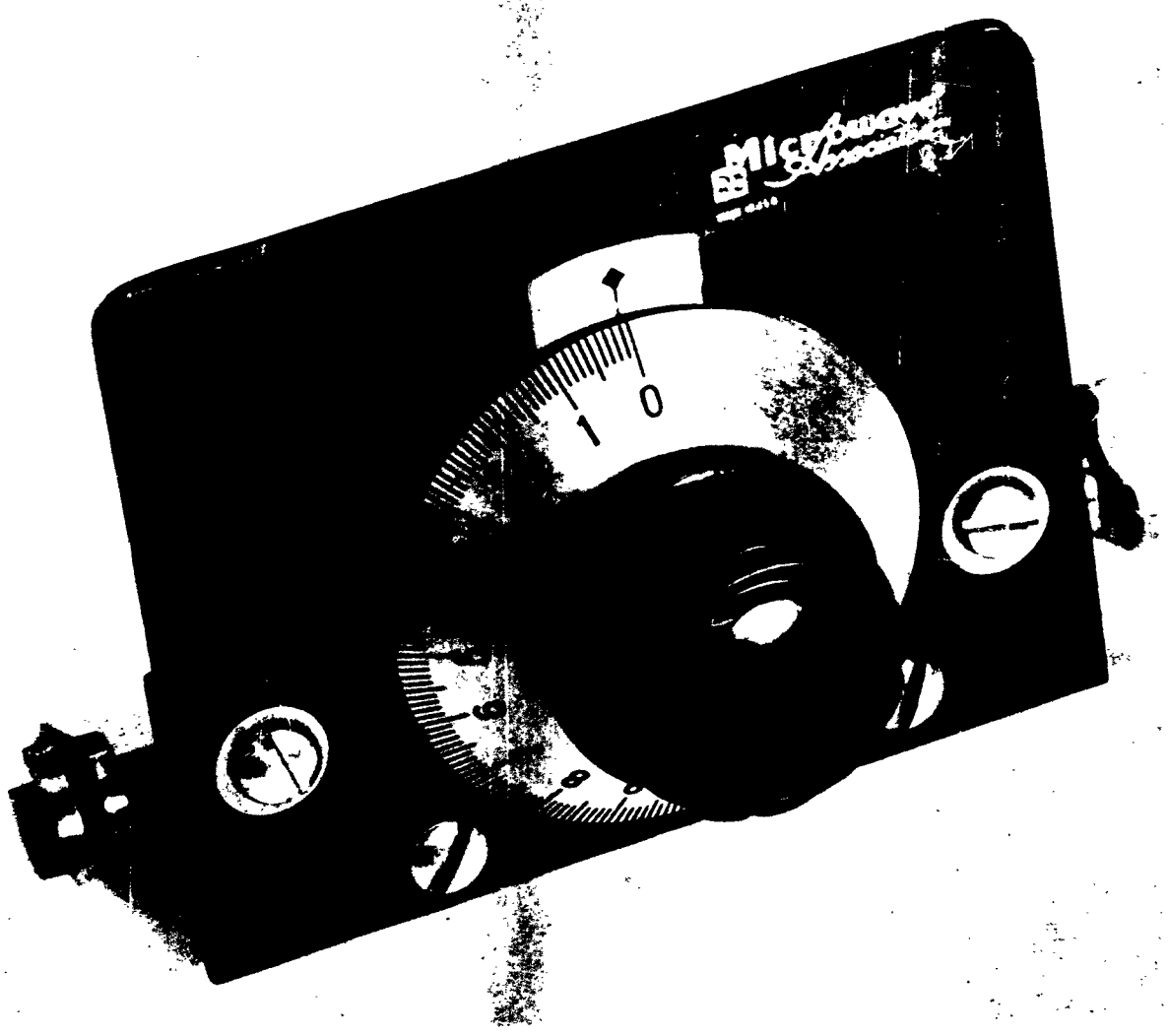

FIGURE 41

CALIBRATED 2 MILLIMETER ATTENUATOR

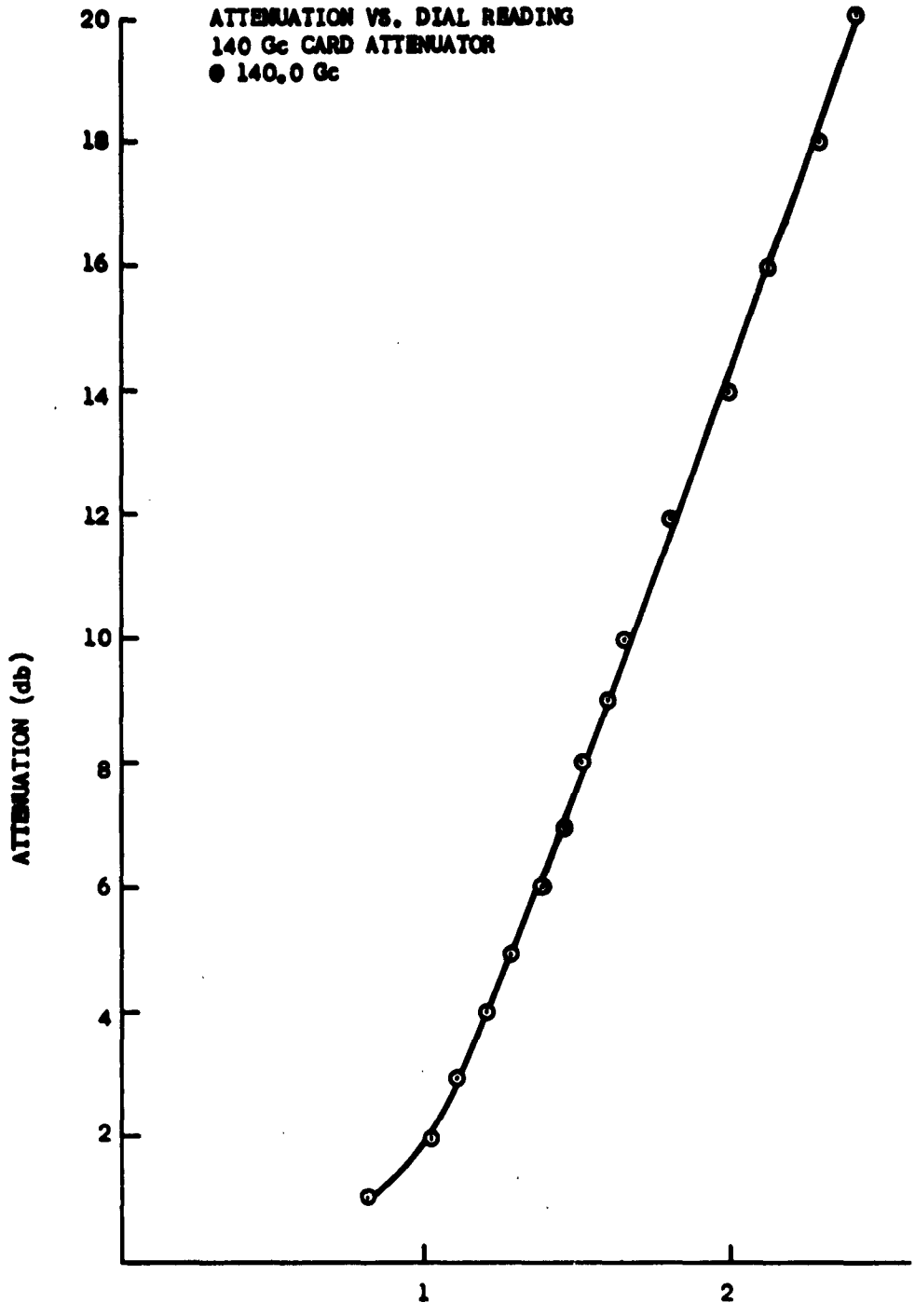

FIGURE 42

ATTENUATOR CALIBRATION CURVE

Diode No.	(mW) Input Power	Lc (db)
1	3.72	-35.7
2	14.3	-41.5
3	3.97	-36.0
4	.22	-23.5
5	36.2	-28.3
6	36.2	-27.3

TABLE XII

HARMONIC GENERATOR CONVERSION LOSS

DISTRIBUTION LIST

	No. of Copies
RADC RALTM/Mr. LoMascolo Griffis Air Force Base New York	6
RADC (RAAPT) Griffiss Air Force Base New York	1
GEEIA (ROZMCAT) Griffiss Air Force Base New York	1
RADC RAIS/Mr. Malloy Griffiss Air Force Base New York	1
AUL (3T) Maxwell Air Force Base Alabama	1
ASD (ASAPRD) Wright-Patterson Air Force Base Ohio	1
Chief, Naval Research Lab Attn: Code 2027 Washington 25, D.C.	1
Commanding Officer U.S. Army Electronics R & D Labs Attn: SELRA/SL-ADT Fort Monmouth, New Jersey	1
RTD (RTGS) Bolling Air Force Base Washington 25, D.C.	1
AFSC (SCSE) Andrews Air Force Base Washington 25, D.C.	1
ASTIA (TISIA-2) Arlington Hall Station Arlington 12, Virginia	10

DISTRIBUTION LIST - CONTINUED

	No. of Copies
Bureau of Ships (691B2C) Electronic Division Attn: Mr. L. V. Gumina Washington 25, D.C.	1
Commanding Officer U. S. Army Electronics R & D Labs Attn: SELRA/SL-PEE/Mr. N. Lipetz Fort Monmouth, New Jersey	1
RADC RAWED/Mr. R. Davis Griffiss Air Force Base New York	1
Bomac Laboratories, Inc. Attn: Mr. A. O. McCoubrey Salem Road Beverly, Massachusetts	1
Commander Hq Detachment 2 AFRD Attn: Mr. C. E. Ellis LG Hanscom Field Bedford, Massachusetts	1
Commander ASD (ASRNRE-1/Mr. R. B. Leasure) Wright-Patterson Air Force Base Ohio	1
University of Illinois Attn: Dr. P. D. Coleman College of Engineering Urbana, Illinois	1
Polytechnic Institute of Brooklyn Attn: Dr. A. A. Oliner Microwave Research Institute 55 Johnson Street Brooklyn, New York	1
FXR Attn: Mr. L. Bertan 26-12 Borough Place Woodside 77, New York	1
Sperry Microwave Company Attn: Mr. R. Duncan Clearwater, Florida	1
MIT Lincoln Laboratory Attn: Dr. Gerald Heller Lexington 73, Massachusetts	1

DISTRIBUTION LIST - CONTINUED

	No. of Copies
TRG Attn: Dr. A. Kay 400 Border Street E. Boston 28, Mass.	1
RADC RAWED/Mr. D. Nicholson Griffiss Air Force Base New York	1
Advisory Group on Electron Devices Attn: Mr. Kramer 346 Broadway New York, New York	3
Electronic Communications, Inc. Attn: Mr. J. Wiltse 1830 York Road Timonium, Maryland	1
Airborne Instruments Laboratory Attn: Mr. J. Taub Deer Park, Long Island, New York	1
Raytheon Company Attn: Dr. P. Debye Spencer Laboratory Burlington, Mass.	1
The Martin Company Attn: Dr. Vernon E. Derr Orlando, Florida	1
Sylvania Electronic Systems Attn: Dr. D. J. Leonard 1100 Wehrle Drive Buffaloe 21, New York	1
General Telephone and Electronics Labs Attn: Daniel E. George Bayside Laboratories Bayside New York	1
American Electronic Labs., Inc. Attn: Leon Riebman Richardson Road Colmar, Pennsylvania	1